ENVIRONMENTAL AND WATER QUALITY
OPERATIONAL STUDIES

TECHNICAL REPORT E-86-7
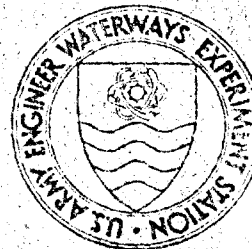
AN ASSESSMENT OF RESERVOIR MIXING PROCESSES

by

Dennis E. Ford, Linda S. Johnson

Ford, Thornton, Norton and Associates, Ltd.
3 Innwood Circle
Little Rock, Arkansas 72211

DTIC
ELECTE
SEP 9 1986
B

July 1986
Final Report

Destroy this report when no longer needed. Do not return
it to the originator.

The findings in this report are not to be construed as an official
Department of the Army position unless so designated
by other authorized documents.

The contents of this report are not to be used for
advertising, publication, or promotional purposes.
Citation of trade names does not constitute an
official endorsement or approval of the use of
such commercial products.

SECURITY CLASSIFICATION OF THIS PAGE (When Data Entered)

REPORT DOCUMENTATION PAGE	READ INSTRUCTIONS BEFORE COMPLETING FORM

1. REPORT NUMBER	2. GOVT ACCESSION NO.	3. RECIPIENT'S CATALOG NUMBER
Technical Report E-86-7	AD-A171 650	

4. TITLE (and Subtitle)	5. TYPE OF REPORT & PERIOD COVERED
AN ASSESSMENT OF RESERVOIR MIXING PROCESSES	Final report
	6. PERFORMING ORG. REPORT NUMBER

7. AUTHOR(s)	8. CONTRACT OR GRANT NUMBER(s)
Dennis E. Ford, Linda S. Johnson	Purchase Order No. DACW39-82-M-2042

9. PERFORMING ORGANIZATION NAME AND ADDRESS	10. PROGRAM ELEMENT, PROJECT, TASK AREA & WORK UNIT NUMBERS
Ford, Thornton, Norton and Associates, Ltd. 3 Innwood Circle Little Rock, Arkansas 72211	EWQOS Work Unit IA.2

11. CONTROLLING OFFICE NAME AND ADDRESS	12. REPORT DATE
DEPARTMENT OF THE ARMY US Army Corps of Engineers Washington, DC 20314-1000	July 1986
	13. NUMBER OF PAGES
	162

14. MONITORING AGENCY NAME & ADDRESS(if different from Controlling Office)	15. SECURITY CLASS. (of this report)
US Army Engineer Waterways Experiment Station Environmental Laboratory PO Box 631, Vicksburg, Mississippi 39180-0631	Unclassified
	15a. DECLASSIFICATION/DOWNGRADING SCHEDULE

16. DISTRIBUTION STATEMENT (of this Report)

Approved for public release; distribution unlimited.

17. DISTRIBUTION STATEMENT (of the abstract entered in Block 20, if different from Report)

18. SUPPLEMENTARY NOTES

19. KEY WORDS (Continue on reverse side if necessary and identify by block number)

Environmental impact analysis
Reservoirs
Water quality

20. ABSTRACT (Continue on reverse side if necessary and identify by block number)
    Since mixing and the resultant hydrothermal regime are dominant factors in determining what takes place chemically and biologically in a reservoir, techniques for predicting the characteristics of the major mixing mechanisms that occur in reservoirs can help the US Army Corps of Engineers (CE) regulate the quality of reservoir and release waters.
    This report provides a literature review of reservoir internal mixing processes, in which general transport processes, reservoir mixing processes and

(Continued)

DD ₁ FORM JAN 73 1473 EDITION OF 1 NOV 65 IS OBSOLETE

SECURITY CLASSIFICATION OF THIS PAGE (When Data Entered)

20. ABSTRACT (Continued).

their effect on water quality, and one-dimensional predictive techniques and computer algorithms are presented and analyzed. The historical development of the recommended predictive techniques, including the assumptions, limitations, and advantages of the techniques used in the development, is also documented.

The recommended one-dimensional mixing algorithm is generalized with respect to CE reservoirs and is not constrained by extensive data requirements nor limited in the mixing processes considered. The algorithm includes all major mixing processes in order to predict changes in the reservoir's mixing regime resulting from changes in hydrometeorological conditions and project operation. The recommended algorithm was used to simulate the thermal structure of over 15 reservoirs and lakes of varying geographical locations, size, hydrometeorological regime, and operational configurations. The recommendations for the mixing algorithm are the opinions of the authors, and all phases of it are not necessarily incorporated in the current one-dimensional CE reservoir model (CE-QUAL-R1).

QUALITY
INSPECTED
4

Accession For

NTIS GRA&I
DTIC TAB
Unannounced
Justification

By
Distribution

Availability Codes

Dist | Avail and/or Special

A-1

DTIC
ELECTE
SEP 9 1986
B

PREFACE

This report was prepared as part of the Environmental and Water Quality Operational Studies (EWQOS) Program, Work Unit IA.2, Develop and Verify Techniques for Describing Internal Reservoir Mixing Processes. The EWQOS Program is sponsored by the Office, Chief of Engineers (OCE), US Army, and is assigned to the US Army Engineer Waterways Experiment Station (WES), under the purview of the Environmental Laboratory (EL). The OCE Technical Monitors were Mr. Earl Eiker, Dr. John Bushman, and Mr. James L. Gottesman. Dr. J. L. Mahloch, EL, is the Program Manager of EWQOS.

The study was conducted by Dr. Dennis E. Ford and Ms. Linda S. Johnson of the Water Quality Modeling Group (WQMG), Environmental Research and Simulation Division (ERSD), EL. The work was conducted under the direct supervision of Mr. Mark Dortch, Chief, WQMG, and under the general supervision of Mr. D. L. Robey, Chief, ERSD, and Dr. John Harrison, Chief, EL. The report was prepared for WES under Purchase Order No. DACW39-82-M-2042 by Ford, Thornton, Norton and Associates, Ltd., Little Rock, Ark.

The report was reviewed and coordinated for publication by Ms. Sandra Bird, WQMG, and was edited by Ms. Jessica S. Ruff of the WES Publications and Graphic Arts Division.

Director of WES was COL Allen F. Grum, USA. Technical Director was Dr. Robert W. Whalin.

CONTENTS

AN ASSESSMENT OF RESERVOIR MIXING PROCESSES

SECTION 1. INTRODUCTION

Mixing refers to all physical transport processes and mechanisms which cause a parcel of water and its associated water quality constituents to blend with or be diluted by another parcel of water. Examples of specific transport processes that are included in this definition are molecular diffusion, dispersion, and convection, among others. The relative importance of any one specific transport process (e.g., dispersion) will vary both temporally and spatially and depend on the physical characteristics of the water body, time of year, and type of forcing event (e.g., the wind).

In lakes and reservoirs, mixing results from the cumulative effects of external energy inputs such as surface heat exchange; absorption of solar radiation with depth; wind magnitude and direction; inflow magnitude, density, and location; outflow magnitude and location; and changes in project operation (i.e., withdrawal depth, pool level changes, etc.). Mixing is therefore dynamic since its effectiveness varies in response to those dynamic forcing events.

A thorough understanding of mixing is required since it and the resultant hydrothermal regime, which includes thermal stratification, is a dominant factor in determining what takes place chemically and biologically in a reservoir. Sensitivity analyses on reservoir water quality models have shown the mixing coefficient to be highly sensitive, indicating the importance of having an accurate formulation for mixing (Thornton et al. 1979).

The objective of this study is twofold:

a. To review and document the major mixing mechanisms in Corps of Engineers (CE) reservoirs and their importance to reservoir water quality.

b. To develop a mathematical algorithm for one-dimensional water quality models (i.e., CE-QUAL-R1, Environmental Laboratory 1982) which realistically represents all major mixing processes occurring in CE reservoirs.

4

The review will emphasize the transport and dispersion of sub-
stances due to a given hydrothermal regime and not the specific details
of the hydrodynamic processes themselves. The mathematical algorithm
must be sufficiently general to be applicable to the majority of CE
reservoirs which vary in size and location and are therefore driven by
different hydrometeorologic forcing events. The algorithm must also be
able to accurately simulate changes in the mixing regime due to changes
in project operations, such as a change in conservation pool level or
withdrawal depth.

SECTION 2. BACKGROUND AND REVIEW

2.1 Introduction

Although the ultimate objective of this review is knowledge of the sum or cumulative effects of all reservoir mixing processes or mechanisms and their impact on reservoir water quality, it is first necessary to review density stratification and the individual transport processes. In many instances, this is not a simple task because the individual transport mechanisms act together, reinforcing one another with unknown synergistic effects. In addition, mixing determines the observed thermal structure, but the thermal (density) stratification modifies the mixing regime. It is therefore impossible to discuss reservoir mixing without knowledge of thermal stratification and to understand thermal stratification and reservoir water quality without an understanding of the individual mixing processes.

In this section, the concepts of thermal stratification and potential energy will first be reviewed. Then, definitions for several fundamental transport processes will be presented. This background information will be used in the next section to construct a complete picture of reservoir mixing based on energy sources and concepts and to determine the significance of mixing on reservoir water quality.

2.2 Density Stratification

2.2.1 Definitions and Importance

Density stratification is the nonhomogeneous layering of a fluid due to differences in density. In reservoirs, density stratification is primarily caused by temperature (i.e., thermal stratification), but density differences resulting from variations in suspended and dissolved solids concentrations can also be important. Density and/or thermal stratification therefore implies incomplete vertical mixing.

Many deep reservoirs exhibit the classical three-layer stratification (Figure 1a). The epilimnion is the upper stratum of warm,

6

c. Inverse winter
   stratification (Lake Eau
   Galle, Wisconsin, 22 Feb 79)

b. Linear stratification
   (Lake Shelbyville,
   Illinois, 6 Jun 73)

a. Classical three-layered
   system (Lake Greeson,
   Arkansas, 6 Oct 72)

Figure 1. Examples of stratification

7

turbulent water. It is usually characterized by relatively uniform temperatures. The deep, cold, relatively undisturbed region is termed the hypolimnion. Between the epilimnion and hypolimnion is a transition zone, the metalimnion, which is characterized by a strong temperature (density) gradient. The plane of inflection or of maximum temperature gradient is termed the thermocline. Other definitions have been proposed for the thermocline (e.g., the 1° C/m criterion), but they are not used herein. Another term illustrated in Figure 1a is the "mixed layer." The mixed layer is, as implied by the name, the overlying isotropic layer. Since the mixed layer refers to the instantaneous depth of the overlying isotropic layer, it differs from the epilimnion, which is an averaged mixed layer, in two respects. First, the mixed layer depth is usually less than the depth of the epilimnion. Second, it is much more dynamic than the epilimnion.

Many shallow reservoirs with short hydraulic residence times do not exhibit a classical three-layered system (e.g., Figure 1b). Instead of having a well-defined hypolimnion, the metalimnion appears to extend to the reservoir bottom. It is also possible to have systems that do not appear to have a well-defined epilimnion.

In cold regions, reservoirs may inversely stratify during the winter months (Figure 1c). At low temperatures (near 4° C), even small quantities of solids can significantly alter the water density and impact the observed thermal structure. In general, there is no well-defined epilimnion and metalimnion in inversely stratified systems. The thickness of the zone of density gradient (i.e., the epilimnion and metalimnion) under the ice varies from a metre or two in small reservoirs to tens of metres in large, deep reservoirs. In deep reservoirs, the effects of hydrostatic pressure (i.e., depth) also modify the density distribution (Farmer and Carmack 1982).

Many other terms are used to describe the thermal structure of a lake. These are defined in Hutchinson (1957), Ruttner (1963), Wetzel (1983), among others. In general, these terms are related either to the number of turnovers (i.e., periods of complete vertical mixing) occurring within a lake or to the strength of the stratification. It is,

however, important to distinguish between holomictic and meromictic
lakes. In holomictic lakes, the entire water column completely circu-
lates or turns over. Lakes that cannot circulate completely and exhibit
a deep stratum that is perennially stagnant in the water column are
termed meromictic lakes (Hutchinson 1957). The reason for this condi-
tion may be physical, chemical, or biological. Turbidity-induced
meromixis has been observed in a CE reservoir (Larson 1979). Whatever
the cause of meromixis, it can have a profound effect on the temperature
and mixing structure and, consequentially, on the water quality of lake.
Bottom withdrawal can be an effective management alternative to elimi-
nate this undesirable condition.

Thermal stratification is important because all chemical and bio-
logical processes are, to some extent, temperature dependent. More
important, however, is the layering of the lake which can isolate the
metalimnion and hypolimnion from light and transfers across the air/
water interface, resulting in vertical variations in water quality.

2.2.2 Factors Affecting Stratification

The principal factors influencing the formation, strength, and
extent of stratification are the density of water; solar radiation and
the heat transfer at the air/water interface; and the mixing resulting
from advection (inflows and outflows) and wind-induced phenomena.

It is well known that the density of water varies with temperature
(Figure 2). The importance of this variation in determining the distri-
bution of heat within a lake was originally documented by Birge (1910).
Two factors are important. First, the maximum density of water occurs
at approximately 4° C. Second, water density decreases at an escalating
rate with both increasing and decreasing temperatures from 4° C. There
is over an order of magnitude difference in the energy requirements to
mix or destratify a 1° C temperature difference at 25° C than at 5° C.

The energy available to warm the waters of a reservoir ultimately
comes from solar radiation, which varies seasonally and with latitude
(Figure 3). The seasonal variation of solar radiation follows a sinu-
soidal curve with a maximum in late June. In addition, diurnal cycles

9
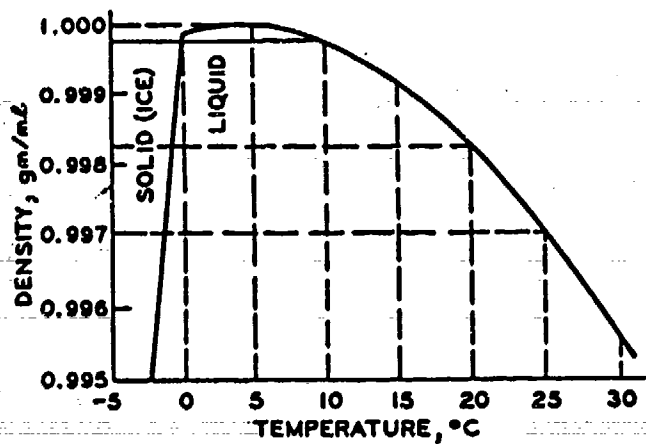
Figure 2. Variations of water
density with temperature
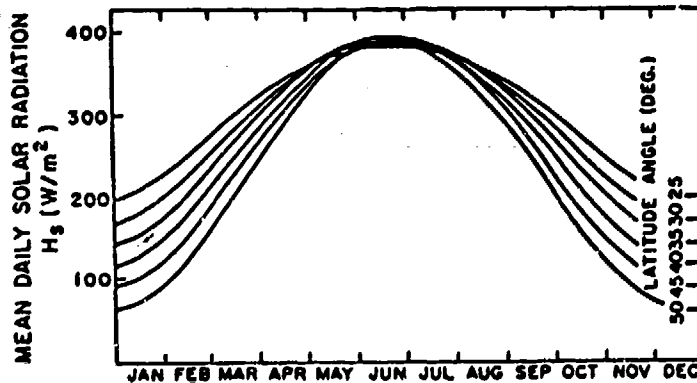
Figure 3. Seasonal variations in
solar radiation (after Koberg 1962)

also occur. Water temperatures respond to both of these cycles with a
slight delay. Solar radiation is absorbed at the water surface and
selectively with depth depending on the wavelength of the light, prop-
erties of the water, and the matter suspended in the water. This
absorption is usually assumed to be exponential with depth (i.e., Beer's
Law), but surface effects result in minor discrepancies in the top metre
or so of a lake (Figure 4).

In contrast to heating, cooling of a water body can occur only at
the water surface. It is therefore possible for the surface water to
decrease in temperature while deeper water increases in temperature. If
the temperature of the surface water drops below the temperature of the

10
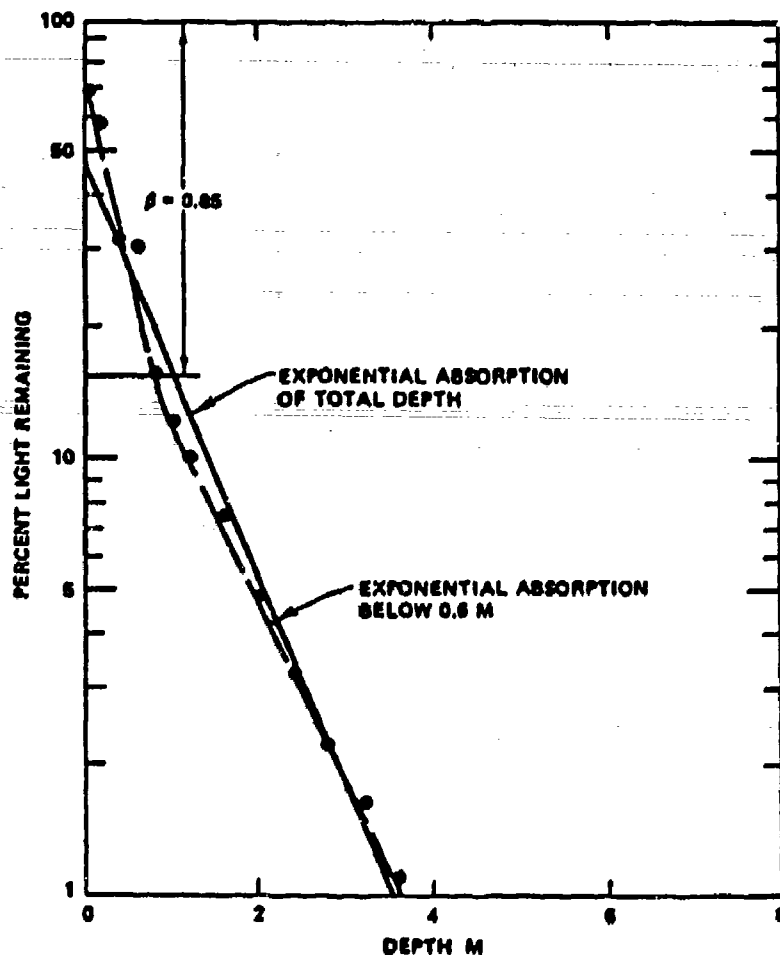
Figure 4. Extinction of light with depth

deeper water and still remains above 4° C, the water column becomes
thermally unstable and natural convection and mixing commence.

Mixing causes the shape of the vertical temperature profile to
change from an exponential decrease with depth (i.e., warming due to
absorption of solar radiation) to the classical profile of a well-mixed
layer overlying a zone of temperature gradient (Figure 5). Reservoir
mixing is discussed in detail in Section 3.

2.2.3 Temporal Variations

Because the factors which determine the thermal stratification are
always changing, the thermal structure is always undergoing change.
There are, however, three distinct cycles of importance: annual, synop-
tic, and diel. The annual cycle has a period of 365 days and exhibits

11

a. Solar heating only   b. Solar heating
                             plus wind
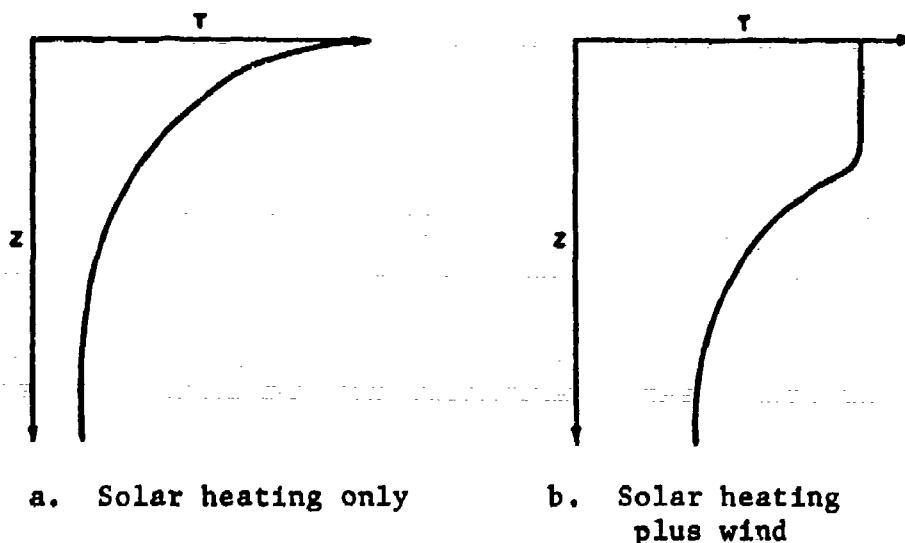
Figure 5. Effect of mixing on the thermal profile

seasonal changes in temperature resulting from seasonal changes in solar
radiation, air temperature, wind, and flow. Synoptic cycles typically
have periods of 5 to 7 days and correspond with the passage of major
weather systems (i.e., warm or cold fronts). Diel cycles have a period
of 24 hr and correspond to daytime heating and nighttime cooling.

Annual cycle. The annual temperature cycle for a large reservoir
with long residence time is shown in Figure 6. During the period of
spring turnover (late February to early March), the entire water column
undergoes complete mixing. The density differences at the low tempera-
tures (4° to 5° C) are insufficient to prevent complete mixing. As the
water column warmed, density differences increase and it becomes more
difficult to mix the entire water column. Stratification started to
form near the bottom of the lake (late March) because the density dif-
ferences and resulting buoyancy forces were small compared to the
kinetic energy input (i.e., wind). As the solar radiation increased,
water temperatures increased, density difference increased, and the
thermocline moved upward because the kinetic energy input could not
overcome the ever-increasing buoyancy forces of density stratification.
The minimum thermocline depth was achieved about the time of summer
solstice or time of maximum heat input (late June). Once stratification
formed, the hypolimnetic temperatures remained relatively constant until

12
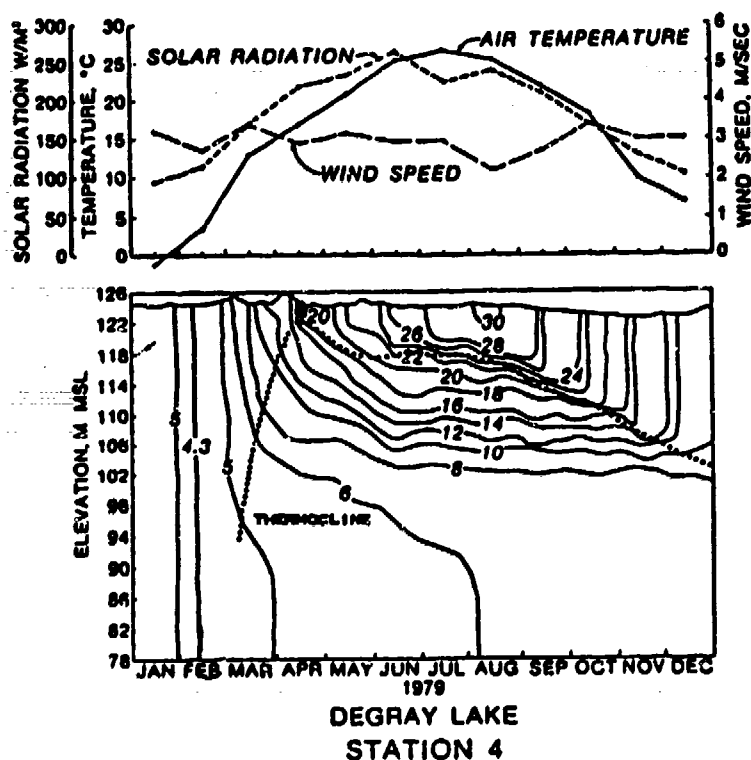
Figure 6. Annual temperature variations in a
deep reservoir with a long residence time

the surface temperatures cooled to near the hypolimnetic temperatures
and complete vertical mixing of the water column occurred (i.e., fall
overturn).

The increased mixing resulting from inflows and outflows in reser-
voirs can result in deviations from the above example. For instance,
periods of overturn may be extended and become more frequent, and the
slope of the isotherms may be increased. If bottom withdrawal is used,
hypolimnetic temperatures may increase. For example, in Figure 7, the
hypolimnetic temperatures in Beltzville Lake, Pennsylvania, during 1976
remained relatively constant when only small amounts of water were
released through the lower ports. In contrast, during 1972, when large
quantities of water were released through the floodgates in response to
Hurricane Agnes, the hypolimnetic temperatures increased. Other
variations such as pumped-storage operations can also increase mixing
and hypolimnion temperatures (Figure 8).

BELTZVILLE LAKE
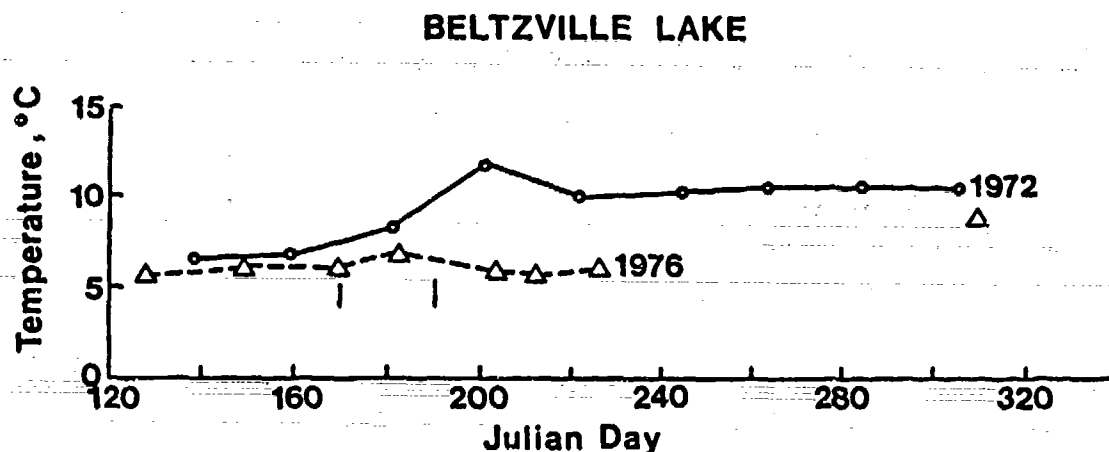
Figure 7. Seasonal variation in hypolimnetic temperature

Synoptic variations. Examples of synoptic temperature variations
are shown in Figure 9. Temporary periods of stratification occur during
periods of warm, calm weather and are destroyed during periods of cold,
windy weather. Synoptic variations are on the order of a few degrees
Celsius.

Diel variations. Diel variations are typically on the order of $1°$
to $2°$ C but can be as large as $7°$ C or more. The actual magnitude will
depend on the depth of the upper mixed layer, the amount of surface mix-
ing, and the quantity of solar insolation. The deeper the mixed layer
and/or the larger the surface mixing, the smaller the diurnal variation.
A typical diel variation is shown in Figure 10.

2.2.4 Horizontal Variations

Horizontal variations in temperature and stratification occur as a
result of differential heating, inflow, or mixing. Differential heating
occurs when the smaller volume of water in the coves, littoral zones,
and headwaters of an impoundment warms or cools more rapidly than the
open-water regions. In large lakes, this phenomenon is significant and
results in the formation of thermal bars. Similarly, rivers flowing
into a reservoir may be of different temperatures, creating longitudinal
variations. Horizontal variations resulting from a river inflow are
illustrated in Figure 11. Horizontal variations resulting from a river

14
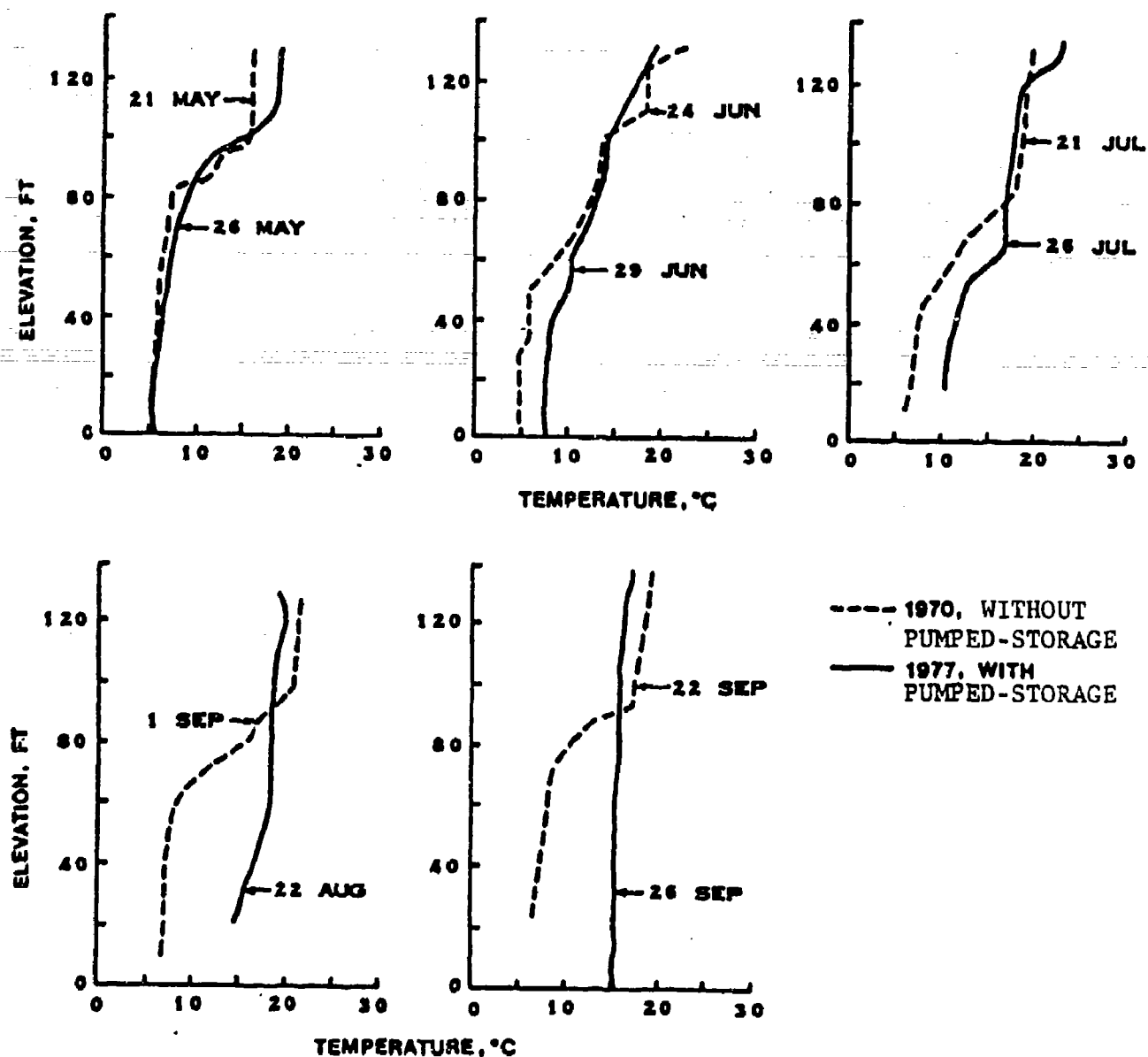
Figure 8. Effect of pumped-storage operations on the thermal structure of Kinzua Lake, Pennsylvania (after Dortch 1981) (to convert feet to metres, multiply by 0.3048)

inflow typically create temperature differences of 1° or 2° C or more. Spatial variations in both the horizontal and vertical directions can also occur as a result of seiching and upwelling (see Sections 3.2.2 and 3.3.2). These variations are highly dynamic.

15
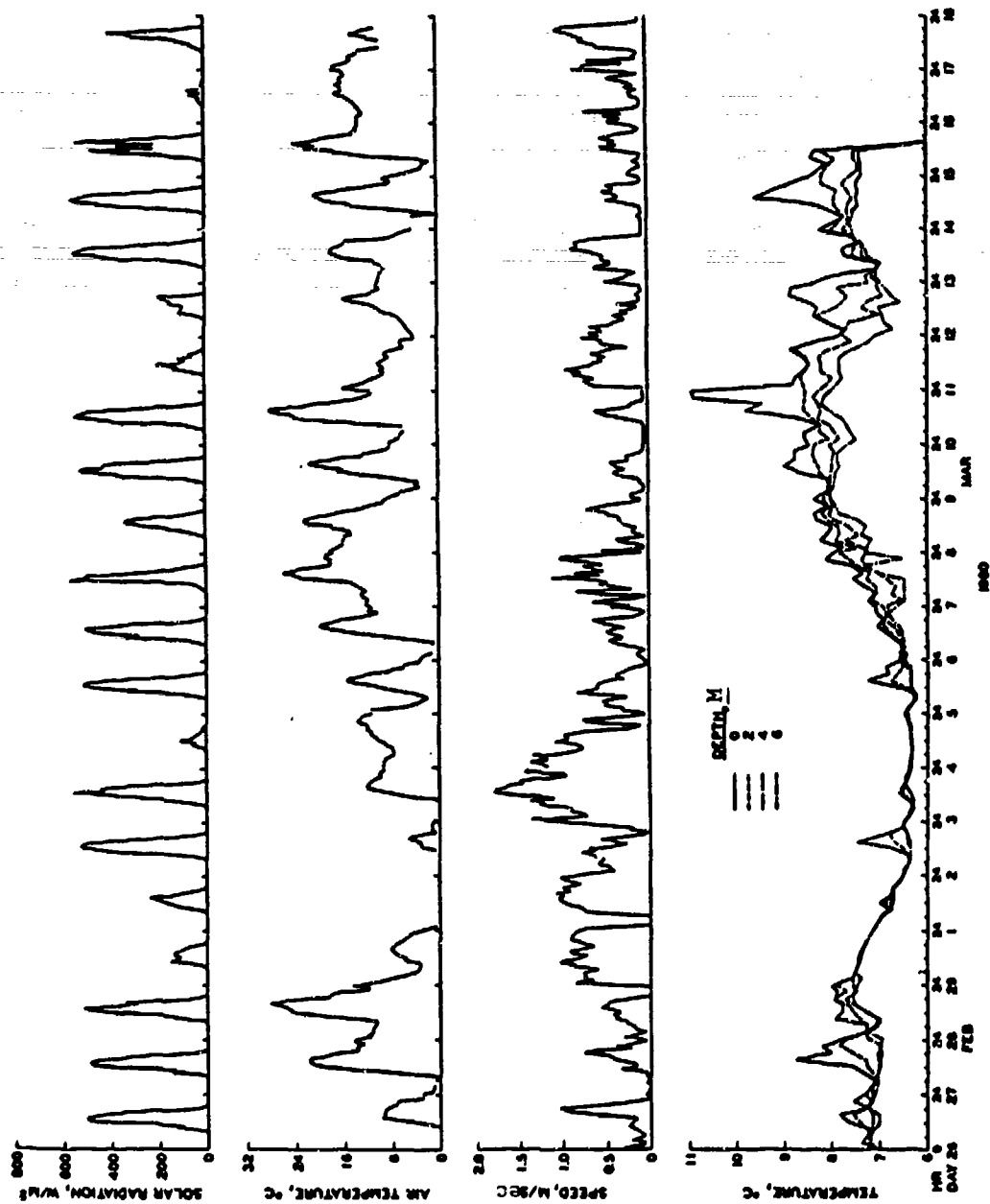
Figure 9. Example of synoptic variations in water temperature, DeGray Lake, Arkansas
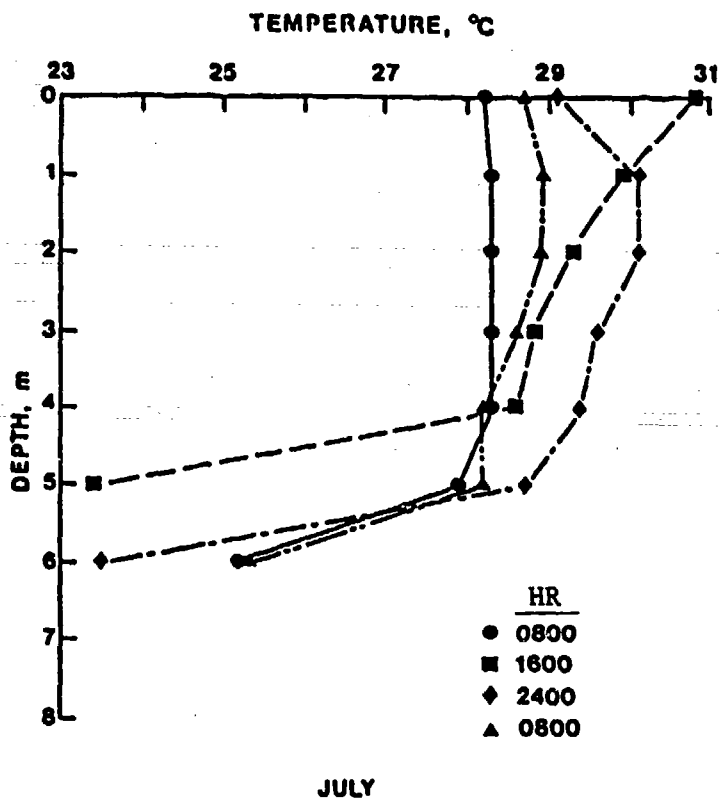
TEMPERATURE, °C

Figure 10. Example of a typical diel
temperature cycle, DeGray Lake, Arkansas
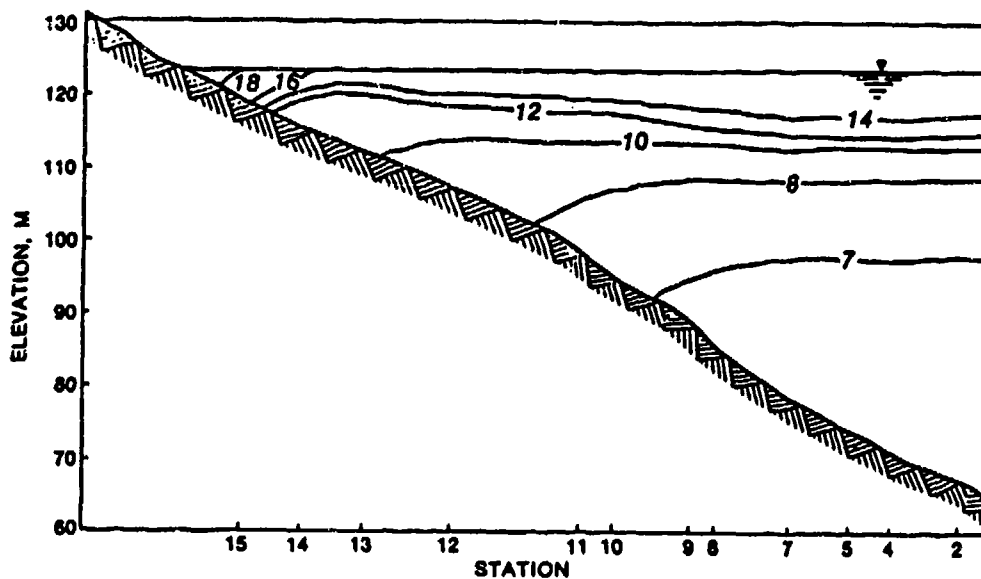
Figure 11. Horizontal variations in temperature resulting
from river inflow, DeGray Lake, Arkansas, 2 Apr 74

17

2.2.5 Data Interpretation and Generalizations

Temperature data interpretation. Much of our knowledge concerning mixing in reservoirs and lakes is based on the interpretation of vertical temperature profile data (i.e., stratification data). In addition to understanding the factors which affect stratification and its temporal and spatial variations (Sections 2.2.2-2.2.4), the correct interpretation of stratification data also requires detailed knowledge of the field sampling (e.g., station location, sampling time, etc.), hydrometeorological conditions (e.g., inflows, wind speed and direction), project operation (e.g., release rates and outlet locations), and reservoir mixing processes. There should be a logical, physically based explanation for all observations (Ford 1978).

For example, most field data are collected during daylight hours and may represent maximum daily water temperature and minimum mixed layer depths (see Figure 10). If there is wind, warm surface water may be pushed to one side of the reservoir (Figure 12) and/or the thermocline may tilt, changing the depth of the upper mixed layer.

When interpreting stratification data, it is usually beneficial to draw isotherms relative to the water surface (e.g., Figure 13). For reservoirs, it is essential that the variation in water surface elevation be considered since there is the potential for large variations in water levels and since the slope of the isotherms indicates the degree of mixing. The relatively flat isotherms in the lower metalimnion (i.e., 16° and 18° C) during midsummer indicate little mixing in this region while the steep slope of the 22° and 24° C isotherms in the upper metalimnion during the same period possibly indicates more intensive mixing. If the variation in the water surface elevation is not taken into consideration, the slope of the isotherms may be misrepresented. Short-term variations in the isotherms (i.e., order of days) indicate seiching and/or internal waves (Section 3.2.2) and should be averaged when comparing isotherm slopes. This should not be a problem if the time interval between sampling dates is greater than 2 weeks.

Once the isotherms are constructed, the importance of inflows, outflows, and light penetration can be determined by comparing periods

18
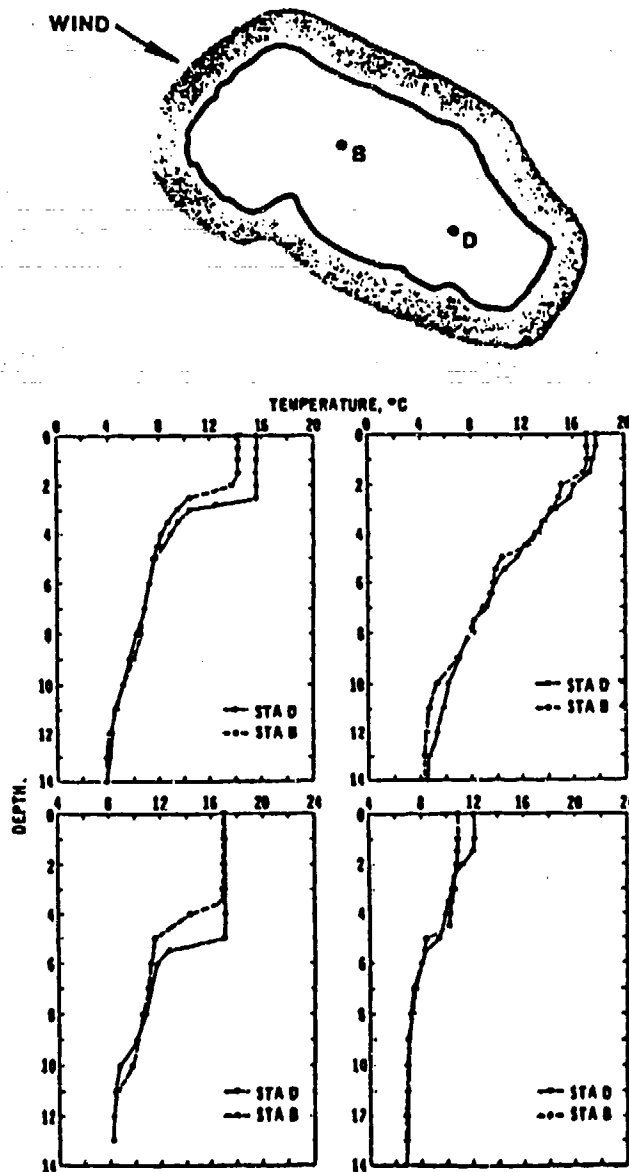
Figure 12. Effect of wind on temperature
profiles, McCarrons Lake, Mi nesota, 1974

and regions of mixing with the inflow quantity and placement (based on
density or temperature) (Figure 14a), the outflow quantity and depth
(Figure 14b), and the seasonal variation in twice the Secchi disc depth
(i.e., ca. 1 percent light level) (Figure 14c). For example, the inten-
sive mixing that occurred during April and May, as evidenced by the

19
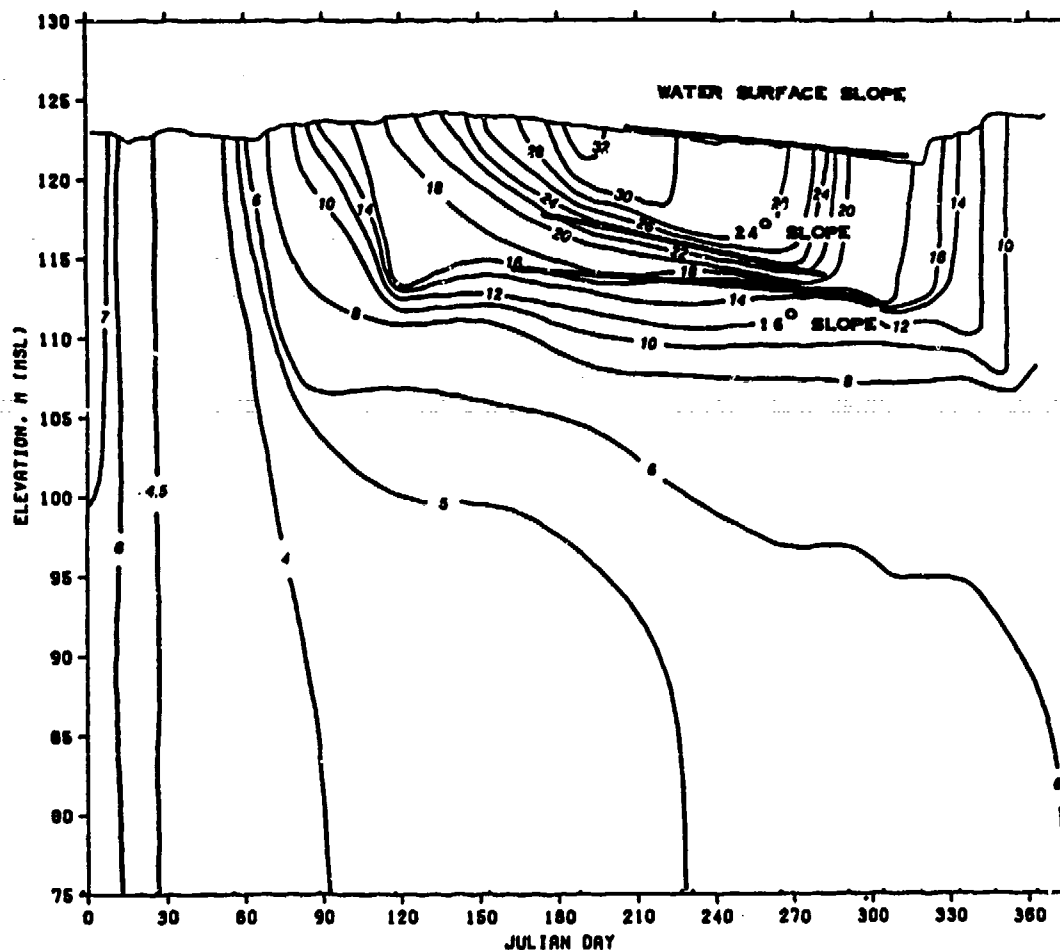
Figure 13. Construction of isotherms relative to
water surface level, DeGray Lake, Arkansas, 1978

steep slope of the 10° to 18° C isotherms, is probably the result of the
large outflows and change in withdrawal depth (Figure 14b) since light
(thermal energy) did not penetrate to these depths (Figure 14c). In
contrast, in Figure 15 the steep gradient of the 14° to 16° C isotherms
during early June is the result of internal absorption of solar radia-
tion since the light penetration increased significantly during this
period and winds and flows were low.

One aspect of data interpretation that is commonly overlooked is
the error associated with field measurements. Because of the intrinsic
variability of temperature in reservoirs and calibration error associ-
ated with field equipment, historical temperature data should be

20
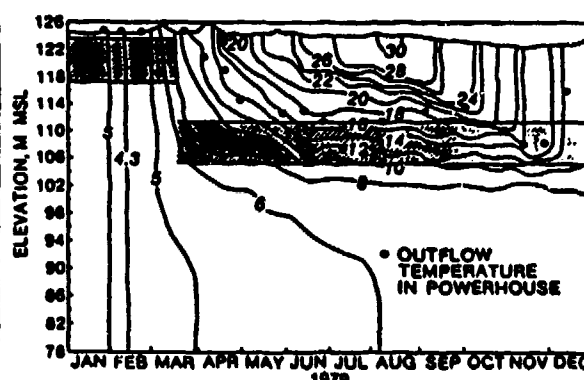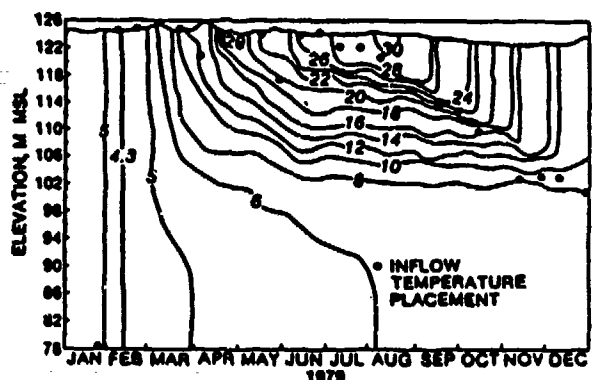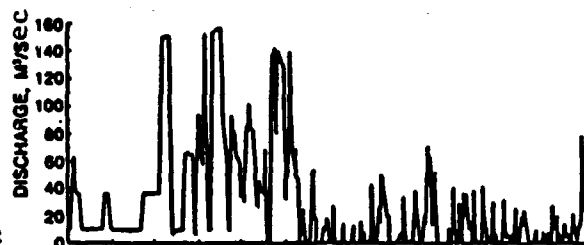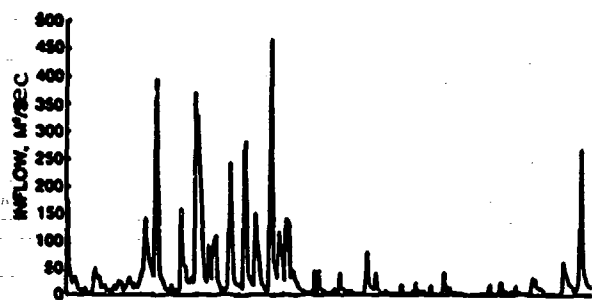
a. Inflow quantity and placement

b. Outflow quantity and withdrawal zone
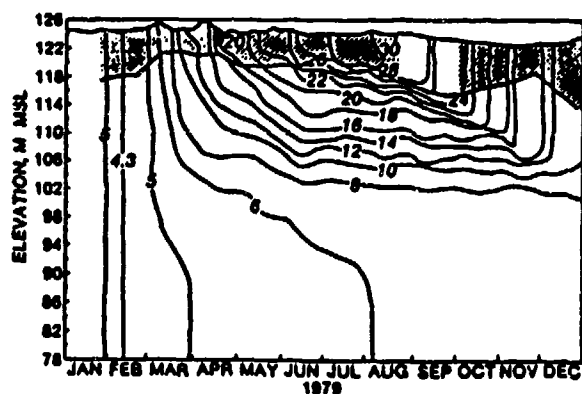
c. Photic zone

Figure 14. DeGray Lake, Arkansas, 1979
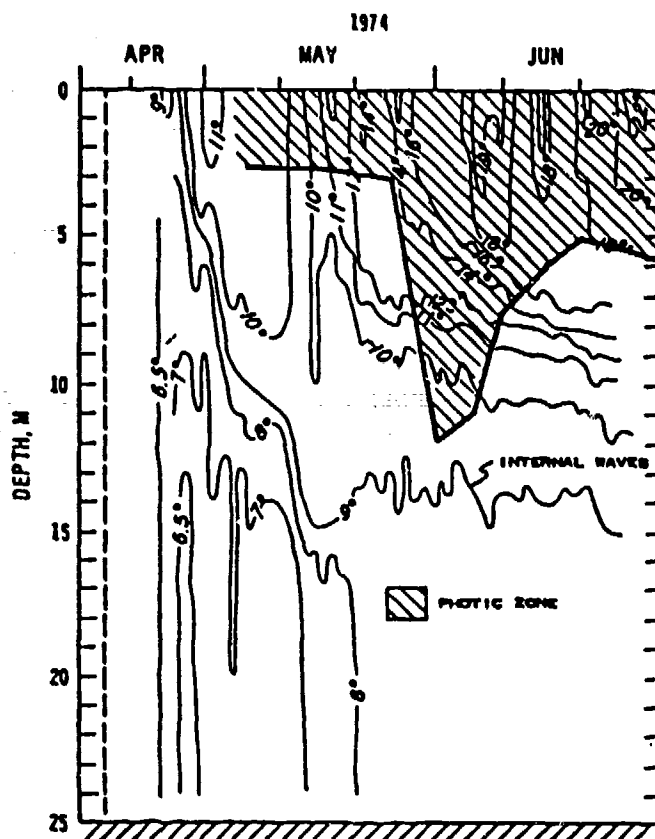
Figure 15. Comparison of isotherms
and photic zone, Lake Calhoun,
Minnesota, 1974

considered no better than ±1° C. For example, pockets of cold water in
the hypolimnion of a lake (Figure 16) are sometimes attributed to an
influx of cold ground water rather than a data error. Such a situation
is highly unlikely since ground-water movement is slow. If it should
occur, it would be apparent in the daily water budget (i.e., change in
pool level or outflow rate) as well as in the temperature profile.

Generalizations concerning stratification. Several generaliza-
tions concerning stratification in CE reservoirs can be made based upon
a review of temperature data collected at reservoirs throughout the
United States. First and foremost, all reservoirs stratify, albeit some
for only a few hours and a few degrees Celsius. Second, if the mean
annual theoretical hydraulic residence time (i.e., volume/mean annual
flow for period of record) is greater than 6 months, the stratification

22
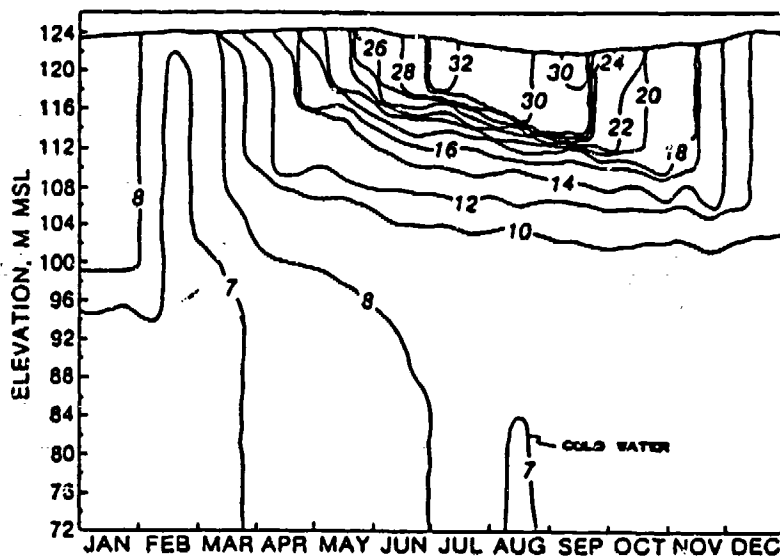
Figure 16. Isotherms for DeGray Lake,
Arkansas, 1980

is dominated by meteorological forcing. Stratification in this type of
lake is characterized by several features:

a. Since the major factors responsible for stratification (e.g.,
wind and solar radiation) act at the air/water interface,
horizontal variations are minimized.

b. There is not much variability in stratification from year to
year. Stratification forms and fall overturn occurs at
approximately the same time each year. Hypolimnetic
temperatures and thermocline depths are similar from year to
year (e.g., Table 1).

c. The larger the surface area, the more wind (kinetic) energy
input, the longer the periods of turnover, the deeper the
upper mixed layer.

d. The deeper the lake, the less wind (kinetic) energy per unit
volume available for mixing, and the stronger the stratifi-
cation.

e. Lakes in similar geographic areas will be exposed to similar
hydrometeorological conditions and exhibit similar stratifi-
cation patterns. For example, Lakes DeGray, Greeson, and
Ouachita are located within 55 km of each other in the
Ouachita Mountains of southwestern Arkansas, are deep (i.e.,
>30 m), have residence times greater than 12 months, and
therefore exhibit similar stratification profiles
(Figure 17).

Third, if the mean annual theoretical hydraulic residence time is
small (less than 20 days), the system is advectively (inflows and

23

Table 1

Variation in August Stratification Characteristics

DeGray Lake, Arkansas

Year	Withdrawal Location	Hypolimnetic Temperature, °C	Thermocline Depth, m
1974	Surface	7.0	8
1975	Surface	8.0	8
1976	Surface	7.0	7
1977	Surface	6.0	7
1978	Surface	6.0	7
1979	Lower	6.5	8
1980	Lower	7.5	8
1981	Lower	6.8	10
1982	Lower	6.2	8
1983	Surface	7.0	8

outflows) dominated, is weakly and intermittently stratified, and will exhibit characteristics similar to the inflows. During storms, the residence times of these projects may be only a few hours, indicating that detailed knowledge of the storm runoff may be required to explain and predict the density (thermal) structure of these projects. Fourth, if the mean annual theoretical hydraulic residence time is greater than 20 days but less than 6 months, the stratification will be controlled both by meteorological forcing and advection. In these projects, it is possible for the stratification pattern to vary significantly from year to year.

Specific guidance concerning criteria to evaluate the stratification potential of a reservoir is given in Appendix A.

2.3 Potential Energy

Closely related to density (thermal) stratification is the concept

24

Figure 17. Comparison of temperature profiles from Lakes DeGray, Greeson, and Quachita, Arkansas, 1982
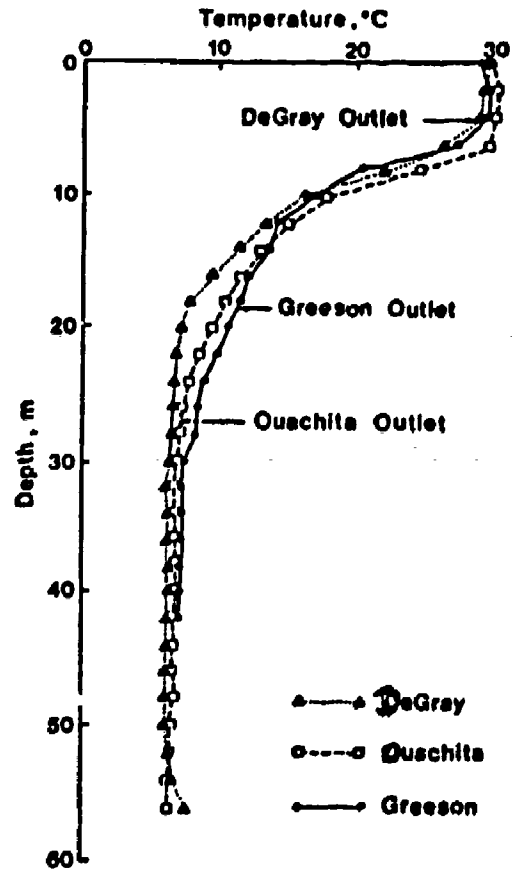
of potential energy (PE*). Potential energy is a form of stored energy that a system possesses because of its configuration. The PE associated with density stratification is dependent on gravity and conservative force, and can be fully recovered and converted into kinetic energy. The PE of a reservoir is defined as:

$$
(1) \qquad PE = mgH = \int_{0}^{Z_m} g\, z\, A(z)\, \rho(z,t)\, dz
$$

where

m = the total mass of the reservoir, kg

g = the acceleration due to gravity, m/sec^2

H = height of the center of mass of the reservoir, m

Z_m = the maximum elevation, m

* For convenience, symbols and abbreviations are listed in the Notation (Appendix B).

z   = the elevation above the reservoir bottom, m

$A(z)$ = the horizontal area of the reservoir at elevation z, m^2

$\rho(z,t)$ = the reservoir density at elevation z and time t, kg/m^3

The PE of a reservoir can therefore be changed by heating or cooling to modify the water density and/or by changing the elevation of the center of mass. For a well-mixed body of water, the center of mass is the center of volume. For a stratified body of water, the surface waters are less dense and the center of mass is deeper. The potential energy concept is similar to Birge's wind work and Schmidt's stability (Hutchinson 1957). For example, Schmidt's stability is the change in PE (using Equation 1) between an initial stratified density profile and the resulting isothermal condition following complete mixing.

The significance of the potential energy concept is its relationship with work and kinetic energy (KE) as defined in classical physics. It indicates that work is required to mix a stably stratified fluid since the center of mass must be raised against the force of gravity. For example, completely mixing the two-layered fluid in Figure 18 changed the PE by $\Delta\rho VH/8$ and raised the center of mass to $H/2$.

The PE, as defined in Equation 1, has limitations when applied to reservoirs because the horizontal areas, $A(z)$, are much larger and dominate over the small differences in water density, $\rho(z,t)$. Additionally, the PE as defined by Equation 1 decreases as stratification increases. A more practical formulation that increases as stratification increases is the relative potential energy (RPE):

$$RPE = \int_0^{Z_m} g \; z \; A(z) \; \left[\rho_m - \rho(z,t) \right] \; dz \qquad (2)$$

where ρ_m = maximum density in water column.

If ρ_m is a constant, the magnitude of the change in PE between two

$$PE = \rho \frac{V}{2} \frac{3H}{4} + (\rho + \Delta\rho) \frac{V}{2} \frac{H}{4}$$

$$= \frac{\rho}{2} VH + \frac{\Delta\rho}{8} VH$$

$$PE = (\rho + \frac{\Delta\rho}{2}) V \frac{H}{2}$$

$$= \frac{\rho}{2} VH + \frac{\Delta\rho}{4} VH$$

$$\Delta PE = \frac{\Delta\rho VH}{8}$$
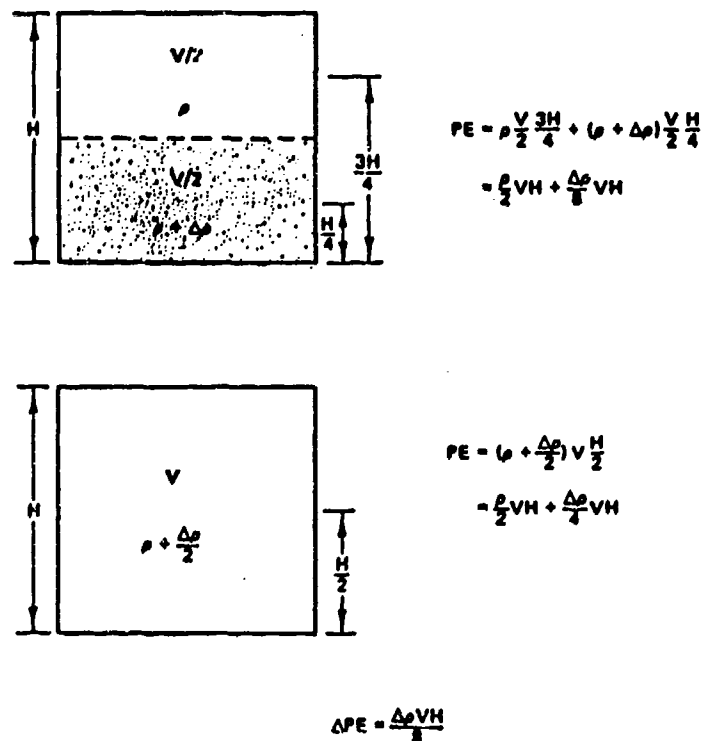
Figure 18. Change in potential energy
resulting from destratification of a
two-layered system

states computed from either Equation 1 or Equation 2 is the same (Ford 1976) but the signs are opposite.

The RPE's for DeGray and Ouachita Lakes, Arkansas, are shown in Figure 19. In February, the reservoirs are isothermal and the entire water column is mixed vertically. The center of mass is therefore located at the center of volume, and the RPE is small since the water density of the entire column is near ρ_m . The maximum RPE occurs in mid- to late-July and coincides with the time of maximum stratification. As the reservoirs cool, mixing occurs, and the RPE decreases.

Figure 19 also illustrates two features of Equation 2. First, the larger the lake, the larger the horizontal areas, $A(z)$, and the larger the RPE. In Figure 19, Lake Ouachita is significantly larger than DeGray Lake. Second, the weaker the stratification, the smaller the RPE. In 1976, DeGray Lake was operated with surface withdrawal and had

27
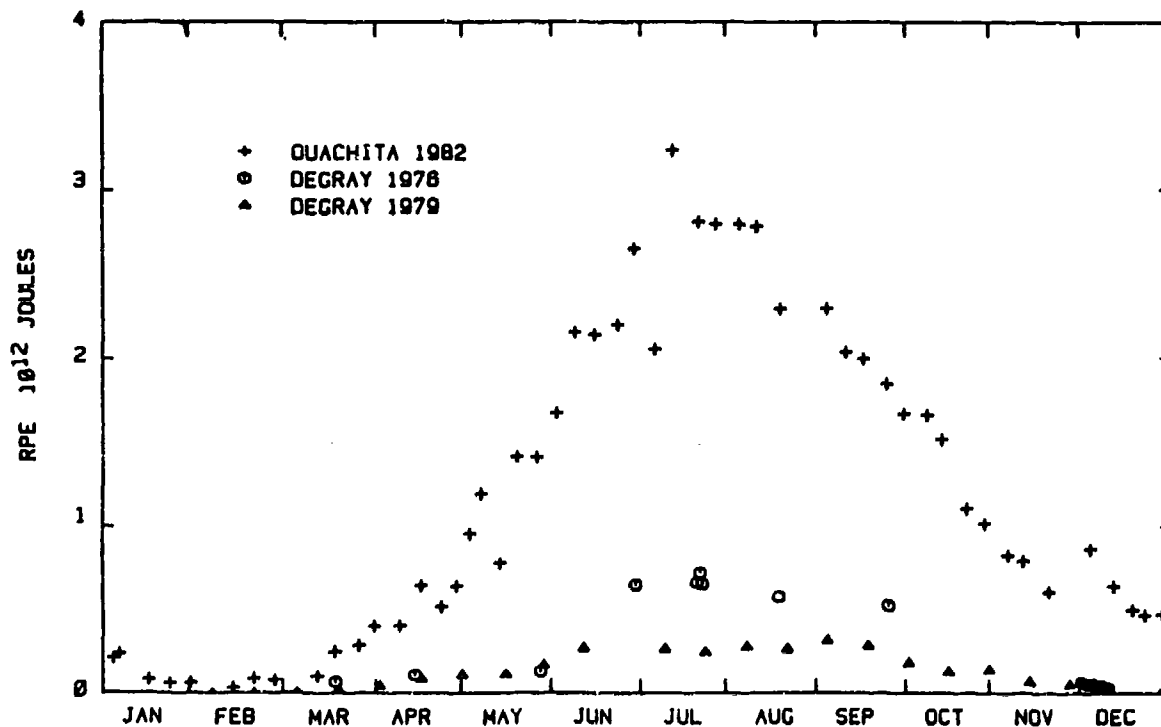
Figure 19. Seasonal variation in potential energy

a stronger stratification than in 1979 when it was operated with bottom withdrawal. The RPE was therefore greater for 1976 than for 1979.

To illustrate how the RPE can be used to explain the annual thermal stratification cycle, the RPE for DeGray Lake in 1979 is compared with the turbulent kinetic energy (TKE) input from the wind and inflows in Figure 20. Specifics concerning the computation of TKE from the wind and inflow rates are described in Sections 3.2.2 and 3.2.5, respectively.

In February, the reservoir was nearly isothermal. The RPE was small since water densities were nearly constant. With little or no stratification, the RPE was not large enough to prevent complete mixing by the TKE. As the water column warmed, stratification increased, RPE increased, and it became more difficult for the TKE to mix the entire water column. Stratification started to form in March at the bottom of the lake (Figure 6) because the density differences and the resulting RPE were small compared to the TKE input from the wind (Ford and Stefan 1980a). As the solar radiation increased, water temperatures increased

28
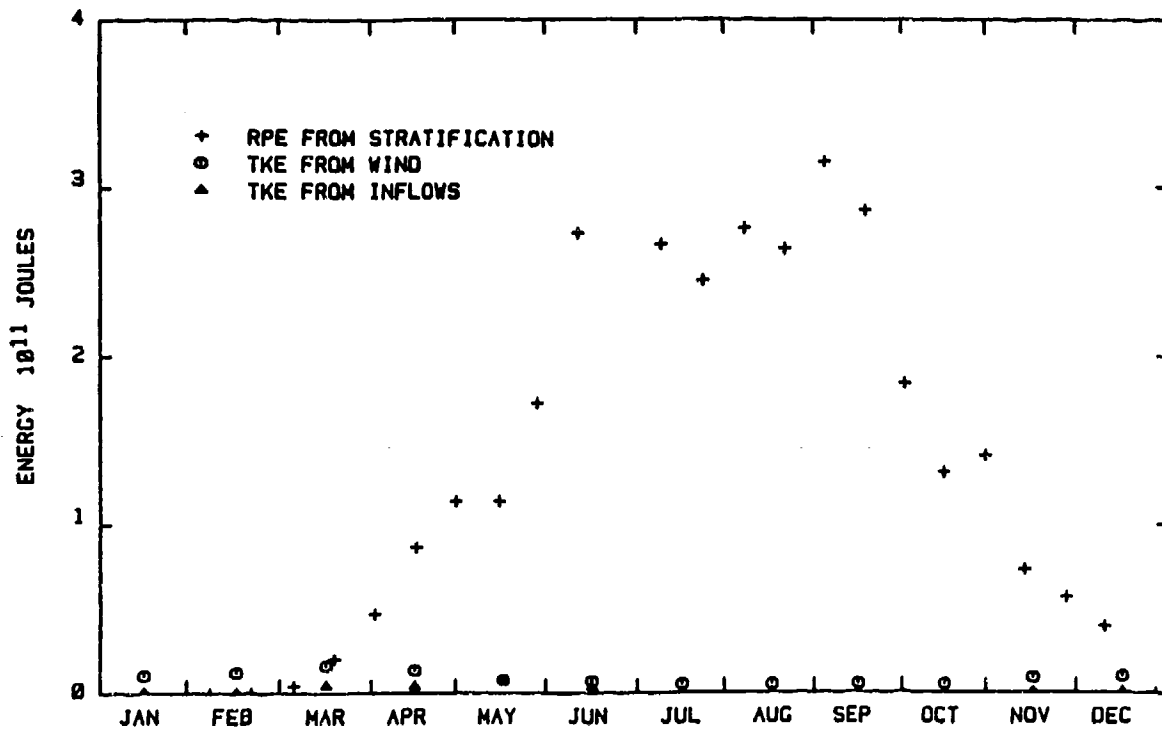
Figure 20. Comparison of RPE with the TKE from the
wind and inflows, DeGray Lake, Arkansas, 1979

and the density differences increased; the thermocline moved upward
because the TKE input could not overcome the ever-increasing RPF. (i.e.,
buoyancy forces). The maximum RPE occurred in mid- to late-July and
coincided with the time of maximum stratification. Once stratification
formed, the hypolimnion temperature remained relatively constant until
fall overturn. As the reservoir cooled, stratification decreased and
the RPE decreased, allowing the available TKE to deepen the thermocline
further, and eventually resulted in complete vertical mixing. When
comparing the RPE of stratification with the TKE input it is important
to note that the RPE varies significantly over the seasonal time scale
(i.e., the time scale of stratification) while the TKE is introduced at
much shorter time scales (i.e., passage of storms).

Figure 21 compares the TKE from the wind with the TKE from the
inflows. Except in May (the wettest month), the TKE from wind is
greater, indicating its dominance over advection (inflows) as a source
of energy and as a mechanism for mixing.

ENERGY 10^{10} JOULES

2.0

1.5

1.0

.5

0

+ TKE FROM WIND
⊙ TKE FROM INFLOWS

JAN FEB MAR APR MAY JUN JUL AUG SEP OCT NOV DEC
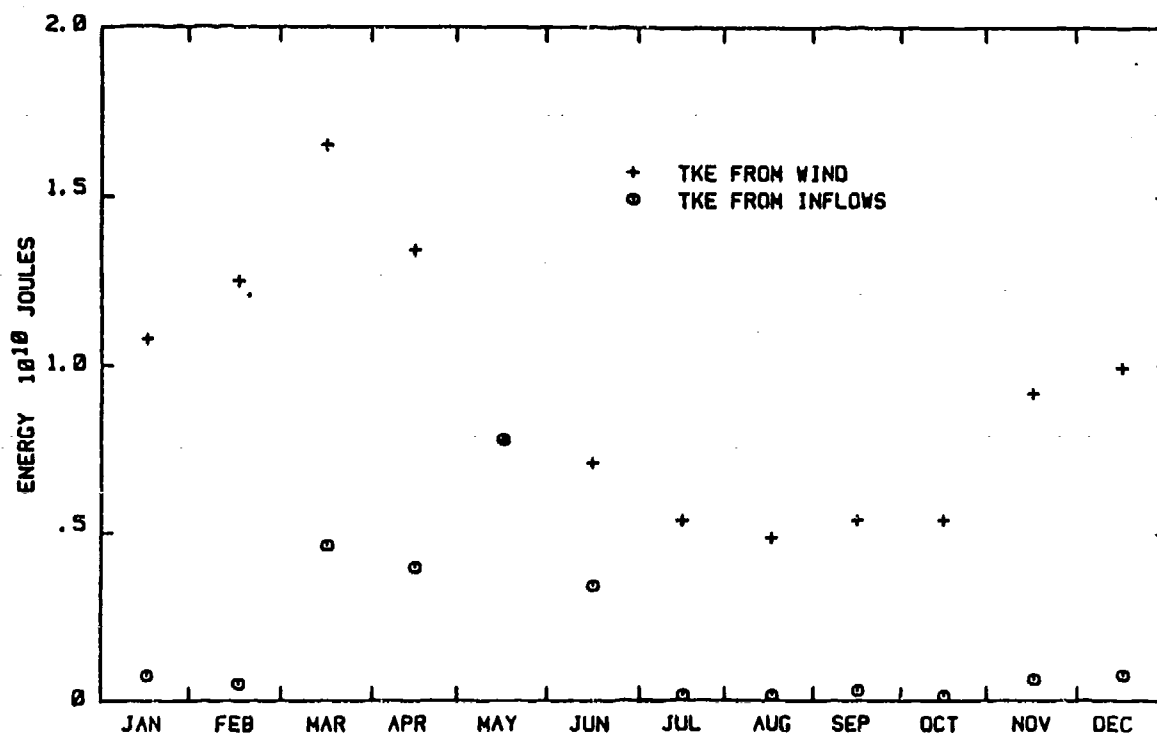
Figure 21. Comparison of TKE from the wind and inflows,
DeGray Lake, Arkansas, 1979

2.4 General Transport Processes

There are several fundamental transport or mixing processes which cause a parcel of fluid to blend with other parcels and which occur in any fluid system, including reservoirs. These are advection, shear, molecular diffusion, turbulence and turbulent diffusion, entrainment, convection, and dispersion. Each of these processes will be defined to form a common base for the remainder of the report. The nomenclature of Fischer et al. (1979) will be followed.

2.4.1 Advection

Advection is transport by the mean motion of the fluid (Figure 22a). If the fluid is moving with velocity U , which has components of U_x , U_y , and U_z in the x, y, z directions, respectively, then the advective transport in the direction of the velocity vector U is UC where C is the concentration of the

30
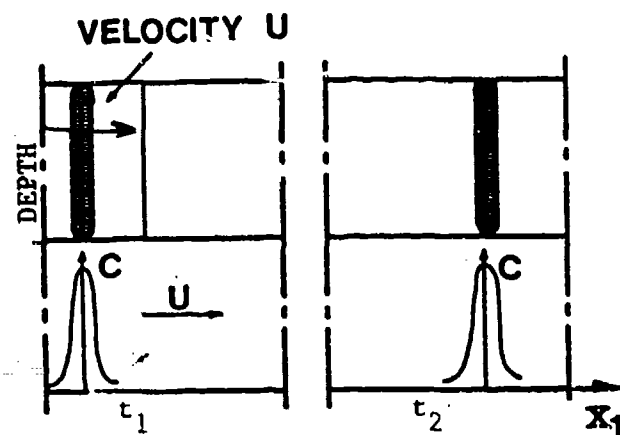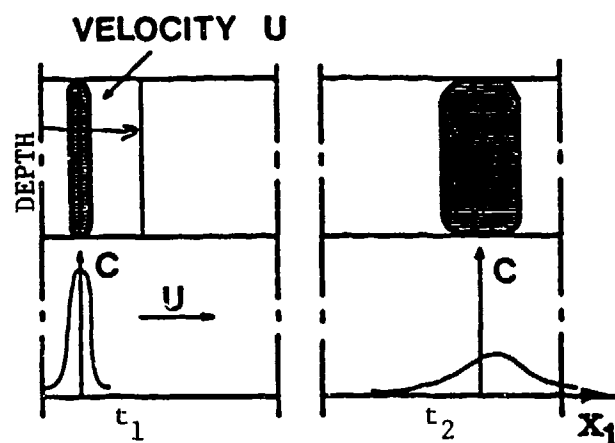
a. Advection

b. Diffusion
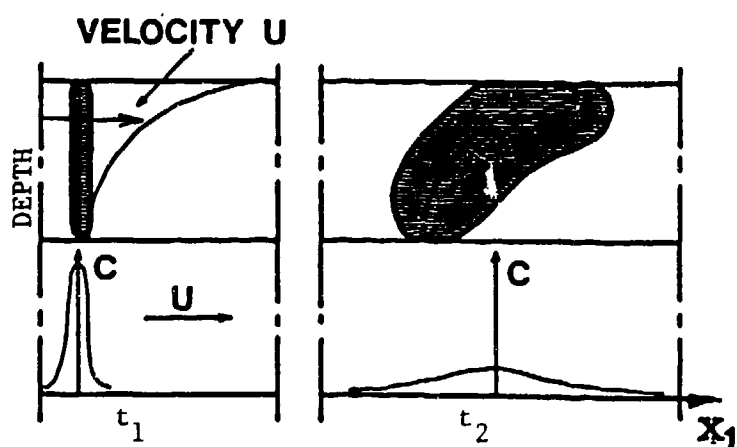
c. Shear and dispersion

Figure 22. Comparison of advection, diffusion, and dispersion

31

solute. The advective transport in the x, y, and z directions is, therefore, U_xC , U_yC , and U_zC , respectively. Since the units of U are L/t (length/time) and the units of C are M/L^3 (mass/length^3), the units of UC are $M/L^2/t$, which represents the rate of mass transport through the unit area L^2 . For transport by advection only, there will be no change in the concentration C provided no other transport mechanisms act on the parcel of fluid.

To be transported by advection, a parcel of fluid must be acted upon by a force. For rivers, this force is gravity. In reservoirs, advection may be caused by inflows, outflows, and wind shear at the air/water interface.

2.4.2 Shear

Shear is advection at different speeds at different locations (i.e., flows with velocity gradients are shear flows) (Figure 22c). Friction or shear forces at boundaries cause velocities to be less near the boundaries than in the center of the flow field. Shear flows vary from simple logarithmic profiles typically found in open-channel flow to complex flow patterns in lakes where velocity vectors vary temporally and spatially both in magnitude and direction. In shear flows, mixing or spreading in the direction of flow is caused primarily by velocity gradients. Since the variability in the velocity profile is proportional to the shear velocity w_* ($w_* \sqrt{\tau/\rho}$, where τ = shear stress and ρ = density) and independent of the mean velocity U , the longitudinal mixing in a shear flow depends on the shear velocity not the mean flow velocity (Fischer et al. 1979).

2.4.3 Molecular Diffusion

Molecular diffusion is a process by which a certain property of a fluid is transferred down a concentration gradient by the random motion of molecules without any overall transport of the fluid taking place. It is important to understand molecular diffusion because molecular diffusion theory is the basis for the turbulent diffusion theory discussed in Section 2.4.4.

The flux or transport of mass or heat per unit cross-sectional area per unit time in a given direction by molecular diffusion is:

$$q_m = -K_m \frac{\partial C}{\partial x} \qquad (3)$$

where

K_m = molecular diffusivity or diffusion coefficient, m^2/sec

$\frac{\partial C}{\partial x}$ = concentration gradient, mg/ℓ/m

The minus sign is required because the transport is from high to low concentrations. The molecular diffusivity is a function both of the solute and the solvent in which it is dissolved (Table 2).

Table 2

Molecular Diffusion Coefficient of Solutes in Water at 20° C

Substance	Diffusion Coefficient, m^2/sec
Temperature	1.42×10^{-7}
Dissolved oxygen	1.80×10^{-9}
Carbon dioxide	1.77×10^{-9}
Nitrogen	1.64×10^{-9}
Sodium chloride	1.35×10^{-9}

SOURCE: "CRC Handbook of Tables for Applied Engineering Science" (Bolz and Tuve 1976).

The diffusion equation:

$$\frac{\partial C}{\partial t} = K_m \frac{\partial^2 C}{\partial x^2} \qquad (4)$$

describes how mass is transferred by molecular or Fickian diffusion. The solution of this equation for an initial slug of mass M released at a point results in a Gaussian distribution of concentration versus

distance at a fixed time. Two properties of this solution are impor-
tant. First, differences in mean concentrations are always reduced.
Second, the variance always grows linearly with time (Figure 22b).

2.4.4 Turbulence and Turbulent Diffusion

Turbulence is the most important source for mixing in lakes
(Ottesen Hansen 1978). It is therefore imperative that turbulence be
understood before mixing in lakes (or reservoirs) can be understood.

Most flows occurring in nature (e.g., atmospheric and surface
water flows) are turbulent. Two notable characteristics of these flows
are: (a) velocities and concentrations at a point in a turbulent flow
are unsteady, and (b) mixing is much faster in turbulent flow than in
laminar flow.

Turbulence is sometimes described as a family of eddies (i.e.,
rotating regions of fluid). These eddies or scales of turbulence can
range in size from the physical limits of the flow (i.e., physical
dimensions of a reservoir) down to molecular motion. At the smallest
scales of turbulence, viscosity is important and the motion dissipates
into heat. One disadvantage of portraying turbulence as a family of
eddies is that it is difficult to separate wave motions from turbulence.
According to Steward (1959), a more precise definition of turbulence is:

> A fluid is said to be turbulent if each component of the
> vorticity is distributed irregularly and aperiodically in
> time and space, if the flow is characterized by a transfer
> of energy from larger to smaller scales of motion, and if
> the mean separation of neighboring fluid particles tends to
> increase with time.

Turbulent flows are therefore irregular (random), diffusive (pro-
duce mixing), rotational (three-dimensional vorticity fluctuations),
time varying, and dissipative (decay rapidly without a continual source
of energy). Turbulent flows are characterized by large Reynolds numbers
(order of 10^6 in lakes) where energy propagates slowly with the speed of
the fluid motion. In contrast, waves can distort a density distribution

34

but cannot permanently change the stratification profile unless the waves break to produce mixing; waves are dispersive but not dissipative, and energy is transferred rapidly through the fluid (Turner 1973).

The energy associated with turbulence or TKE is defined as

$$TKE = \overline{(u_x^2 + u_y^2 + u_z^2)}/2 \qquad (5)$$

where u_x, u_y, u_z = turbulent fluctuations in the x, y, and z velocity components, m/sec.

The fluctuating velocity components are related to the instantaneous and mean velocity components by

$$U_x = \bar{U}_x + u_x \qquad (6a)$$

$$U_y = \bar{U}_y + u_y \qquad (6b)$$

$$U_z = \bar{U}_z + u_z \qquad (6c)$$

where

U_x, U_y, U_z = instantaneous velocity components, m/sec

$\bar{U}_x$, $\bar{U}_y$, $\bar{U}_z$ = mean velocity components, m/sec

Tennekes and Lumley (1972) develop and discuss this concept in detail.

In lakes, turbulence can be generated directly at a boundary (external process) or internally through a shear instability. The only way a fluid element outside a turbulent region can become turbulent (i.e., acquire vorticity) is through viscous diffusion of vorticity. Once a fluid element is turbulent (i.e., possesses vorticity), its turbulence or vorticity can be amplified by the straining set up by neighboring turbulence. Because of this straining, the vorticity and energy of smaller eddies can increase at the expense of the energy of larger eddies. Energy, therefore, flows from large to small eddies. Without a continual source of energy at the larger scales, turbulence could not be maintained and would rapidly decay. Generally, the larger

35

eddies move slowly and last longer than the smaller eddies. The larger
eddies are also responsible for most of the transport of momentum and
mass. At the very small scales, viscosity smooths the velocity fluctua-
tions by dissipating small-scale motion into heat.

Density stratification inhibits turbulence and mixing. The reason
for the decreased mixing in a zone of stable density stratification is
that turbulent eddies lose energy not only through viscous dissipation,
as previously described, but also through the performance of work
against gravity in the density gradient (Section 2.3). The Richardson
number

$$Ri = \frac{g \frac{d\rho}{dz}}{\rho \left(\frac{dU}{dz}\right)^2} \tag{7}$$

compares the energy required to do work against the density gradient
($d\rho/dz$) with the energy supply of the shearing form (dU/dz).

The scattering of particles by turbulent motion can be considered
analogous to molecular diffusion with a larger turbulent diffusion coef-
ficient replacing the molecular diffusion coefficient. The turbulence
flux q_t in the x direction if therefore given by

$$q_t = -K_t \frac{\partial C}{\partial x} \tag{8}$$

where K_t = turbulent diffusion coefficient, m^2/sec.

The turbulent diffusion coefficient is equivalent to the product of the
Lagrangian length scale l_L and the intensity of turbulence $<u^2>^{1/2}$

$$K_t = l_L <u^2>^{1/2} \tag{9}$$

where

$$\langle\ \rangle = \text{ensemble mean (i.e., mean over many trials)}$$

$$\langle u^2 \rangle^{1/2} = \text{root mean square velocity, m/sec}$$

The Lagrangian length scale is that distance a particle must travel before it forgets its initial velocity. This turbulent diffusion approach is not valid for lengths smaller than l_L or times less than the Lagrangian time scale (i.e., the time required for a particle to move l_L). Individual clouds of dimension less than l_L grow at a rate that increases with size (i.e., Richardson diffusion) and varies from cloud to cloud. There is an intermediate range where clouds grow in proportion to the 4/3 law (i.e., proportional to $l_L^{4/3}$), but this requires homogeneous turbulence and no boundary effects.

2.4.5 Entrainment

When a nonturbulent body of water is stirred at a boundary, the turbulence generated at that boundary will advance into the nonturbulent regions of the fluid. Entrainment is the term used to describe this one-way advective type transport which is characteristic of most free turbulent shear flows. If the fluid is homogeneous, entrainment will proceed unhindered, and the thickness of the layer being stirred will increase linearly with time until another boundary is reached or another force becomes limiting (e.g., Coriolis effect).

Visual observations in laboratory experiments (Turner 1973) showed the interface between the turbulent and nonturbulent regions to be sharp but convoluted. In the stratified fluids where the densities of the stirred layer and nonturbulent regions differ, turbulence and convolutions at the interface are generally suppressed by buoyancy forces. Under these conditions, entrainment is the result of wisps or thin sheets of fluid being scoured into the turbulent region by turbulent eddies.

The rate at which the mean position of the interface advances into the nonturbulent fluid is usually expressed in terms of an entrainment velocity w_e. The entrainment velocity is usually assumed to be a

37

function of the overall Richardson number

$$Ri_* = \frac{g \; \Delta\rho \; h}{\rho \; w_*^2} \qquad (10)$$

where

g = acceleration due to gravity, m/sec^2

$\Delta\rho$ = density difference between turbulent layer (i.e.,
layer being stirred) and nonturbulent layer (i.e.,
layer being entrained), kg/m^3

h = depth of turbulent layer, m

ρ = density, kg/m^3

w_* = shear velocity in turbulent layer, m/sec

such that

$$\frac{w_e}{w_*} = f(Ri_*) \qquad (11)$$

There is little reason to expect Equation 11 to be a simple func-
tion because of the complex and different physical processes involved in
entrainment. It is, however, appealing to assume

$$\frac{w_e}{w_*} = c \; Ri_*^{-1} \qquad (12)$$

where c = proportionality constant , because the rate of increase of
potential energy is then equal to the rate of mechanical energy input.
This law, however, falls apart as $Ri_* \to 0$ and as $Ri_* \to \infty$
(Phillips 1977).

2.4.6 Convection

In order to distinguish vertical transport induced by density
instabilities from advective transport generated by other forces or
sources of energy, convection is defined as a buoyancy-induced flow that
occurs in a fluid when it becomes unstable due to density (temperature)

differences. If the mixed-layer depth increases as he, t is removed but no changes occur in the thermal profiles below the mixed layer, the increase in thickness of the mixed layer is termed encroachment by Tennekes and Driedonks (1980) (Figure 23a). If instead, some of the TKE generated by cooling at the air/water interface is used to entrain stably stratified water into the mixed layer and thereby modify the thermal profiles below the mixed layer, the convective entrainment is termed penetrative convection (Figure 23b). Reviews of penetrative convection can be found in Turner (1973) and Denton (1978).

In order to explain the process of convection, Denton (1978) divided the water column into three zones (Figure 24). The thin layer at the water surface is the buoyancy production zone. This layer is a molecular diffusion boundary layer that builds up due to cooling at the air/water interface. At some critical point, the layer becomes unstable and breaks up. At the time of breakup, Denton (1978) observed the formation of long, irregular rolls that eventually broke into single clumps of fluid (thermals). Since these thermals are heavier than the ambient fluid, they sink into the mixed layer. After the breakup of the boundary layer, a new layer begins to form which, in turn, will eventually become unstable and break up. In general, the thickness of the production layer is negligible compared to the total thickness of the mixed layer.

The mixed layer, as implied by its name, is uniformly mixed with respect to all properties. Dye observations and continuous temperature measurements in the mixed layer indicate that the thermals generated in the production layer pass through the mixed layer as discrete elements (not plumes as sometimes described), the net effect being to keep the layer turbulent.

Below the mixed layer is the region of the stably stratified fluid. The density gradient is usually assumed to be discontinuous at the interface to be consistent with entrainment experiments that report a sharpening of the gradient. When the thermals encounter the interface, they penetrate a short distance and sometimes rebound (Linden 1973). Through various mechanisms that are not completely understood,

NATURAL CONVECTION

a. Encroachment

b. Penetrative
   convection
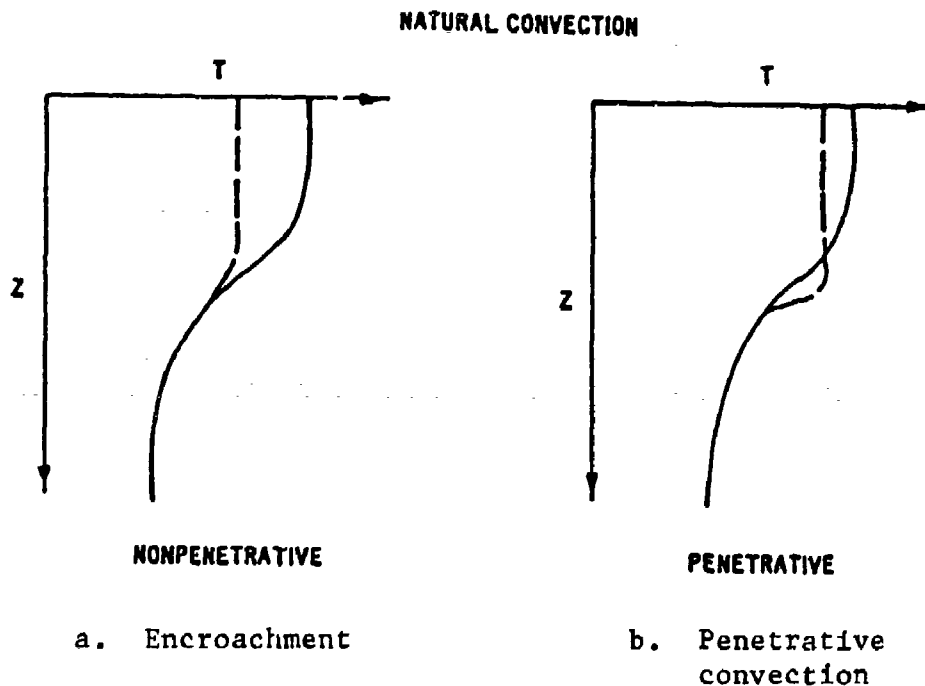
Figure 23. Comparison of encroachment and penetrative convection

some of the stratified fluid is entrained into the mixed layer.
According to Tennekes and Driedonks (1980), 10 to 50 percent of the
potential energy released during cooling is converted to TKE and used
for entrainment. Denton (1978) concluded this fraction is not constant
but attains a maximum at a Richardson number of 0.91 and decreases with
increasing and decreasing Richardson number. The mixing and entrainment
resulting from penetrative convection is restricted to the diffusive
layer (Figure 24), which has a thickness of approximately 0.2 times the
mixed layer depth.

2.4.7 Dispersion

Dispersion includes the combined effects of shear and diffusion.
Shear causes particles to move at different rates. Diffusion causes
particles to move across the velocity gradient. After a certain period
of time, a particle experiences all velocities and the longitudinal dis-
tribution appears Gaussian (Figure 25). The mixing can then be de-
scribed by

O
DENSITY ρ

BUOYANCY
PRODUCTION LAYER

TURBULENT MIXED
LAYER

d_m — TURBULENT INTERFACE

$\dfrac{\partial \rho}{\partial Z}\bigg]_i$

INTERFACIAL
DENSITY GRADIENT

DIFFUSION REGION

Z
DEPTH
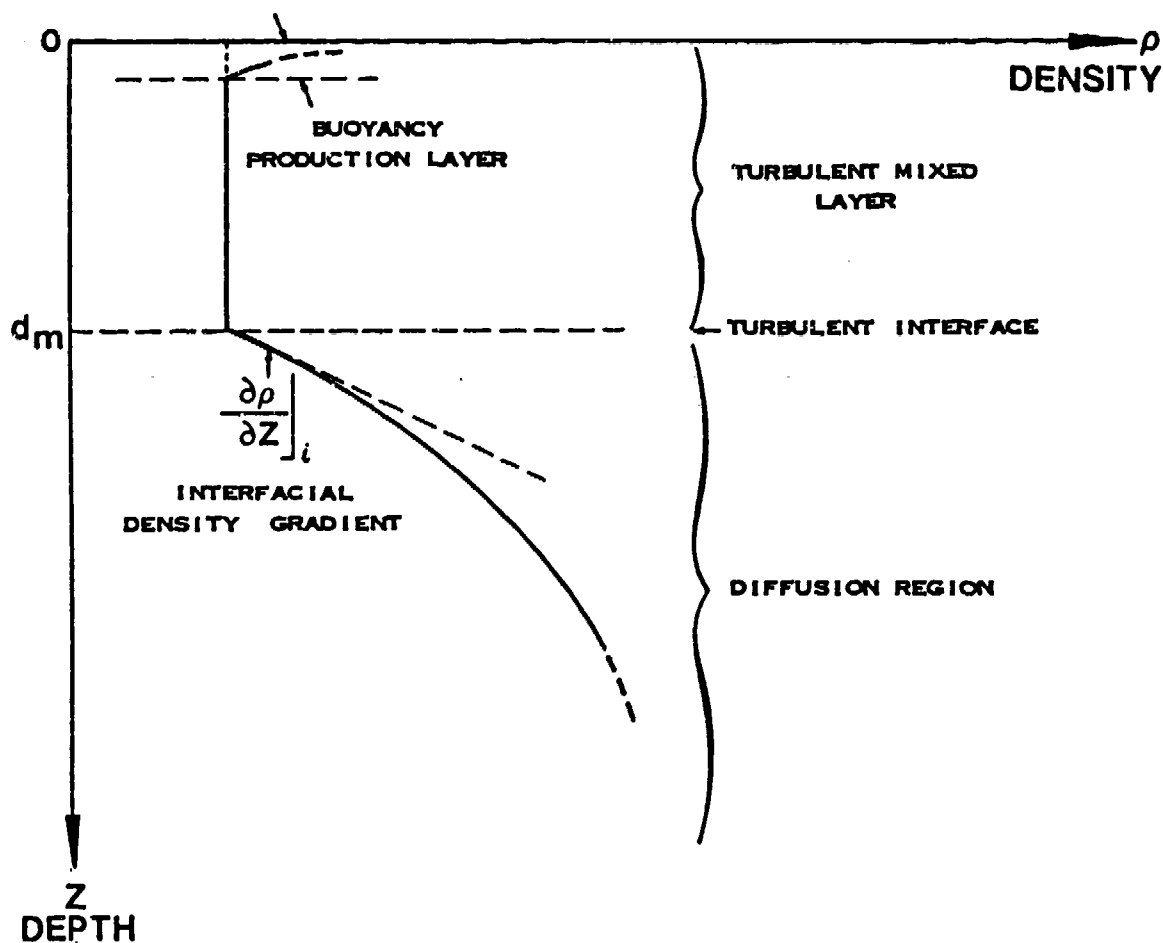
Figure 24. Schematic of convective zones

$$q_d = K_d \frac{\partial C}{\partial x} \tag{13}$$

where

K_d = dispersion coefficient, m^2/sec

q_d = flux due to dispersion, $kg/(m^2\text{-}sec)$

In riverine systems, the concentration is sometimes skewed (Figure 25) because of edge effects. Material is trapped along the banks and released at a later time, causing the longitudinal distribution to be skewed in an upstream direction. Fischer et al. (1979) discuss dispersion in detail.

41
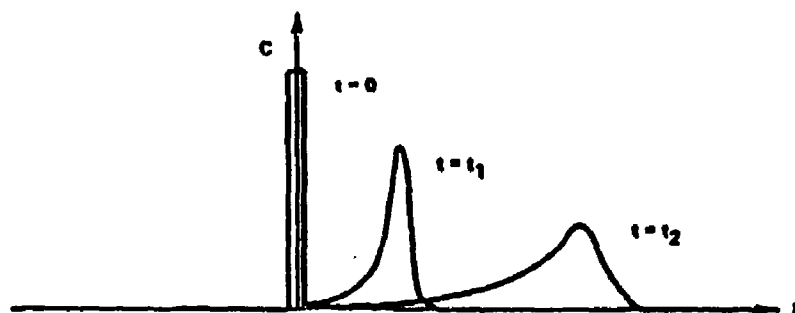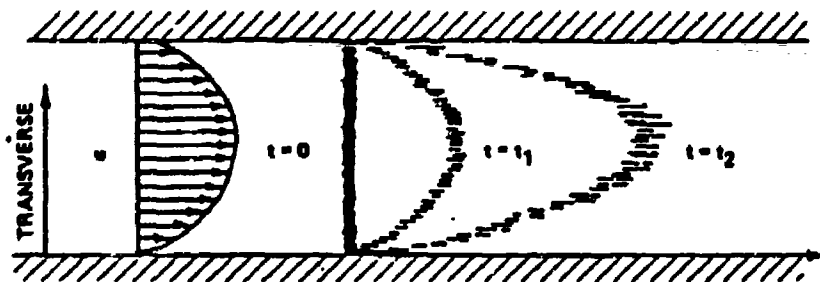
Figure 25. Longitudinal dispersion

SECTION 3. RESERVOIR MIXING AND WATER QUALITY

3.1 Introduction

It was shown in Section 2.3 that energy is required to mix a stably stratified fluid. The energy is used to perform work and raise the center of mass. The major sources of energy potentially available to mix a reservoir are atmospheric heating (cooling), wind, inflows, outflows, barometric pressure, and gravity. Although several reviews have been published on lake mixing and hydrodynamics, these reviews tend to emphasize specific types of lakes or specific mixing processes. In general, these reviews do not consider all aspects of mixing and reservoir operation and their impacts on reservoir water quality. For example, Boyce (1974), Mortimer (1974), and Csanady (1975) reviewed the hydrodynamics of large lakes; Smith (1979) reviewed the hydraulics of isothermal lakes; Ottesen Hansen (1978), Fischer et al. (1979), and Imberger and Hamblin (1982) reviewed mixing mechanisms; Ford and Johnson (1983) reviewed inflow dynamics; Roberts and Dortch (1985) reviewed entrainment of pumped-storage inflow jets; and Imberger (1980) reviewed outflow dynamics and selective withdrawal. In addition, oceanographic reviews on internal waves by Garrett and Munk (1979), mixed layer dynamics by Kraus (1977), and microstructure by Gregg and Briscoe (1979) are directly applicable to mixing in reservoirs.

In this section, reservoir mixing will be reviewed and discussed with respect to energy inputs and water quality impacts. The section concludes with a summary of mixing processes that must be considered when developing a mathematical algorithm to predict water quality changes.

3.2 Description of Reservoir Mixing Processes

3.2.1 Atmospheric Heating (Cooling)

The major surface heat exchange processes acting on a water body are summarized in Figure 26. The numbers in parentheses indicate the

43

H_s · SHORT WAVE SOLAR RADIATION (50 TO 400 W/m²)

H_a · LONG WAVE ATMOSPHERIC RADIATION (30 TO 450 W/m²)

H_{br} · BACK RADIATION (300 TO 500 W/m²)

H_e · EVAPORATIVE HEAT LOSS (100 TO 600 W/m²)

H_c · CONDUCTIVE HEAT LOSS (100 TO 600 W/m²)

H_{sr} · REFLECTED SOLAR RADIATION (5 TO 30 W/m²)

H_{ar} · REFLECTED ATMOSPHERIC RADIATION (10 TO 15 W/m²)
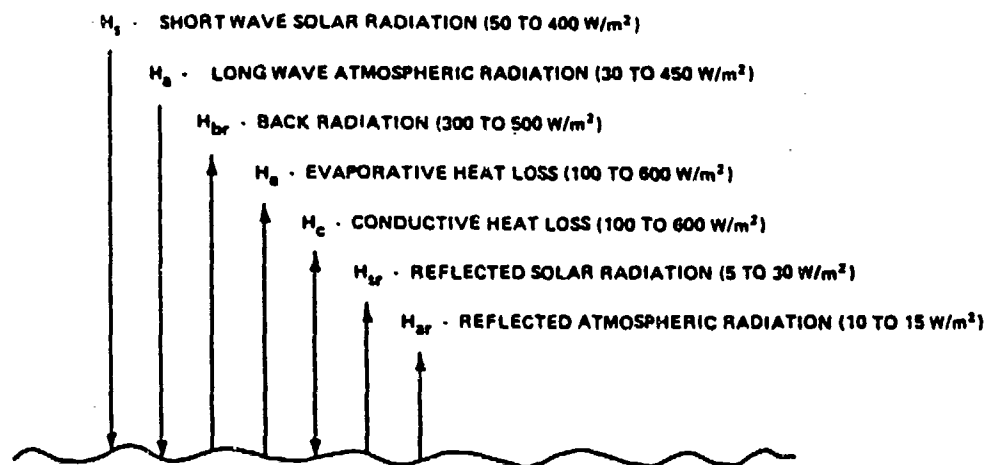
Figure 26. Major heat exchange processes
(after Edinger, Brady, and Geyer 1974)

relative magnitudes and ranges of mean daily values at midlatitude. A
complete description of these processes and their measurement and/or
computation can be found in Tennessee Valley Authority (TVA) (1972);
Edinger, Brady, and Geyer (1974); and other references. The relative
magnitude of these processes depends primarily on the time of day and
year, location on the earth's surface (i.e., latitude, longitude, and
elevation), surrounding terrain and horizon angle, amount of water in
the atmosphere, and meteorological conditions such as air temperature,
cloud cover, wind speed and direction, and dew point temperature.

Atmospheric heating and cooling impact the mixing regime in reser-
voirs by: (a) adding and removing heat, thereby changing the water
density and RPE, and (b) producing TKE during periods of heat loss and
convective mixing. The seasonal variation in atmospheric heating for
central Arkansas is shown in Figure 27. It indicates that periods of
cooling and convective mixing typically occur during late summer, fall,
and winter when heat losses exceed heat gains. Convective mixing can
also occur during the other periods because of diurnal heating and cool-
ing (Figure 28). Hirshburg, Goodling, and Maples (1976) analyzed this
mixing process and developed a seasonal temperature model based on this
concept. They showed that convective mixing due to diurnal cooling is
an important mixing mechanism, but a short time increment (~1 hr) m
be used to model convective mixing.
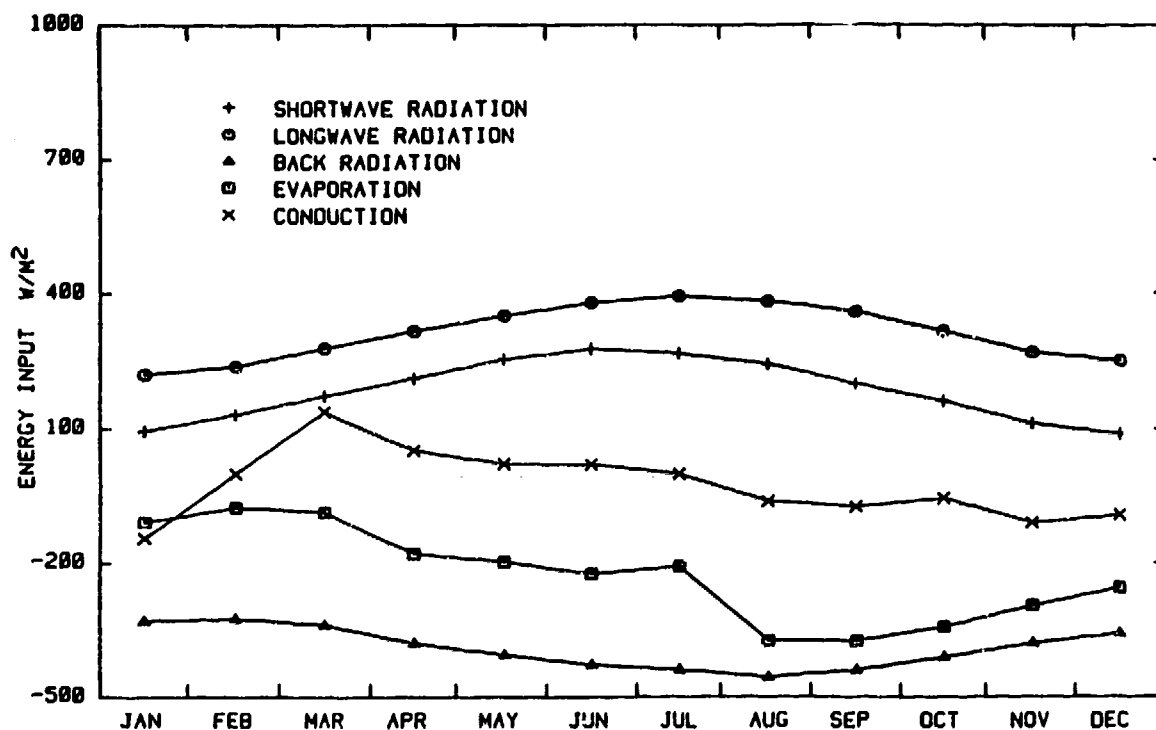
Figure 27. Seasonal variation in atmospheric
heating, central Arkansas

3.2.2 Wind Processes

The wind is the major source of energy for many physical phenomena
which either directly or indirectly cause mixing. These phenomena
include surface waves, circulation currents, seiches, internal waves,
turbulence, and Langmuir circulation.

Wind shear. When the wind blows across a water surface, it
creates a shear stress that transmits energy to the water body
(Figure 29). Part of this energy is used for surface waves, part for
circulation currents, and part for the direct production of turbulence.
The magnitude of the shear stress is determined from

$$\tau_s = \rho_a \, C_d \, W^2 \tag{14}$$

where

τ_s = surface shear stress, $kg/(m\text{-}sec^2)$

ρ_a = density of air, $1.177 \ kg/m^3$

C_d = drag coefficient (order of 10^{-3}), dimensionless

W = wind speed at a specified elevation, m/sec

45
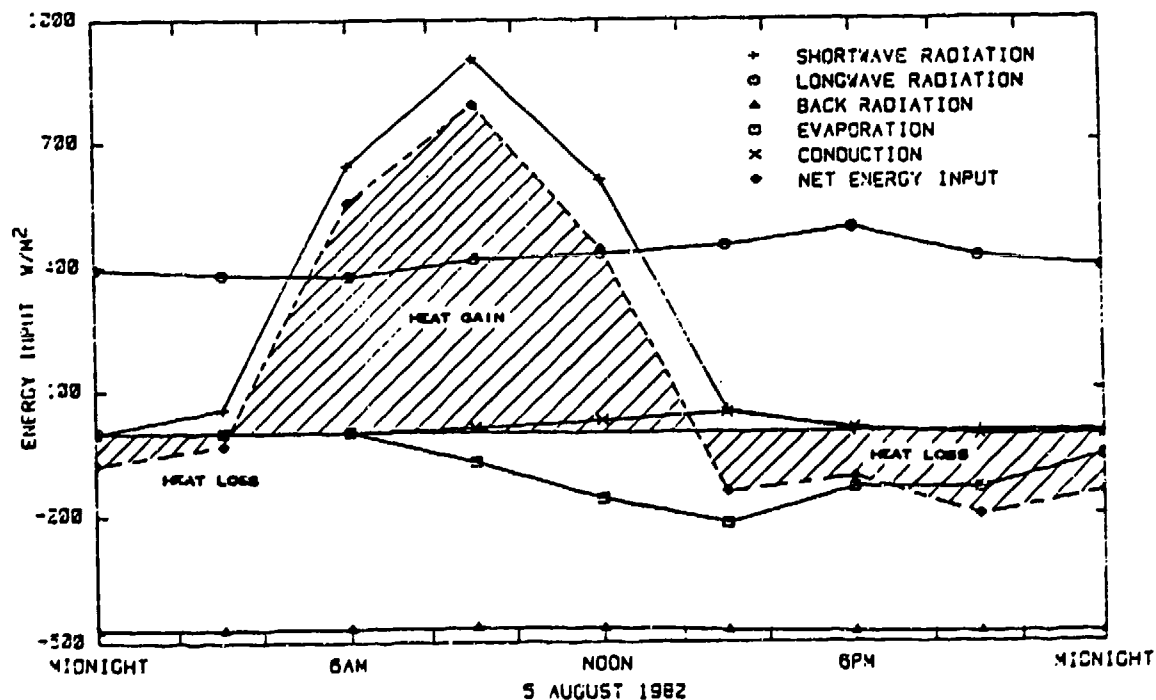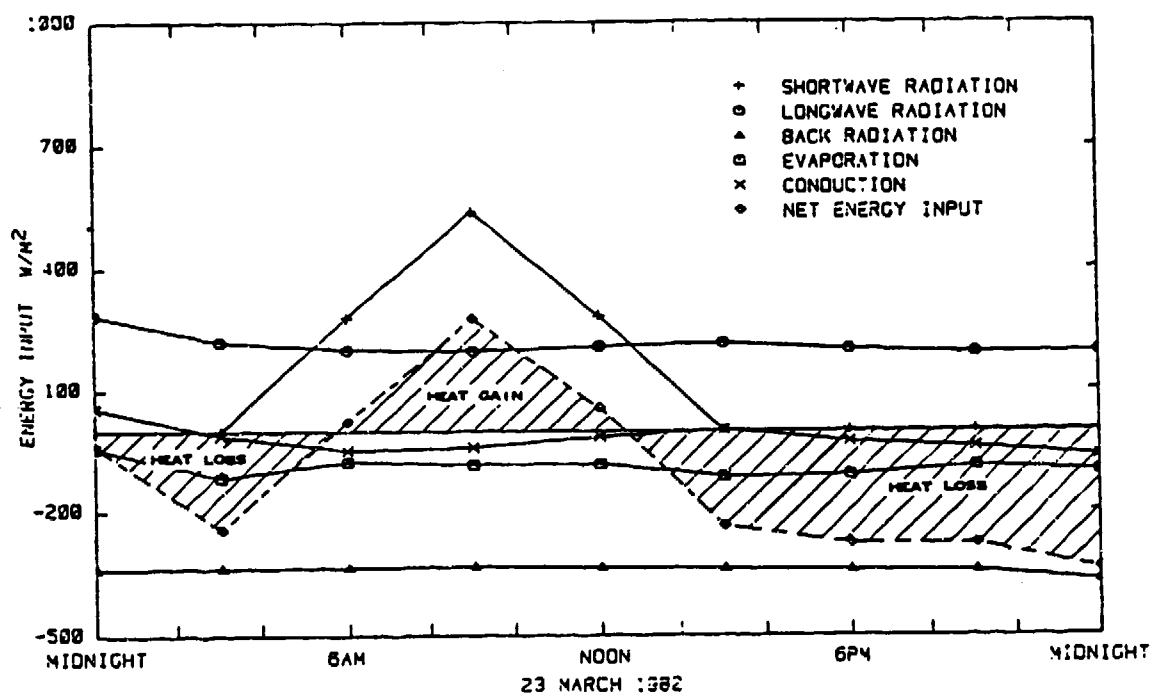
Figure 28. Diurnal heating and cooling cycles
for central Arkansas (Continued)

46
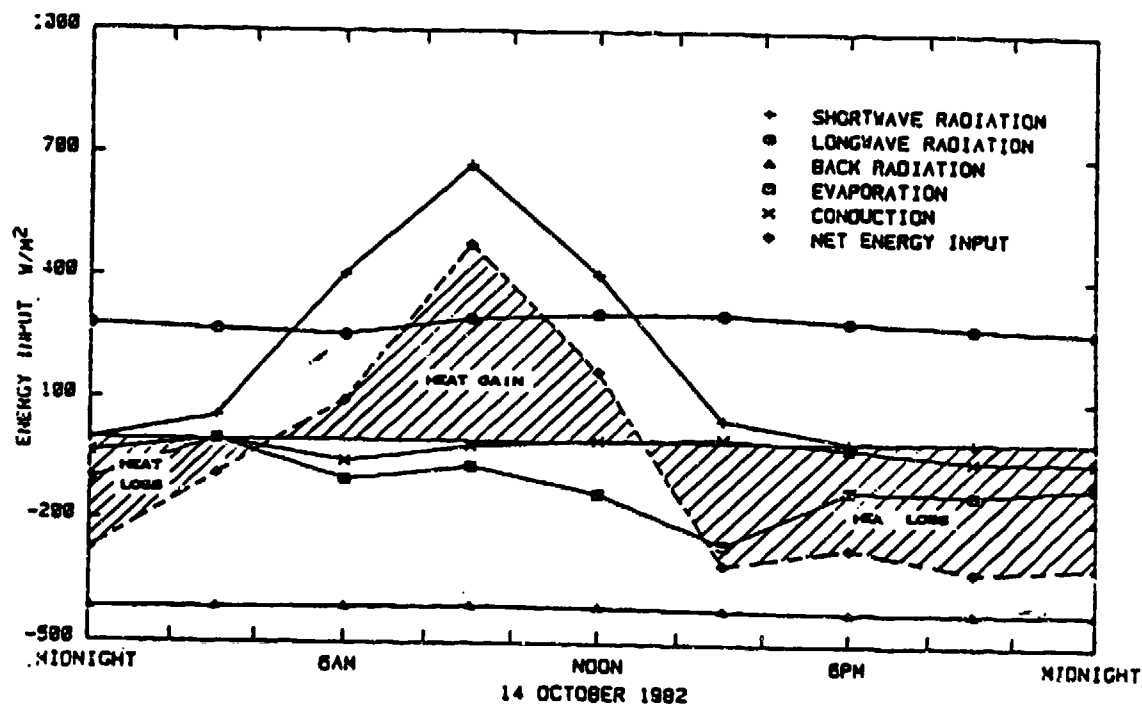
Figure 28. (Concluded)
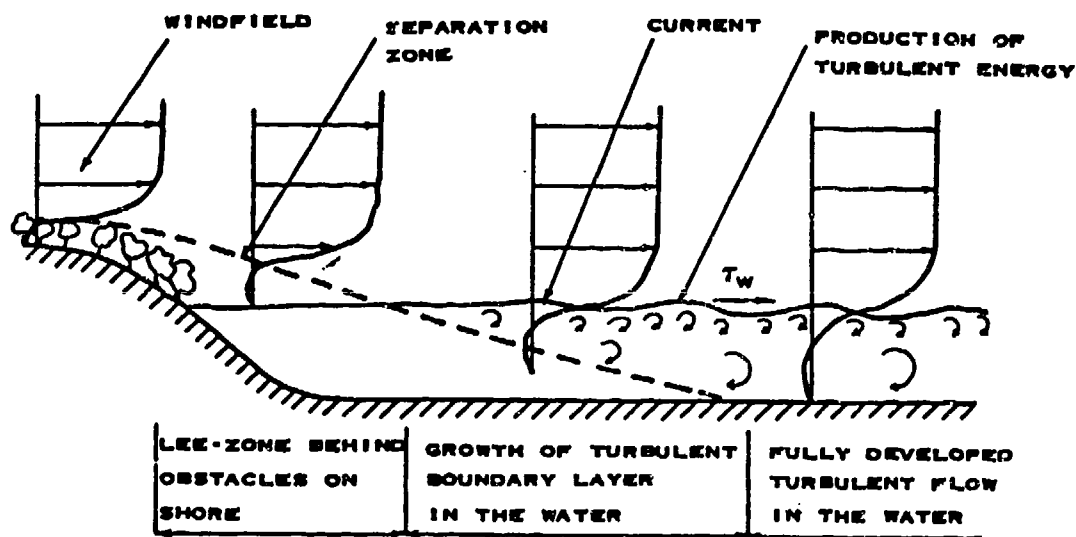
Figure 29. Wind shear on water surface
(after Ottesen Hansen 1978)

The drag coefficient can be determined from empirical formulas developed by Safaie (1978), Wu (1980), and others. The rate of energy input to the water body is

$$\frac{d(TKE)}{dt} = \int_{A_s} u_s \, \tau_s \, dA \tag{15}$$

where

A_s = water surface area, m^2

u_s = surface drift velocity, m/sec

The surface drift velocity is usually assumed to scale with the wind friction velocity in water (w_*), which is defined by

$$w_* = \sqrt{\frac{\tau_s}{\rho_w}} \propto u_s \tag{16}$$

where ρ_w = water density, kg/m^3.

From Equations 14-16, it is evident that the energy available to create waves, turbulence, and currents and, hence, mixing is dependent on the wind speed to the third power and on the surface area of the reservoir. Depending on the surrounding terrain and shape of the reservoir, measured wind speeds and surface areas may not be appropriate for use in Equations 14 and 15. If the terrain surrounding a reservoir consists of high hills, trees, bluffs, etc., the terrain may shelter the water surface from the wind force. As a rule of thumb, the sheltering effects extend into the lake a distance of approximately eight times the vertical elevation (Ford 1976). The wind speed can also increase over a water surface because of the decrease in surface roughness going from land to water. Using boundary layer theory, Ford and Stefan (1980b) developed a relationship to predict the increase in wind speed based on fetch and roughness lengths. For complete reviews on this subject, the reader is referred to Haugen (1973) and Smith (1975). Dendritic reservoirs with many islands may experience funneling and variability in wind speed and direction which further complicate the determination of wind shear.

48

Surface waves. The significance of wave action with respect to mixing results from the orbital motion of water particles beneath the water surface (Figure 30). In isothermal lakes or in the mixed layer of a stratified lake, the depth of water affected by wave action is approximately one-half the wave length (λ) (Smith 1979). This depth is also used to define the shore zone or that region of a lake where the wave form is distorted by bottom interference.
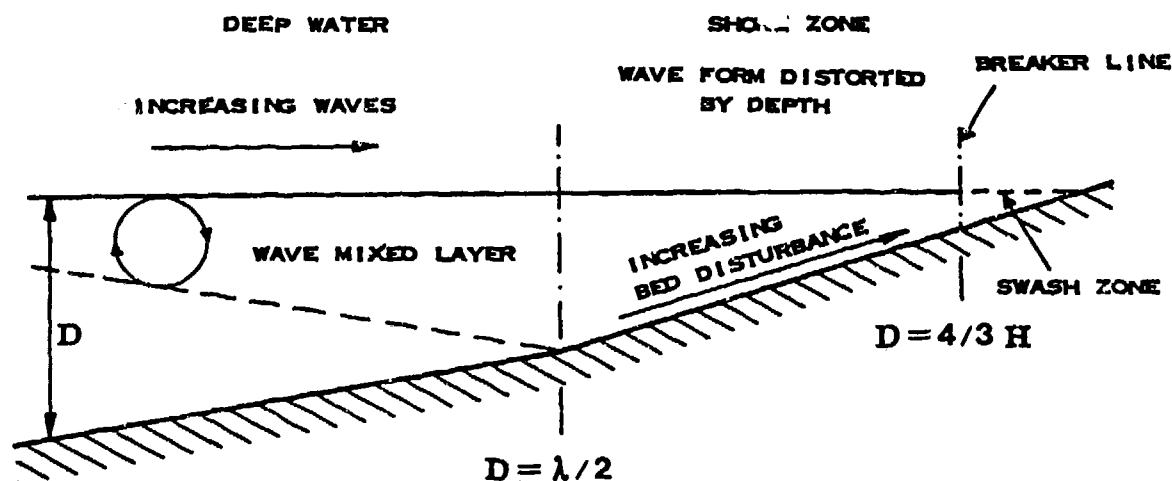
Figure 30. Schematic of surface waves (after Smith 1979)

The waves become unstable and break when the water depth is equal to four-thirds the wave height (H). This point is the break line and defines the swash zone as the area where the waves break out of shore. Since the orbitals are not truly circular and do not completely close, there is a net transport by wave motion in the direction of the wind. This transport is usually negligible compared to the transport by currents (Smith 1979).

3.2.3 Circulation Currents

General. Circulation currents are averaged water movements controlled by Coriolis, external, and friction forces. Circulation patterns in reservoirs are complicated by basin configurations, density stratification, fluctuating wind speeds and directions, reservoir

operating plans (e.g., hydropower and flood control), and secondary circulations from differential heating and convective currents. In addition, the principle of continuity requires that any movement of water out of any part of a reservoir be balanced by the return of an equal volume of water or a change in water surface level.

Coriolis forces, which result from the earth's rotation about its axis, cause currents in the northern hemisphere to deflect to the right when looking in the direction of the flow. For example, Pharo and Carmack (1979) determined that Coriolis effects caused the Thompson River inflow to Kamloops Lake, British Columbia, to be deflected along the shore. According to Mortimer (1974), Coriolis forces or rotational effects become significant when the width of a lake is greater than 5r and dominant when the lake width is greater than 20r. The radius of the inertial circle r is defined by

$$r = \frac{U}{f} \qquad (17)$$

where

U = water velocity, m/sec

f = Coriolis parameter ($f = 2\bar{\omega} \sin \emptyset$)

$\}$ = angular velocity of the earth's rotation (7.29×10^{-5} rad/sec)

$\emptyset$ = latitude

For a typical velocity U of 0.1 m/sec and a latitude $\emptyset$ of 40 deg, r = 1.06 km and rotational effects become significant for lakes with widths greater than 5 km. Because r is inversely related to the sine of the latitude $\emptyset$, rotational effects become significant at a smaller width with increasing latitude. In large lakes, which are dominated by rotational effects, the classical Ekman spiral can limit the depth of the upper mixed layer to the Ekman layer depth and thereby affect the mixing regime (Smith 1979).

The wind is a major external force governing circulation patterns in lakes and reservoirs. As previously discussed, the fraction of the

50

wind shear that is used to generate currents is unknown. It is, how-
ever, usually assumed that the surface current speed is 1 to 3 percent
of the wind speed. Bengtsson (1978) and others have found that:
(a) the percentage is not a constant even for a specific case, (b) the
percentage decreases with increasing wind speed, and (c) the percentage
increases with increasing lake dimensions. Figure 31 illustrates the
complex surface current patterns that can develop in a lake. Although
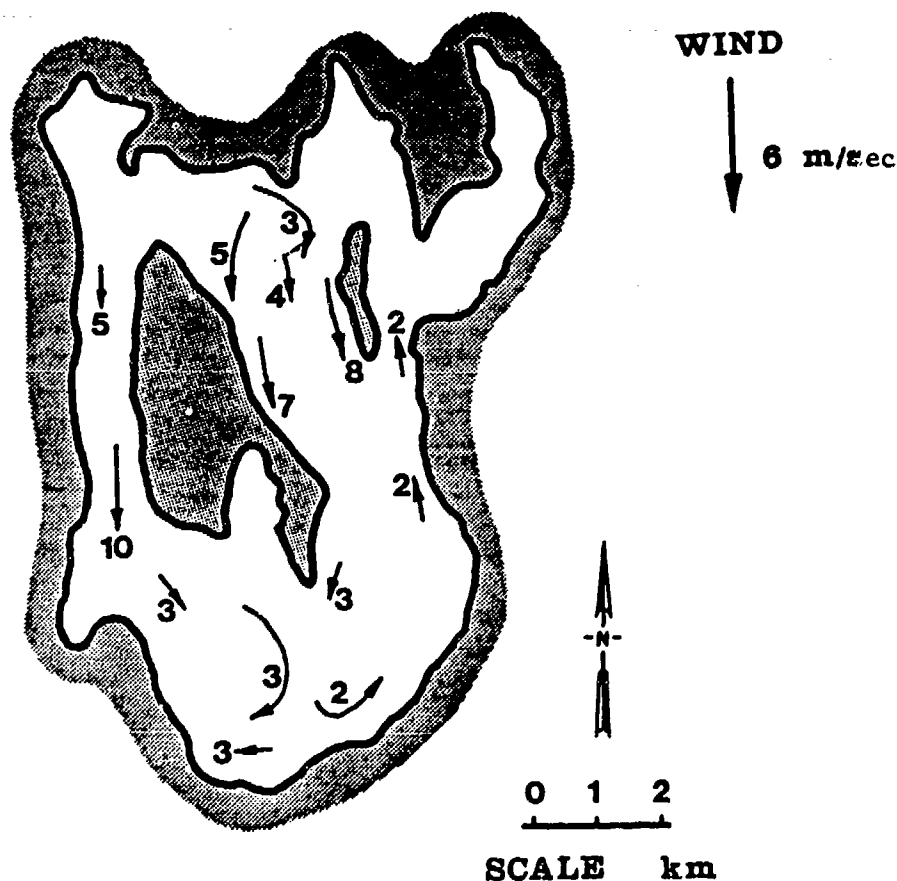
Figure 31. Surface currents in Lake Ivo,
Sweden (after Bengtsson 1978)

it is usually assumed that the current speeds decline exponentially with
depth, the actual shape of the current vertical profile will depend on
the nature of all external forces, stratification, inflow and outflow
distributions, and the location of all lake boundaries. Friction at the
lake boundaries causes a boundary layer to form that can be described by

a logarithmic velocity profile such that the current speed at the bed is zero. The random variability of the wind and the geometrical complexities of reservoir basins result in a temporally changing and spatially nonuniform water. Smith (1979) discusses many of these and other factors controlling lake circulation in detail.

In reservoirs, the existence of well-defined inflow density currents (Ford and Johnson 1983), withdrawal zones (Bohan and Grace 1973, Imberger 1980), and possibly pumpback jets (Roberts 1981) probably significantly perturbs classical wind-generated circulation patterns, but little is known of these interactions. In addition, reservoir operating procedures that result in pool-level fluctuations also generate currents that must interact with the wind-generated current field. Again, little is known about the synergistic effects of these currents and mixing mechanisms except that, once water is set in motion, it cannot respond instantaneously to a change in flow regime.

Seiches. When a steady wind blows across a water surface, water is transported to the windward side of the lake and the water surface slope is determined by

$$ S = \frac{\Delta D}{L} = \frac{\tau_s}{\rho g D} \tag{18} $$

where

$\qquad$ S = water surface slope

$\qquad$ ΔD = setup of water surface, L

$\qquad$ L = length of lake, L

$\qquad$ τ_s = surface shear stress, F/L^2

$\qquad$ D = water depth, L

In this equation, the wind force is balanced by the change in hydrostatic pressure. If the water body is stratified such that it can be represented as a two-layered system, the interface responds to the wind force by tilting in the opposite direction (Figure 32) with a slope of

52

$$S_i = \frac{\tau_s S}{\frac{\Delta \rho}{\rho} g D_i} \qquad (19)$$

where

S_i = interface slope

$\Delta \rho$ = density difference between two layers, m/L^3

D_i = thickness of top layer, L
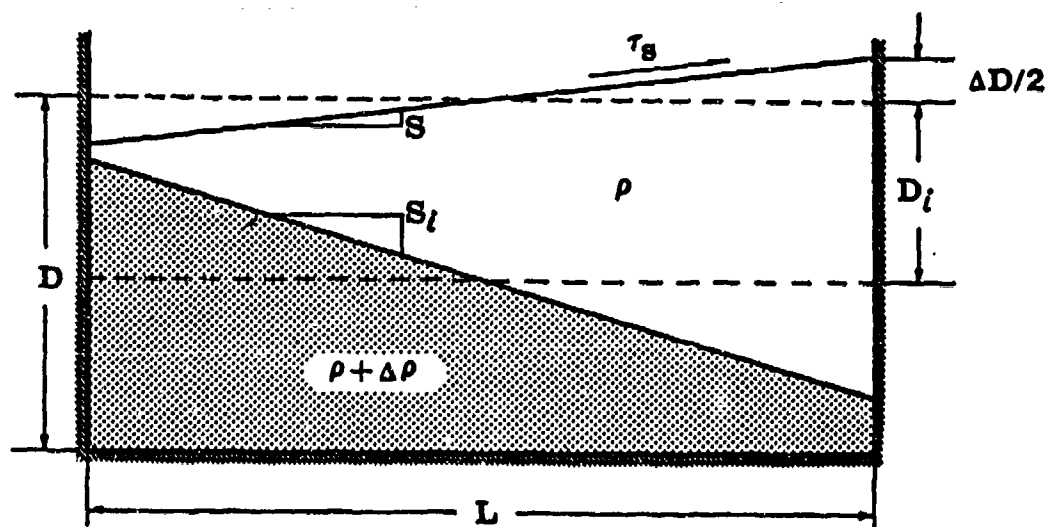
Figure 32. Nomenclature for an internal seiche

If the wind force (τ_s) is sufficiently large, the interface slope may become large enough so that the lower layer is exposed to the water surface. This phenomenon is termed upwelling and can result in the hypolimnetic water being mixed into the surface waters (Blanton 1973).

When the wind force is removed, the potential energy associated with the water surface and interface is converted into kinetic energy and flow. The result is an oscillating motion called seiching, which decays with time. The time for one cycle of the surface seiche (i.e., the seiche period) is

$$t_s = \frac{2L}{\sqrt{gD}} \qquad (20)$$

53

where the terms are as previously defined. A seiche is one indirect mechanism for energy from the wind to become available for mixing in the hypolimnion of a lake. A more detailed review of seiches and upwelli is found in Monismith (1983).

3.2.4 Internal Waves

All stably stratified fluids possess the ability to sustain internal wave motion. The waves can be generated locally by turbulence or externally by an outside perturbation such as hydropower operation. Internal waves transport momentum and can exist without breaking and forming turbulence. It is only after they break that turbulence is generated and mixing is possible.

Internal waves impact the mixing regime because they radiate energy away from the place where they were generated. They can reduce entrainment into the mixed layer by creating a local energy loss from the mixed layer (Kantha, Phillips, and Azad 1977). Internal waves can increase mixing by transporting energy into a region where it would not otherwise be available.

Turbulence. Part of the energy input from the wind shear is used to directly produce turbulence and TKE. This turbulence interacts with turbulence produced by breaking waves (surface and internal), cooling at the air/water interface, and current shear to keep the upper layer (epilimnion) well mixed and to entrain metalimnetic water into the epilimnicn. If the turbulence is generated at a length scale less than the thickness of the mixed layer, viscous dissipation with depth will result in a negligible fraction of the energy being available for entrainment at the epilimnetic/metalimnetic interface. If there is a simultaneous heat (buoyancy) flux across the air/water interface, all of the wind-generated TKE may be used to maintain the well-mixed layer and not be available for additional entrainment.

Langmuir circulation. Langmuir circulations are counter-rotating concentric vortices in the surface layers of water bodies (Figure 33). Their existence is readily observed because materials accumulating in the zones of convergence appear as streaks or bands on the water
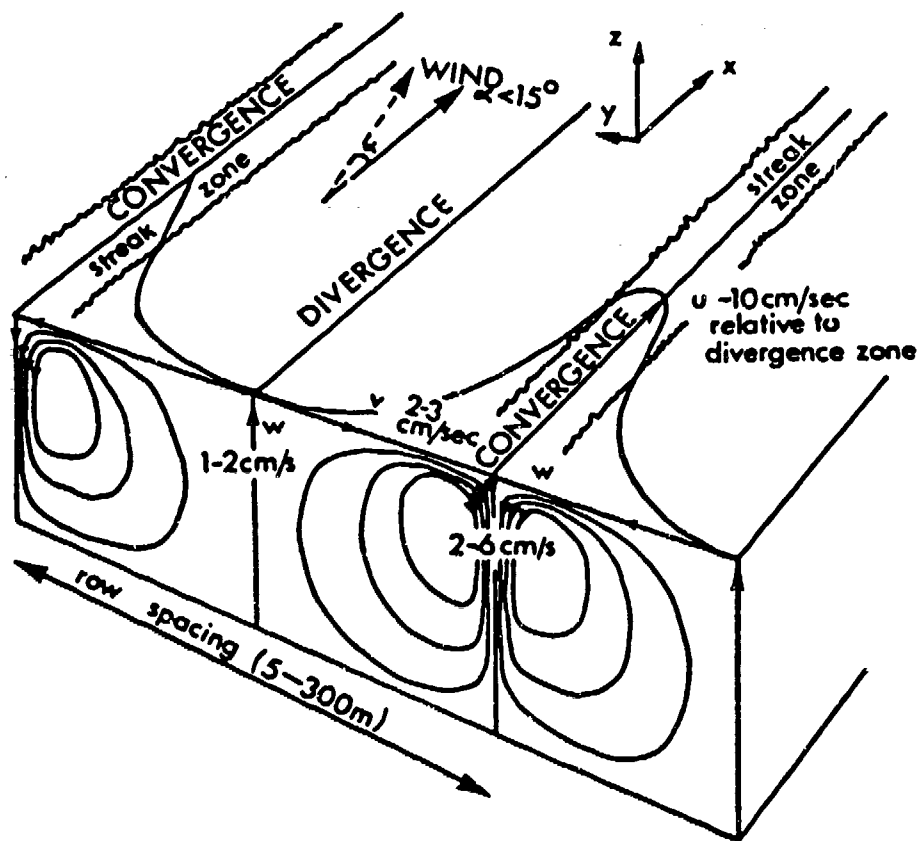
Figure 33. Schematic of a Langmuir circulation
cell (after Pollard 1977)

surface. In some instances, compressed films dampen the capillary
waves, giving the streaks a smoother appearance. Langmuir (1938) was
the first to show that the commonly observed surface streaks or windrows
were a manifestation of a more complex circulation pattern related to
the wind. Langmuir also concluded that the vortices were responsible
for the formation of stratification and the maintenance of a well-mixed
layer. Recent laboratory and theoretical studies have shown that both
waves and current shear are required for the Langmuir cells to form
(Leibovich 1983). Earlier models that related the formation of Langmuir
circulation to instabilities and thermal convection are now considered
invalid. In a comprehensive review of Langmuir circulation, Leibovich
(1983) summarizes the results from several field studies. These
include:

<u>a</u>. Langmuir cells form and align within a few degrees of the wind
    direction.

<u>b</u>. Cells form within a few minutes of onset of a wind of 3 m/sec
    or faster.

<u>c</u>. Spacing of windrows varies from 1 m to hundreds of metres.

<u>d</u>. Depth of penetration of cells is limited to the first
    significant density gradient.

<u>e</u>. The spacing between the largest windrows is approximately
    twice the depth of the cells.

Although there is evidence to suggest Langmuir cells are important
mixing mechanisms in reservoirs, there is no direct proof (Leibovich
1983).

3.2.5 Inflows

Since tributary inflow density usually differs from the density of
the reservoir surface waters, inflows enter and move through reservoirs
as density currents. Depending on the sign and magnitude of this den-
sity difference, density currents can enter the epilimnion, metalimnion,
or hypolimnion (Figure 34) and thereby modify the mixing regime in these
regions since inflows are a source of both buoyant potential energy and
turbulent kinetic energy. The rate of the PE input is dependent on the
inflow density, the flow rate, and the in-lake density distribution:

$$\frac{d(PE)}{dt} = \frac{d}{dt} (mgH) = \Delta\rho_j Q_j g Z_j \tag{21}$$

where

$\Delta\rho_j$ = density difference between inflow and reservoir surface
waters, kg/m^3

Q_j = inflow rate, m^3/sec

Z_j = difference in depth between center of mass of inflow and
center of mass of inflow placement, m

56
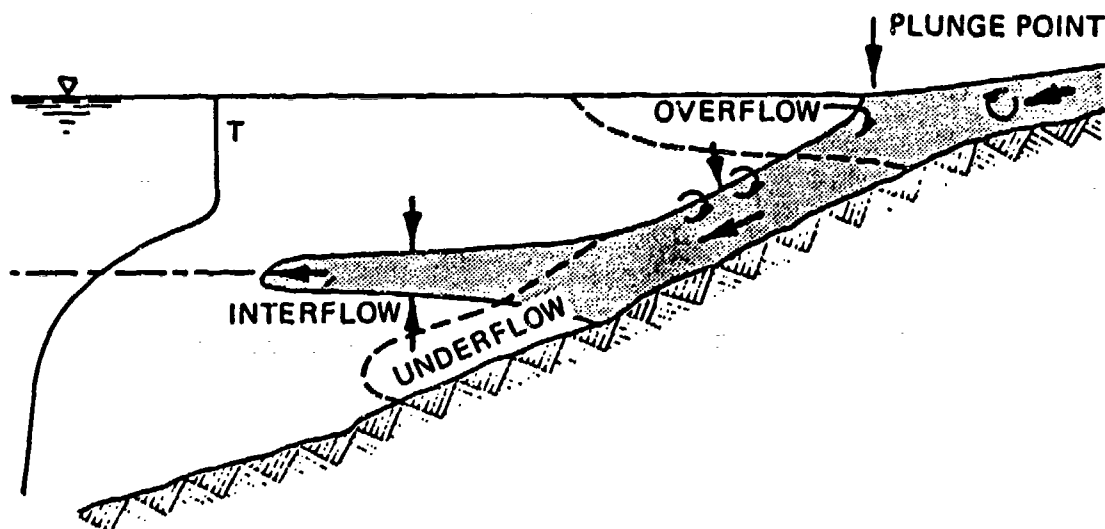
Figure 34. Inflow density currents

The rate of TKE input is also dependent on the flow rate:

$$\frac{d}{dt} \text{(TKE)} = \frac{d}{dt} \left(\frac{1}{2} mU_j^2\right) = \frac{1}{2} \rho_j \, Q_j \, U_j^2 \qquad (22)$$

where

U_j = inflow velocity = Q_j/A_j, m/sec
ρ_j = inflow density, kg/m^3
A_j = cross-sectional area perpendicular to inflow, m^2

Since the mixing resulting from inflows is dependent on the energy input, the magnitude of inflow mixing is highly dependent on the flow rate. A complete analysis of reservoir inflows is found in Ford and Johnson (1983).

When the inflow density is less than the surface water density, the inflow will float on the water surface as an overflow. This condition typically occurs in the spring when inflows warm more rapidly than reservoirs. In an overflow, the excess hydrostatic pressure in the density current causes the current to flow in all directions not obstructed by boundaries. Overflows are susceptible to mixing from wind-induced mechanisms and diurnal heating and cooling processes. Wind

57

shear can direct the overflow into a cove or prevent it from moving downstream. Vertical mixing in the mixed layer can be enhanced with an overflow if the density difference is small and flow rate is large (i.e., large TKE input) or suppressed if the flow rate is small and density difference is large (this situation frequently exists with thermal discharges).

If the inflow density is greater than the water surface density, the inflow will push the reservoir water ahead until the buoyancy forces dominate and the inflow plunges beneath the water surface. The plunge point is sometimes made visible because of turbidity or the accumulation of floating debris, which may indicate a stagnation point. The location of the plunge point is determined by a balance between the stream momentum, the pressure gradient across the interface separating the river and reservoir waters, and the resisting shear forces. Some mixing (termed initial mixing) occurs at the plunge point because of the large eddies formed by flow reversals and pooling of the inflowing water (Akiyama and Stefan 1981). Ford and Johnson (1983) estimated this mixing to be on the order of 25 percent of the inflow volume. Knapp (1942) noticed that the flow in the vicinity of the plunge point occurred at the bottom of this pooled mixing zone (Figure 35). Ford, Johnson, and Monismith (1980) and Kennedy, Gunkel, and Carlile (1983) substantiated this pooling phenomenon during dye studies on DeGray Lake, Arkansas, and West Point Lake, Georgia, respectively, when the dye clouds appeared to have stalled at the plunge point. The location of the plunge point can also be influenced by morphological factors. Changes in the bed slope (e.g., due to sediment deposition), bed friction, and cross-sectional area may
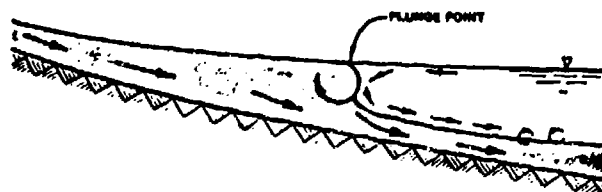
MIXING AT PLUNGE POINT

Figure 35. Flow in the vicinity of
the plunge point

affect location of the plunge point. For a river entering a wide lake, the plunge point may actually be a point rather than a line.

After the inflow plunges, it follows the old river channel (thalweg) as an underflow. The speed and thickness of the underflow is determined by a flow balance between the shear forces and the acceleration due to gravity (i.e., gradually varying flow theory). An underflow will entrain overlying reservoir water due to shear and turbulence generated by bottom roughness. Changes in the underflow density from entrainment must be quantified before a density interflow or intrusion can be analyzed, or estimates of the vertical placement of an interflow can be incorrect.

An interflow or intrusion occurs when a density current leaves the river bottom and propagates horizontally into a stratified body of water. Intrusions differ from overflows and underflows because an intrusion moves through a reservoir at a elevation where the intrusion and reservoir densities are similar. Intrusions require a continuous inflow and/or outflow for movement, or they stall and collapse (i.e., dissipate). Turbulence is usually quickly dissipated in an intrusion since the metalimnetic density gradient creates strong buoyancy forces which inhibit mixing. Mixing still occurs, however, because of the flow gradient.

3.2.6 Outflows

Manmade reservoirs differ from natural lakes in many respects, but especially with respect to the importance of outflows. In natural lakes, outflows are usually uncontrolled surface withdrawals with the outflow rate dependent on the water surface elevation. In reservoirs, outflows are usually regulated by gates and/or a structure, and the withdrawal depth is not necessarily near the water surface. For example, many flood control projects have bottom outlets while multipurpose projects may have multilevel outlets (i.e., selective withdrawal structures.

Outflows contribute to the in-lake mixing regime through withdrawal currents and turbulence associated with them. Withdrawal

currents are generated because the PE associated with the water level
(i.e., the head) is converted into TKE and causes water to flow through
an outlet (see Figure 36). The characteristics of the withdrawal cur-
rents will be dependent on the withdrawal rate (i.e., gate or structure
setting), ambient in-lake stratification, outlet location, and lake
geometry. If the outlet is located in the hypolimnion of a strongly
stratified lake, the withdrawal zone may also be limited to the
hypolimnion of the lake. Withdrawal zones can also be limited to the
epilimnion or metalimnion of a lake depending on the outlet location,
flow rate, and ambient stratification. Withdrawal zones can be computed
using formulas provided by Bohan and Grace (1973), Imberger (1980), and
Davis, Holland, and Wilhelms (1985).

OUTFLOW

$$\frac{d}{dt}(KE) = \frac{1}{2}V^2\frac{dm}{dt} = \frac{1}{2}V^2\rho Q$$

$V = \sqrt{2gH}$
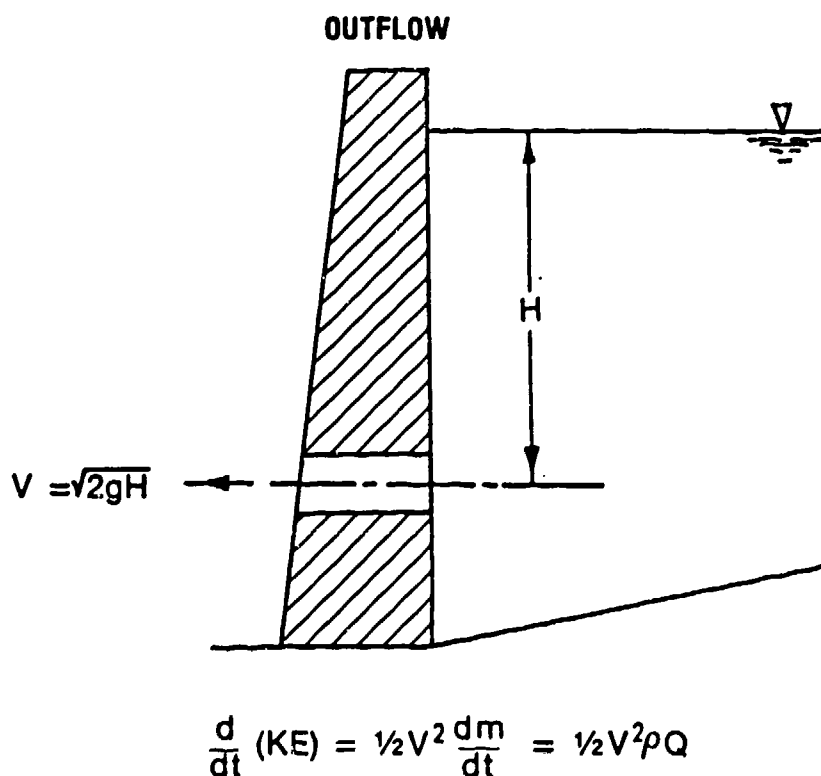
Figure 36. Energy conversion associated with an outlet

3.2.7 Barometric Pressure and Gravity

On large lakes, horizontal variations in barometric pressure can
result in surface seiching. As indicated in Section 3.2.2., seiching

can impact the mixing regime as internal waves and seiches form and break. Tidal movement resulting from the gravitational attraction of the moon and the sun has been observed in very large lakes (e.g., Lake Superior, Minnesota and Wisconsin, and Lake Baikal, Siberia) (Wetzel 1983) but is probably negligible in most reservoirs.

3.2.8 Summary

In the preceding discussion of reservoir mixing, it was shown that the observed thermal structure in a reservoir results from the cumulative effects of a number of complex, nonlinear, interdependent mixing processes. Although the sources of TKE for mixing are limited (i.e., solar and atmospheric heating, wind, inflows, and outflows (including outlet location)) and well known, quantitative knowledge of specific mixing mechanisms is limited. TKE budgets for the entire lake do, however, clearly expose the physical causes of observed motion and thermal stratification.

The observed temperature structure in a lake is actually a signature of past mixing events. The relative timing of these events is important. For example, the occurrence of spring floods after stratification forms can result in a significantly different thermal structure than if the floods occur prior to stratification. Identification of the mixing events is crucial to understanding the thermal structure of a lake.

3.3 Influence of Mixing on Reservoir Water Quality

While the mixing mechanisms of inflows and outflows, upwelling and seiches, turbulence, and others are highly interactive, the influence of each of these processes on chemical and biological processes will be discussed separately for convenience. It must be recognized, however, that reservoir water quality is a function of the interactions among the dynamic mixing processes and of the chemical and biological responses to mixing.

3.3.1 Inflows and Outflows

Reservoir inflows usually represent the major contributions of both dissolved and particulate constituents to the reservoir mass budget. Ground-water and atmospheric contributions are generally minimal.

As an inflow enters the lake, velocity and turbulence decrease, coarse particulate or suspended materials settle, and the water clarity increases. Turbulence generated through bottom shear generally is sufficient to maintain silt- and clay-sized particles in suspension. Nutrients, bacteria, and organic constituents may be transported into the reservoir since these constituents generally sorb to particles in the clay-silt size range (Frink 1969; Pita and Hyne 1974; Sharpley and Segers 1979; De Pinto, Young, and Martin 1982). Depending on the density structure of the lake and inflow, the inflow can enter the epilimnion, metalimnion, or hypolimnion (Figure 34).

An overflow situation may have the greatest initial influence on reservoir water quality by introducing oxygen-demanding material, nutrients, and bacteria directly into the surface waters or euphotic zone. Available nutrients can be assimilated by phytoplankton and may stimulate plankton blooms; bacteria concentrations may exceed body contact recreation standards; and oxygen-demanding material may depress mixed-layer dissolved oxygen (DO) concentrations. Even though the euphotic zone thickness would probably be decreased due to increased turbidity, circulation and mixing in the mixed layer would circulate phytoplankton between the nutrient-rich inflow and euphotic zone. With overflow conditions, phytoplankton concentration would probably attain a maximum in the headwater regions and decrease in the downstream direction (Kimmel, Lind, and Paulson 1984).

Interflows and underflows have similar influences on water quality. At the plunge point, the inflow waters sink to form a density current flowing along the bottom. Bottom-generated turbulence results in entrainment of surface waters into the density current. This also may

introduce nutrients, organic matter, and bacteria into the overlying surface water and euphotic zone.

Once the density current enters the metalimnion as an interflow, the inflowing constituents are temporarily isolated from the mixed layer. These constituents may be entrained into the mixed layer during storm events if wind gusts deepen the mixed layer or as the thermocline erodes due to penetrative convective mixing. Since the metalimnion is isolated from oxygen exchange with the surface, oxygen-demanding material in the interflow may depress metalimnetic DO concentrations. In most stratified reservoirs, a metalimnetic DO minimum typically develops with anoxic conditions developing in some systems (Hannan and Cole 1984).

Underflows not only introduce inflowing constituents into the hypolimnion but also increase turbulent diffusion across the sediment/ water interface because of bottom shear. This can increase oxygen depletion by increasing oxygen transfer across the diffusion-limited sediment/water interface. It also can increase the transfer of reduced and resolubilized constituents such as ammonia, phosphorus, iron, manganese, and hydrogen sulfide from the sediment into the overlying water column.

Interflows and underflows have been proposed as major transport processes for reduced and resolubilized species such as manganese and phosphorus from the upper reservoir to downstream areas (Nix 1981, 1984; Davison, Woof, and Rigg 1982). Since anoxic conditions generally begin in the upstream area of the reservoir, inflow mixing processes can promote the movement of this anoxic front further into the reservoir. Many dissolved nutrient species are in a readily available form for phytoplankton assimilation.

Underflows also can improve reservoir water quality. Cold, well-oxygenated outflows from Lake Ouachita, Arkansas, maintain an aerobic hypolimnion in the old thalweg of Lake Hamilton, Arkansas, downstream, even though the Lake Hamilton coves become anoxic.

The above situation can be altered depending on how the project is operated (i.e., how water is released). If a reservoir has a multilevel

withdrawal structure, water may be released at a similar elevation as the inflow enters the reservoir. Under such conditions the inflow waters can be short-circuited through the reservoir. If the residence time of a density overflow is less than the response time (i.e., doubling time) of phytoplankton under natural conditions, phytoplankton blooms may be minimized. Lund, Mackereth, and Mortimer (1963) report natural doubling times for *Asterionella formosa* to be 5 to 7 days. Doubling times for other species under natural conditions are on the order of 5 to 30 days (Ford and Thornton 1979). Therefore, when the residence time or short-circuited residence time is less than approximately 5 days, phytoplankton washout is probable. For Lake Windermere, England, a natural lake, Lund (1950) concluded losses due to overflow were approximately compensated for by inflowing nutrients. Lund, Mackereth, and Mortimer (1963) found outflow losses to be the major loss for *Asterionella*. Residence times of 5 days or less for overflows imply that the inflow water quality will dominate the mixed layer quality.

If the outflow is released from a different level than the inflow enters, mixing within the reservoir may be increased. Transport of nutrients from the metalimnion to the epilimnion and euphotic zone, for example, can be increased when inflows enter as interflows or underflows and the project is operated with surface discharge. Bottom withdrawal may promote movement of interflows and underflows through the reservoir and minimize the interaction between the inflowing constituents and the euphotic zone. Bottom withdrawal also may purge an anoxic hypolimnion of reduced and resolubilized constituents. Dunst (1974) found that bottom discharge from several Wisconsin reservoirs with anoxic hypolimnia significantly reduced the hypolimnetic phosphorus load. During fall overturn, then, this phosphorus load would not be available for mixing throughout the water column and phytoplankton assimilation.

Many reservoirs are operated to store water for downstream flood control. The pool elevation therefore rises to accommodate the inflowing water. Water also flows into littoral zones and coves, carrying with it inflowing constituents. These constituents can remain within these zones and coves and impact water quality later in the season.

Nutrients, for example, may be assimilated by phytoplankton, and organic loadings may contribute to the onset of anoxic conditions. When there is a net outflow from a reservoir, there is also a net transport from the littoral zones and coves into the main body of the reservoir. Increased horizontal transport also results in increased vertical transport.

3.3.2 Upwelling, Seiches, and Internal Waves

The water quality significance of upwelling and seiches is severalfold. First, upwelling is one mechanism whereby the waters of the metalimnion, and possibly the hypolimnion, are temporarily exposed to the surface. Upwelling of anoxic hypolimnetic water near the dam in C. J. Brown Lake, Ohio, depressed surface DO concentrations to about 2 mg/ℓ with increased surface nutrient concentrations and hydrogen sulfide odors. This upwelling occurred because of the passage of a large storm front. The colder, nutrient-rich water may initiate a phytoplankton bloom of different composition than previously occurred within the lake.

Second, seiches may alter the mixed-layer depth and light regime to which plankton are exposed. Horizontal variations are also expected because the wind may concentrate phytoplankton at the downwind end of the lake, creating differences in mixed-layer depths and light penetration within the mixed layer. The correlation between upwelling and phytoplankton blooms is well established for coastal zones (Fogg 1975, Rao 1977) and is also found in natural lakes (Coulter 1968). The high rate of production throughout the year in Lake Victoria, Africa, is attributed to efficient mixing resulting from seiche action (Fogg 1975).

Seiche motion may indirectly initiate hypolimnetic mixing. As the water oscillates in the reservoir, bottom shear may create turbulence that increases mixing in the hypolimnion. This mixing may increase transfer of DO and reduced constituents across the sediment/water interface.

Seiche motion may result directly from project operation, particularly in peaking hydropower reservoirs. During generation, water

movement is established toward the dam. When generation ceases, water continues to move toward the dam and piles up at the dam with the establishment of oscillations of this water as the water surface seeks equilibrium. Seiche activity may explain the observed hypolimnetic DO fluctuations in Lake Sidney Lanier, Georgia. Hypolimnetic DO concentrations at a given depth near Buford Dam increased about 2 mg/ℓ around 1000 hr from Tuesday through Saturday but were not evident on Sunday or Monday. Over long weekends with no generation, the increase was delayed until the day following the initiation of generation. Apparently, a seiche was created through generation with a frequency in phase with the generation cycle. This seiche motion created by hydropower generation may also increase hypolimnetic mixing through bottom shear.

While internal waves do not promote mixing unless these waves break, the vertical displacement of water by internal waves can significantly alter the light regime of phytoplankton in the metalimnion. Metalimnetic nutrient concentrations may be higher than in the mixed layer due to interflow loadings and microbial decomposition of organic matter settling from the epilimnion. Light may be the factor limiting phytoplankton production in the metalimnion. Internal waves with an amplitude of 2 to 15 m and a period of 15 min to 12 hr have been observed in coastal areas (Reid 1956, LaFond 1962). Armstrong and LaFond (1966) have observed vertical displacements of nutrient layers by these waves. As the metalimnion is displaced by the internal waves, this layer may enter the euphotic zone where available light may stimulate plankton production (Denman and Gargett 1983). Plankton production may increase metalimnetic DO concentrations during the day, but increased respiration at night may deplete DO concentrations below acceptable thresholds for aquatic life. Metalimnetic plankton assemblages may be entrained into the mixed layer and initiate plankton blooms.

Breaking internal waves may increase metalimnetic and hypolimnetic mixing. Many reservoirs are not completely cleared of timber when impounded, so these trees act as barriers to wave movement. The turbulence generated through breaking waves can mix metalimnetic constituent

66

concentrations and increase diffusion across the epilimnetic/ metalimnetic interface. An anoxic metalimnion may contribute dissolved nutrients; reduced species such as manganese, iron, and hydrogen sulfide; and organic compounds to the mixed layer.

Project operation has the potential to generate internal waves of varying amplitudes and periods. Hydropower generation may result in internal waves with relatively regular periods while storm flows can result in internal waves with relatively large amplitudes.

3.3.3 Turbulence, Turbulent Mixing, and Entrainment

In the vertical dimension, the turbulent mixing and the resulting constituent distributions are determined primarily by density stratification. During periods of turbulent mixing, the upper well-mixed layer is usually isotropic despite settling and vertical variations in light intensity. Fee (1976) gives several examples where in vivo chlorophyll was isotropic in the upper mixed layer.

Below the upper mixed layer, in the metalimnion, the density gradient is usually strong enough to inhibit turbulent mixing. Measurements of temperature microstructure in freshwater lakes (Simpson and Woods 1970; Neal, Neshyba, and Denner 1971) show that the density structure in the metalimnion is not smooth as traditionally thought, but rather is made up of a series of steps on very small length-scales (e.g., Figure 37). These isotropic layers of intense mixing separated by strong gradients can have significant ecological effects. For example, Whitney (1938) found microstratification on the scale of centimetres based on transparency in several inland lakes. Whitney also was able to relate these abrupt changes in transparency to organic content and bacterial counts. More recently, Fee (1976) found narrow bands of high chlorophyll concentrations in the metalimnion and hypolimnion of several small, clear, well-stratified inland lakes. Thornton, Nix, and Bragg (1980) found narrow bands of high coliform bacteria concentrations in DeGray Lake, Arkansas. Density stratification and turbulence can therefore greatly affect vertical constituent distributions.
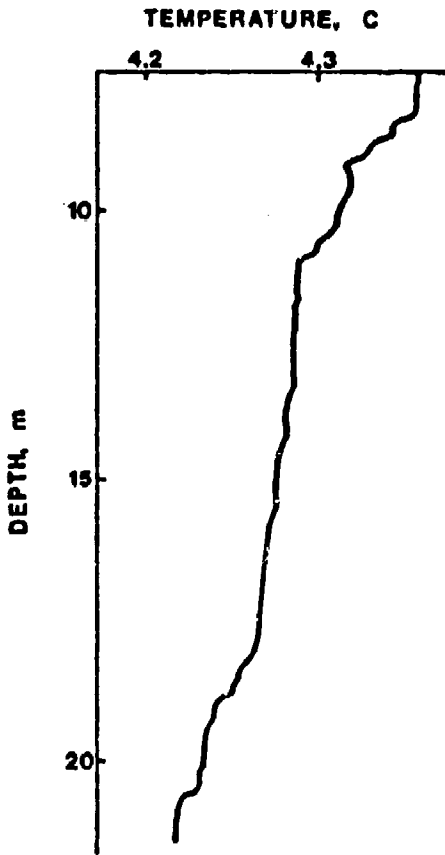
TEMPERATURE, C

Figure 37. Example of temperature microstructure (after Neal, Neshyba, and Denner 1971)

Simultaneous measurements of chlorophyll a (a measure of phytoplankton biomass) and various physical parameters have been used to determine the importance of physical transport on phytoplankton distributions (Abbott et al. 1984). Using a time series of chlorophyll and temperature at a fixed location and fixed depth in the mixed layer, Platt (1972) found the power spectra of chlorophyll a followed a -5/3 law which is characteristic of three-dimensional isotropic turbulence. Using the same data, Denman and Platt (1975) found significant coherence between temperature and chlorophyll a at each depth but not between depths. In summarizing these studies and others, Platt and Denman (1975b) concluded that for length scales between 100 m and 5 km, the observed variations in temperature and chlorophyll a resulted primarily from physical transport mechanisms including internal waves. For length scales less than 100 m, the fluctuations were damped out by turbulent diffusion. Powell et al. (1975) arrived at a similar conclusion using spectra of current speeds and chlorophyll a from the mixed layer of Lake

Tahoe, Nevada. This limit for turbulent diffusion is also consistent with the critical length scale of 50 m calculated by Platt and Denman (1975a) for the smallest patch of phytoplankton that can maintain itself against diffusion. Recently, Abbott et al. (1984) found the formation and dynamics of deep chlorophyll maxima were regulated by the interaction of three important processes: turbulent diffusion, nutrient supply rate, and light availability. Harris (1980) provides an excellent discussion of the important temporal and spatial scales in phytoplankton ecology and interaction of physical processes and plankton assemblages.

The case for a common physical mechanism controlling the distribution of both temperature and chlorophyll a at selected length scales was further substantiated by Denman (1976) and Fasham and Pugh (1976). In both studies, significant coherence was found between temperature and chlorophyll a measured at the same depth. The shapes of the power spectra of the two parameters were also similar. The gradual steepening of the power spectra at high frequencies was attributed to internal waves by Denman (1976). Denman (1976) also found that when the chlorophyll a variance was high (i.e., periods of high biological activity), the coherence between chlorophyll and temperature was low.

To investigate the vertical structure in more detail, Denman (1977) used a series of vertical profiles of chlorophyll a and temperature. The results suggested that most of the chlorophyll variation was due to horizontal advection of patches past the observation site and not to internal wave motion. Denman (1977) concluded that for a period characterized by little biological and physical activity, a single depth series of chlorophyll could depict changes in total chlorophyll only if the depth is located in an area of no appreciable vertical density gradient.

Closely related to turbulent diffusion is turbulent entrainment (Section 2.4.5). Entrainment is precisely what happens during the seasonal stratification cycle in temperate lakes. Examples of the onset and breakdown of stratification influencing phytoplankton blooms are numerous and well established (Lund 1954, Reynolds and Rogers 1976,

69

Kaeff and Knoechel 1978, etc.). Influences on the blooms include
entraining cells living on the sediment surface at fall overturn (Lund
1954); entraining previously produced chlorophyll from the metalimnion
and hypolimnion (Fee 1976); entraining nutrients from the metalimnion
(Stauffer and Lee 1974); and diluting the food concentrations to a level
too low for successful feeding (Fogg 1975). Turbulent entrainment also
occurs at shorter time frames such as the passage of synoptic weather
fronts. Gusting winds during storm events can increase the depth of the
mixed layer and entrain constituents from an anoxic metalimnion and/or
hypolimnion.

3.3.4 Langmuir Circulation

A special case of turbulent mixing in the surface waters is
Langmuir circulation (Section 3.2.4). Observations of Langmuir cells
indicate that drift velocities are generally strongest in the zones of
convergence. The cells are asymmetrical with downwelling velocities
being larger than upwelling velocities. Downwelling velocities on the
order of 5 cm/sec (4.3×10^3 m/day) are typical and are several orders
of magnitude larger than typical settling velocities (i.e., 0.01 to
1 m/day). The currents in Langmuir circulations are more than suffi-
cient to keep phytoplankton and other particulate constituents (i.e.,
bacteria) suspended (Denman and Gargett 1983).

Langmuir cells can transport phytoplankton, bacteria, and other
constituents into and out of the euphotic zone. This transport can pass
plankton and other cells through microstratification layers of higher
nutrient or organic concentrations. Since nutrient uptake is usually
much faster than growth, luxury uptake of nutrients by plankton as they
pass through these microstrata can maintain or promote plankton growth.

3.4 Synthesis

The preceding review of reservoir mixing processes and the
influence of mixing on reservoir water quality indicated that in order
to achieve the second objective of this study (i.e., develop a

mathematical algorithm for one-dimensional water quality models which realistically represents all major mixing processes occurring in CE reservoirs), the mixing algorithm should be capable of accurately predicting the:

a. Onset of stratification.

b. Daily variations in mixed-layer depths and dynamics of short-term mixing events.

c. Metalimnetic gradient.

d. Variable mixing in the hypolimnion.

e. Fall overturn.

f. Inverse stratification during winter months.

g. Effects of project operation.

An accurate representation of the onset of stratification is required to accurately predict, for example, the depletion of dissolved oxygen and the onset of phytoplankton blooms. As previously explained (Section 2.2), reservoir stratification starts at the bottom of a lake and moves upward, not from the water surface downward. The extent of metalimnetic and hypolimnetic DO depletion may depend on the relation between spring runoff and the onset of stratification. If spring runoff occurs prior to stratification, the nutrients and organic load may be distributed throughout the water column or proceed as a density overflow. If the onset of stratification has occurred before the spring runoff, an interflow may occur that can result in a significant load to the metalimnion or upper part of the hypolimnion. This load may exert an oxygen demand that results in the development of an anoxic metalimnion or hypolimnion. An accurate representation of the onset of stratification is also critical for simulating the water quality of lakes that exhibit weak or intermittent stratification.

Daily variations in mixed-layer depths are required to accurately simulate the entrainment of nutrient-rich metalimnetic waters into the epilimnion. This water, when released in the euphotic zone, may result in phytoplankton blooms. The depth of the mixed layer, relative to the

depth of the euphotic zone, can also impact the timing, magnitude, and composition of a phytoplankton bloom.

Materials tend to accumulate in the metalimnion because density gradients inhibit mixing. It is necessary to simulate this accumulation for entrainment into the epilimnion and to predict metalimnetic oxygen minima. An accurate representation of the metalimnetic gradient is also required to compute withdrawal zones and inflow placement.

Variable mixing in the hypolimnion is required to accurately simulate the depletion of dissolved oxygen and material exchanges across the sediment/water interface. It is also required to predict hypolimnetic temperatures required to meet downstream temperature objectives. Although little is known about hypolimnetic mixing, it is known that mixing levels increase with hydrometeorological forcing and use of bottom gates.

With fall overturn, complete vertical mixing returns and water quality problems associated with stratification are eliminated. If a significant oxygen demand builds up during the stratified period, oxygen levels may be depressed for a few days at overturn to satisfy the existing oxygen demand. Fall overturn also signifies the time when it is no longer possible to control release quality (e.g., temperature) through project operation (i.e., selective withdrawal).

Many CE reservoirs are located in cold climates and experience water quality problems during winter months when ice and snow covers isolate the lakes from exchanges across the air/water interface. During this period the lakes can become inversely stratified, and mixing is dominated by inflow and outflow processes.

Project operation influences both reservoir mixing processes and water quality. Bottom withdrawal can promote interflows and underflows, increase hypolimnetic mixing and mass transfer across the sediment/water interface, and decrease the buildup of anoxic constituents in the hypolimnion. Bottom withdrawal can also decrease the thermal stability of the reservoir by depleting the colder hypolimnetic water and hastening fall overturn. Since phytoplankton succession is dictated, in part, by the stratification pattern in the reservoir, the successional pattern

can be altered by project operation. Superimposing peaking hydropower generation and bottom withdrawal can create additional mixing through fluctuating water levels, Kelvin-Helmholtz instabilities, and epimeta-limnetic and metahypolimnetic interfacial shear due to return currents established by project operation.

SECTION 4. REVIEW OF ONE-DIMENSIONAL PREDICTIVE TECHNIQUES

4.1 Introduction

Since the early to mid 1960's, one-dimensional lake and reservoir
models have been proven to be effective tools for analyzing in-lake and
downstream temperature and water quality problems because temperature
and many water quality parameters tend to vary more along a vertical
distance of tens of metres than along a horizontal distance of thousands
of metres. One-dimensional models solve a set of one-dimensional con-
servation equations for heat and mass. The major difficulty in solving
these equations is finding expressions for the turbulent fluxes for heat
and mass.

Following Niiler and Kraus (1977), one-dimensional material trans-
port models for reservoirs can be grouped into four types depending on
how the turbulent fluxes are expressed. These types include determin-
istic solutions, turbulence closure models, eddy coefficient models, and
mixed-layer models. Deterministic solutions directly determine the
fluctuating velocities from the primitive equations and thereby avoid
the problem of specifying the turbulent fluxes. Since this approach
requires a very fine space scale and correspondingly high time reso-
lution, it is too expensive and time consuming for practical problems.
An example of its use is found in Deardorff (1970). Turbulence closure
models express the turbulent fluxes in terms of higher order moments
(i.e., averaged triple products of the fluctuating quantities) which in
turn must be parameterized in terms of empirical coefficients and com-
putable (bulk) quantities or be represented by another set of equations
involving fourth-order moments. Mellor and Yamada (1974) describe this
process as a hierarchy of turbulent closure models with the classical
eddy coefficient models at the lowest level. With the exception of this
lowest level, the equations solved in these models are cumbersome and
difficult to solve. Eddy coefficient models assume the turbulent fluxes
can be expressed by the gradient of the transported quantity multiplied
by an eddy diffusion coefficient which is a complicated function of

space and local stability. Mixed-layer models assume, as implied by the
name, that the upper layer is well mixed. This assumption permits the
vertical integration and solution of the turbulent energy equation in
terms of the upper mixed-layer depth. According to Niiler and Kraus
(1977), this approach is probably the most effective tool for prediction
of upper ocean temperatures and heat storage.

In this section, the one-dimensional assumption and its implica-
tions are examined, and existing eddy coefficient and mixed-layer models
are reviewed. Deterministic solutions and turbulence closure models
were not considered cost-effective tools for the solution of practical
problems.

4.2 One-Dimensional Assumption

Vertical one-dimensionality assumes that forcing across the air/
water interface and vertical variations (gradients) play a dominant role
with transverse and longitudinal variations playing a secondary role.
The one-dimensional assumption therefore assumes that reservoirs are
represented by a vertical series of horizontal slices (Figure 38). Each
horizontal slice is assumed to be well mixed laterally and longitudi-
nally. Inputs to a horizontal layer are assumed to be instantaneously
mixed throughout the layer. Since vertical density gradients (i.e.,
strong stratification) inhibit vertical motions (i.e., act to keep the
isotherms horizontal), the use of a one-dimensional assumption for
stratified systems is often justified.

Ford and Thornton (1979) analyzed the time and length scales char-
acterizing the hydrodynamics, chemistry, and biology of lakes and showed
that there is both an upper and lower bound to the lake size that can be
characterized by a one-dimensional model. The lower bound was set at
horizontal dimensions on the order of 0.05 to 0.5 km to minimize hori-
zontal gradients caused by near-field effects such as local runoff and
upwelling. The upper bound was set at horizontal dimensions on the
order of 10 to 1.0 km to minimize horizontal variations caused by vari-
ations in the synoptic forcing functions.
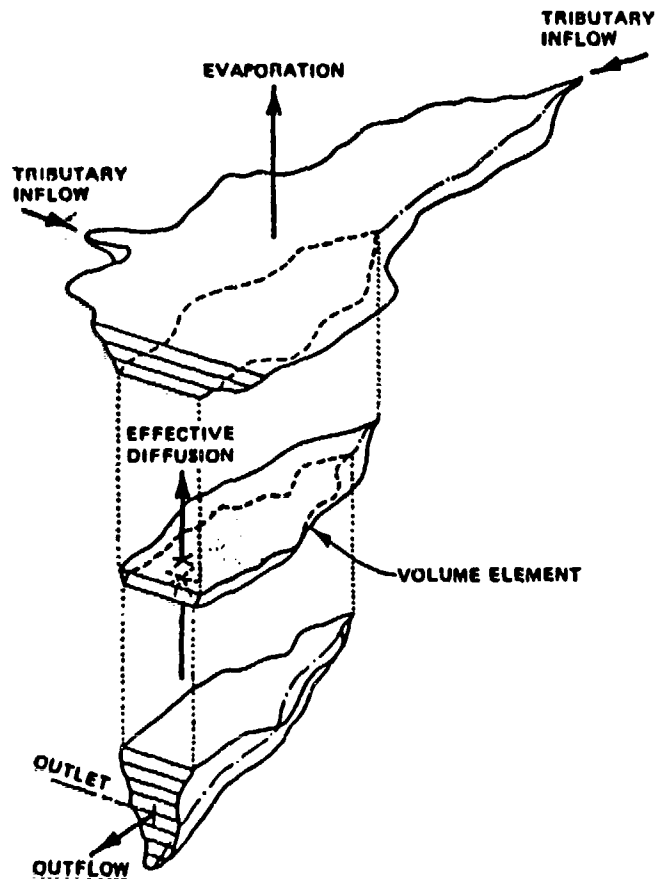
Figure 38. Vertical one-dimensional
representation

When evaluating the appropriateness of the one-dimensional assump-
tion for reservoirs, two physical factors must be specifically consid-
ered in addition to the ideas presented by Ford and Thornton (1979).
These factors are the wind setup and the horizontal penetration of the
inflow (i.e., plunge point). When the wind blows across the water sur-
face, the resulting shear stress causes the isotherms to tilt
(Section 3.2.2). If the wind is sufficiently strong, metalimnetic and
hypolimnetic waters may become exposed to the surface (upwelling) and
become mixed with epilimnetic waters. The magnitude of the wind setup
at the water surface can be estimated by comparing the applied wind
shear force

76

$$\tau_s A_s = \rho_a C_d W^2 A_s = \rho_w w_*^2 A_s \tag{23}$$

where

τ_s = shear stress, $kg/(m\text{-}sec^2)$

A_s = surface area, m^2

ρ_a = density of air, $1.177 \ kg/m^3$

W = wind speed, m/sec

ρ_w = density of water, kg/m^3

w_* = shear velocity in water, m/sec

with the pressure force (potential energy) that builds up

$$PE = \rho_w \ g \ \frac{dz}{dx} \ D \tag{24}$$

where

g = acceleration due to gravity, m/sec^2

$\frac{dz}{dx}$ = slope of water surface, m/m

D = depth of lake, m

This balance assumes no bottom shear. The slope of the water surface is

$$\frac{dz}{dx} = \frac{w_*^2}{gD} \tag{25}$$

and the slope of the thermocline

$$\frac{dz}{dx_i} = \frac{dz}{dx} \frac{\rho_w}{\Delta\rho} = \frac{w_*^2}{\frac{\Delta\rho \ Dg}{\rho}} \tag{26}$$

If (dz/dx) is approximated by $\Delta D/L$, Imberger's Wedderburn number (We) is obtained

$$We = \frac{\frac{\Delta\rho}{\rho}\, g\, \Delta D}{w_*^2}\, \frac{\Delta D}{L} \qquad (27)$$

The Wedderburn number therefore compares the slope of the interface with wind forcing. It can be used to determine if upwelling is significant. If We >> 1, upwelling is not sufficient and the one-dimensional assumption is valid.

The plunge point location provides an indication of where the riverine zone stops and the lake begins (Section 3.2.5). If the riverine zone extends a significant distance into the reservoir, the reservoir is dominated by advective forces and cannot be considered to be vertically one-dimensional. Following the recommendations of Ford and Johnson (1983), the depth of the plunge point can be determined by

$$h_p = 1.6 \left(\frac{Q_j^2}{B_c^2\, g\, \frac{\Delta\rho_j}{\rho}} \right)^{1/3} \qquad (28)$$

where

h_p = hydraulic plunge depth, m

Q_j = inflow rate, m^3/sec

B_c = width of zone of conveyance, m

$\Delta\rho_j$ = density difference between inflow and reservoir, kg/m^3

If h_p/Z_m , where Z_m is the maximum reservoir depth, is less than 1/3, the reservoir is one-dimensional.

4.3 Eddy Coefficient (Diffusion) Models

4.3.1 Description

Eddy diffusion models were initially used in the mid-1960's to predict temperature changes in deep, stratified reservoirs. They have

78

been routinely used by the CE since the late 1960's and form the basis for many one-dimensional water quality/ecological models. Eddy diffusion models are based on the vertical one-dimensional thermal energy equation:

$$
\underbrace{\frac{\partial T}{\partial t}}_{(1)} + \underbrace{\frac{1}{A(z)} \frac{\partial}{\partial z} (Q_v T)}_{(2)} = \underbrace{\frac{1}{A(z)} \frac{\partial}{\partial z} \left[(K_m + K_z) A(z) \frac{\partial T}{\partial z} \right.}_{(3)}
$$

$$
\left. + \underbrace{\frac{B(z)}{A(z)} \left[u_j(z) T_j - u_o(z) T \right]}_{(4)} \right.
$$

$$
+ \underbrace{\frac{1}{\rho_w c_p A(z)} \frac{\partial}{\partial z} \left[H_z A(z) \right]}_{(5)} \tag{29}
$$

where

T = water temperature, °C

t = time, sec

$A(z)$ = horizontal area of reservoir at elevation z, m^2

z = vertical elevation, m

Q_v = vertical flow rate, m^3/sec

K_m = molecular diffusion coefficient, m^2/sec

K_z = global vertical diffusion coefficient, m^2/sec

$B(z)$ = reservoir width at elevation z, m

$u_j(z)$ = inflow velocity distribution, m/sec

T_j = inflow temperature, °C

$u_o(z)$ = outflow velocity distribution, m/sec

ρ_w = density of water, kg/m^3

c_p = heat capacity of water, J/(kg-°C)

H_z = heat flux at elevation z, W/m^2

Term (1) on the left side is the time rate of change of temperature. Term (2) is the vertical advective transport term. It represents the flow between internal elements that is required to balance inflows and outflows and maintain continuity. If a Lagrangian or variable layer

79

scheme is used (Section 5.4.3), there is no flow between elements $(Q_v = 0)$, and term (2) is not required. Term (3) (the first term on right side of Equation 29) is the diffusion term. The molecular diffusion coefficient K_m, is usually neglected or incorporated into the turbulent diffusion coefficient K_z. Various formulations for K_z are discussed in Section 4.3.2. Term (4) of Equation 29 represents the heat input from tributaries and heat loss from outflows. The inflow and outflow velocity distributions are usually based on empirical relationships developed from laboratory experiments (e.g., Bohan and Grace 1973). Many diffusion models developed for natural lakes (e.g., Sundaram and Rehm 1973; Henderson-Sellers 1976; Walters, Carey, and Winter 1978) ignore the fourth term. For many CE reservoirs characterized by short residence times (i.e., less than 60 days), this term dominates Equation 29. Term (5), the last term in Equation 29, represents the local heat source which includes the internal heating from solar radiation. The various components of this term were discussed in Section 3.2.1.

Equation 29 can be solved by various computational techniques knowing the initial conditions, boundary conditions (i.e., heat transfer at air/water interface, inflow and outflow velocity distributions, heat transfer at sediment/water interface), and reservoir geometry (i.e., $A(z)$ and $B(z)$). In addition to these requirements, the only major difficulties remaining to solve Equation 29 are the specifications of the internal absorption of solar radiation H_z and the eddy diffusion coefficient K_z. As indicated in Section 2.2.2, the specification of H_z requires knowledge of both dissolved and particulate materials in the water. Although thermal simulations in some systems are sensitive to the attenuation of shortwave radiation, it will not be discussed further. Reviews on light penetration can be found in Williams et al. (1981).

4.3.2 Eddy Coefficient Formulations

Field measurements. Since the eddy diffusion coefficient includes the dynamics of all mixing processes, it is a complicated function of

time, space, and local stability. It is therefore informative to review results from field measurements of eddy diffusion coefficients prior to discussing the various formulations for K_z. According to Imberger and Hamblin (1982), there are no direct measurements of local values of vertical diffusion coefficients in either lakes or oceans, only basin averaged K_z values derived from global thermal budgets or tracer budgets. Since this study is concerned only with one-dimensional formulations, global- or basin-averaged coefficients are consistent with study assumptions.

In the global thermal budget approach, estimates of K_z are back-calculated from Equation 29, temperature data, and information on the internal absorption of solar radiation H_z, assuming no vertical and horizontal advective transport (i.e., terms (2) and (4) in Equation 29 are assumed to be 0). This assumption is usually valid for lakes and reservoirs with long residence times. If Equation 29 is integrated down the water column from depth z to the maximum depth Z_m, then

$$K_z = \int_z^{Z_m}\left(\frac{\partial T}{\partial t} - H_z\right)\bigg/\left(-\frac{\partial T}{\partial z}\right) \tag{30}$$

and K_z can be determined either graphically or with the aid of a computer. Typical results are shown in Figure 39, which illustrates decreased values for K_z in the metalimnion or regions of temperature gradient. The K_z values computed by the method represent an average value over the period between temperature profiles. Figure 40 illustrates that different values can be obtained if different integration periods are used. The smaller the period, the more variation in K_z. Computed K_z values may vary over several orders of magnitude from one day to the next. As discussed in Jassby and Powell (1975), it is essential that the internal absorption of solar radiation be considered when back-calculating K_z. For this reason and others, K_z should not be computed for the epilimnion using this method.

81
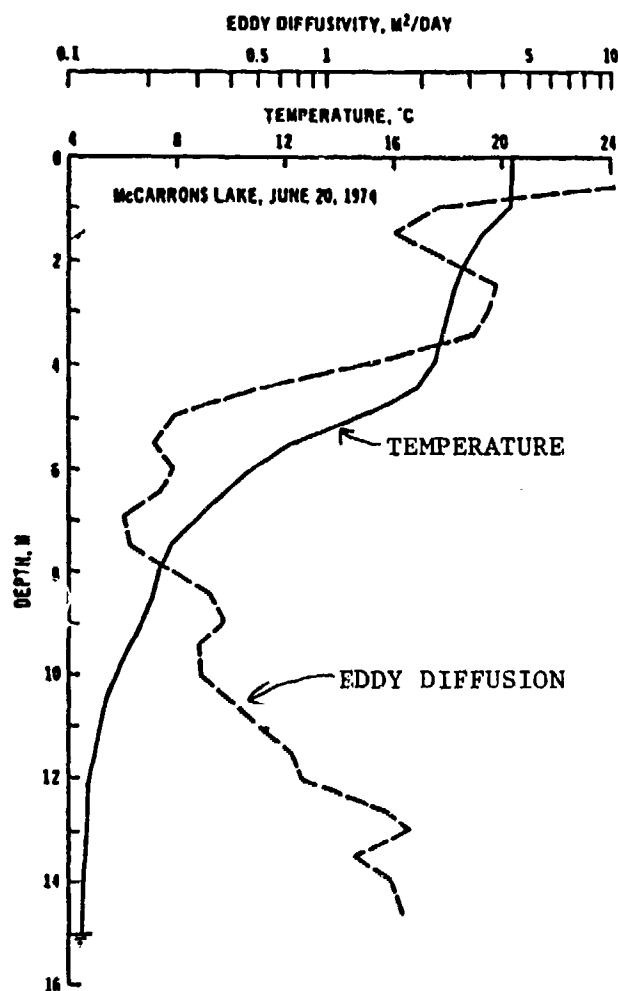
Figure 39. Vertical variation in eddy
diffusion coefficients

Eddy diffusion coefficients can also be computed from passive
tracer budgets using the one-dimensional, unsteady diffusion equation
(i.e., a modified version of Equation 29) and/or the method of moments
(Fischer et al. 1979). Examples of tracer studies include Kullenburg,
Murthy, and Westerberg (1973) using dye; Imboden et al. (1977) using
tritium; Imboden and Emerson (1978) using radon and phosphorus, and Quay
et al. (1980) using tritium. The K_z values computed from these stud-
ies represent the time scale over which the study took place. In many
instances this period is shorter than those computed by the thermal
budget approach.
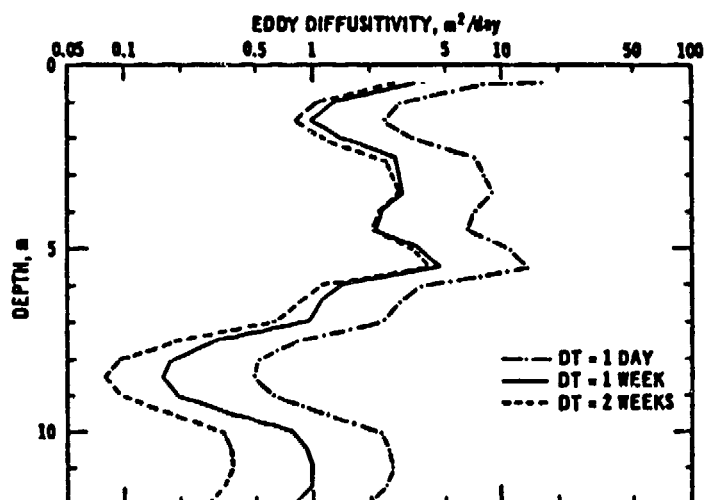
Figure 40. Variation in computed eddy
diffusion coefficients with integration
time, McCarrons Lake, Minnesota

Field studies using the thermal budget approach, tracers, or a
combination of both substantiate the following conclusions concerning
vertical diffusion coefficients. First, vertical diffusivities of heat
range from molecular (i.e., 1.42×10^{-7} m^2/sec) up to values of
10^{-4} m^2/sec (Figure 41). They are several orders of magnitude less than
horizontal eddy diffusion coefficients but greater than molecular diffu-
sion coefficients for gases and salts.

Second, vertical diffusion coefficients for heat and mass are
about the same in the hypolimnion but differ in the metalimnion. Quay
et al. (1980) found that heat diffuses faster than mass in the metalim-
nion, indicating molecular diffusion is important in determining the
rate of vertical transport in the metalimnion. As shown in Table 2, the
molecular diffusion coefficient for heat and mass differ significantly.

Third, the diffusivity is usually higher during periods of strong
winds and large inflows or outflows. Bengtsson (1978) found an almost
linear increase in log K_z with wind speed (Figure 42).

Fourth, the diffusivity decreases with increasing stability (i.e.,
stratification) according to the following relationship

83
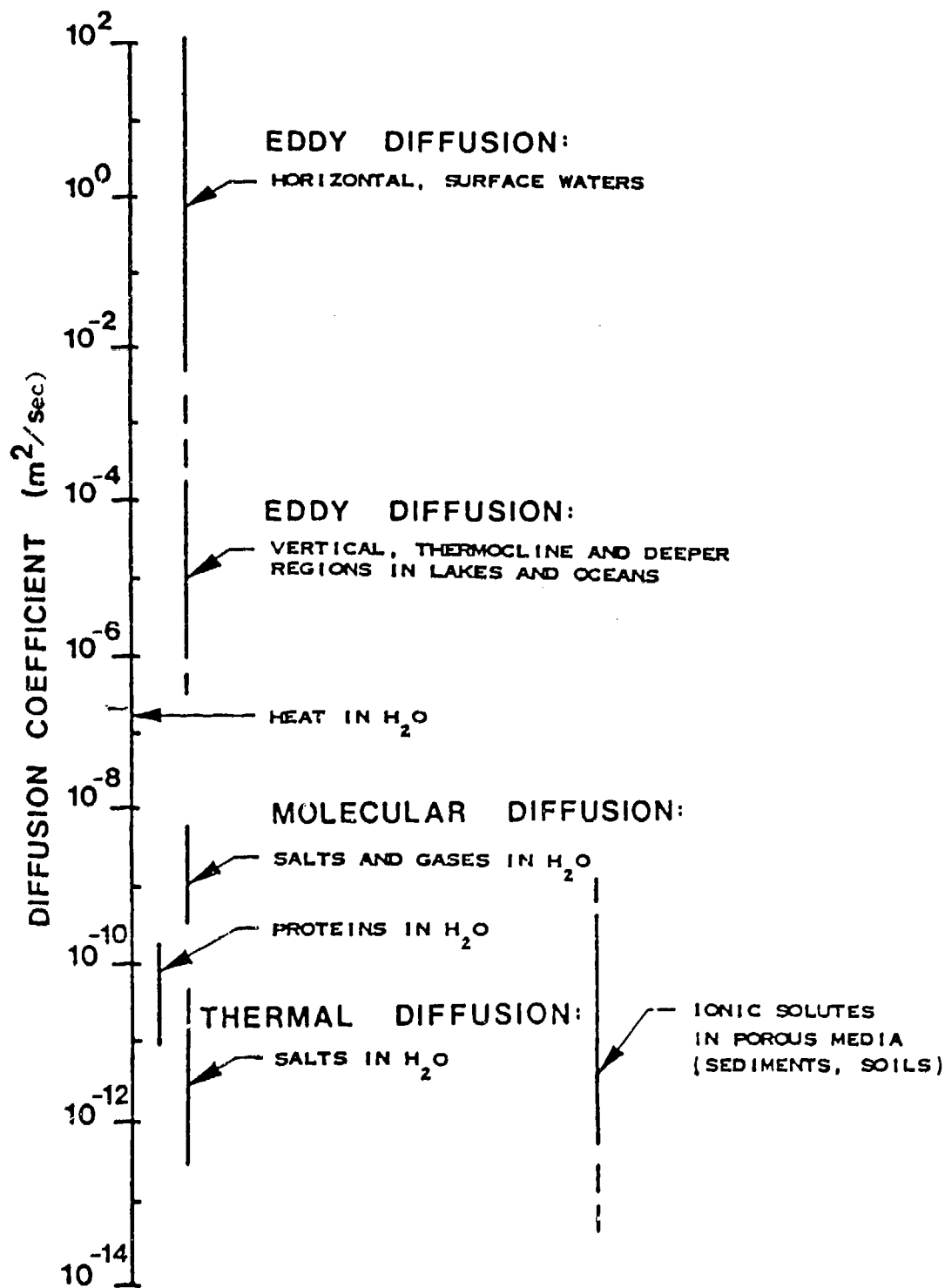
Figure 41. Comparative ranges for diffusion
coefficients (after Lerman 1971)
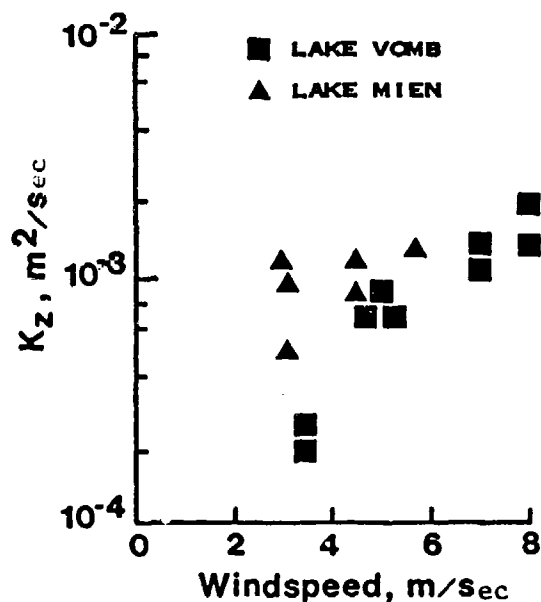
Figure 42. Increase in K_z with wind speed (after Bengtsson 1978)

$$K_z = a(N^2)^{-n} \tag{31}$$

where

a = proportionality coefficient, units vary

$N^2 = \dfrac{g}{\rho} \dfrac{\partial \rho}{\partial z}$ = buoyancy frequency, sec^{-2}

n = coefficient, dimensionless

Values for n vary from 0.25 (Hutchinson 1941) to almost 2.0 (Blanton 1973). Using dimensional analysis, Welander (1968) attributed different coefficients to different physical processes. For example, $n = 0.5$ is a local shear process and $n = 1$ is for a cascade process. Figure 43 illustrates the variation in K_z with N^2.

Fifth, diffusion coefficients generally increase with lake size. Ward (1977) related K_z to the surface area of lakes

$$K_z = 3.3 \times 10^{-9} A_s^{1/2} \tag{32}$$

85
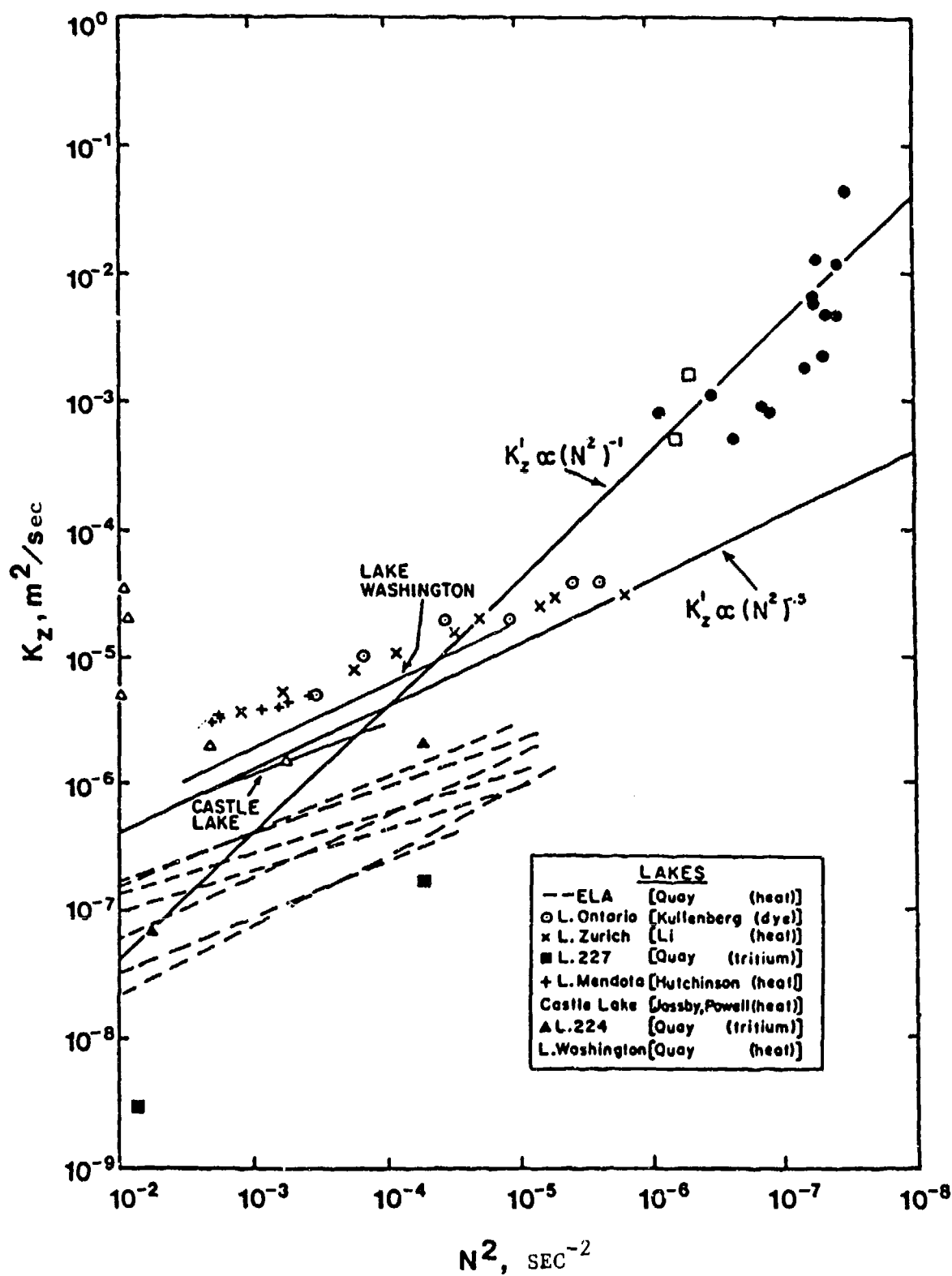
Figure 43. Variation in K_z with stratification stability N^2 (after Quay et al. 1980)

where A_s = surface area, m^2.

This relationship is consistent with the data published by Ford (1978) (Figure 44).
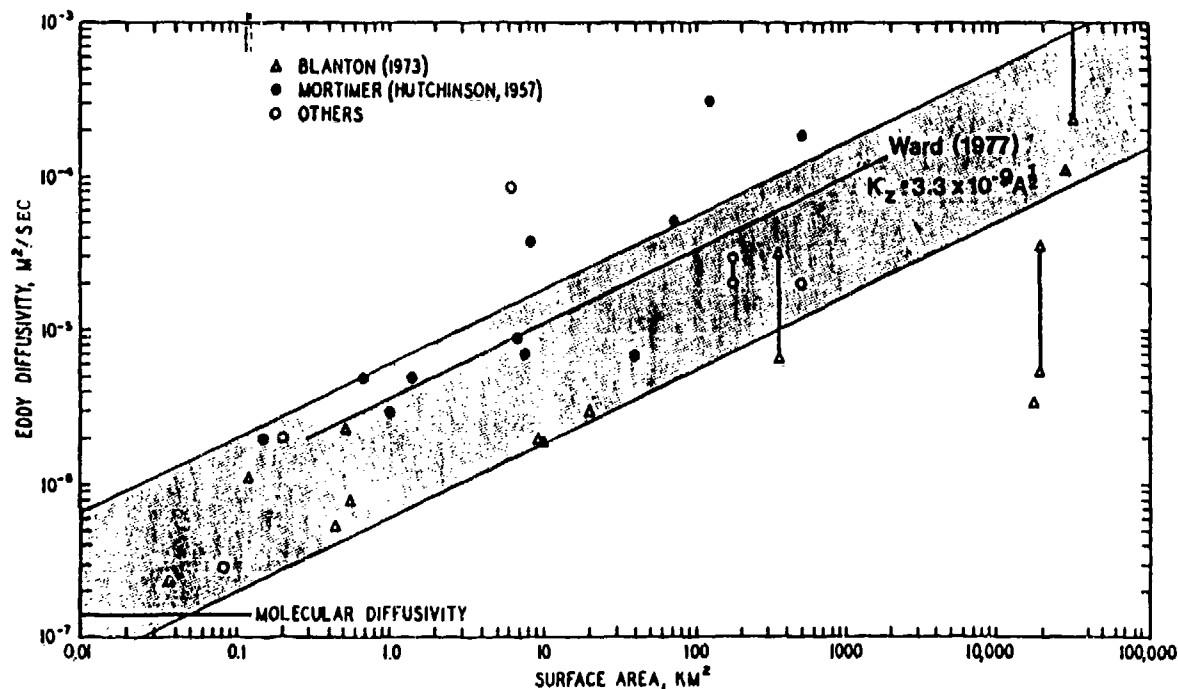
Figure 44. Variation in K_z with lake surface area

Formulations. The specification of K_z varies from model to model. If turbulent diffusion is assumed to be much larger than molecular diffusion, molecular diffusion can be incorporated into the turbulent term without any loss in precision. Some early thermal models (e.g., MIT model (Huber and Harleman 1968); Eiker Model (USAE District, Baltimore 1974)) considered the turbulent diffusivity to be constant with depth; others considered it to be dependent on the density structure and, therefore, depth dependent.

Historically, the steady-state model of Munk and Anderson (1948) was probably the first to provide insight into the interplay of turbulence, stratification, and heat flow. They assumed the eddy diffusion coefficient was related to the Richardson number by

87

$$K_z = K_{zo} (1 + a \, Ri)^{-3/2} \tag{33}$$

where

K_{zo} = eddy diffusion coefficient at neutral stability, m^2/sec

a = dimensionless coefficient

Ri = Richardson number, dimensionless

Since then, variations of this formulation have been used by Sundaram and Rehm (1971, 1973); Henderson-Sellers (1976); Walters, Carey, and Winter (1978); and others. Specific differences between formulations centered around the specification of K_{zo} , Ri , and the power (i.e., -3/2). Some specific models (e.g., Sundaram and Rehm) modify the formulation after stratification forms to account for the smaller eddy diffusivities that are normally found in the hypolimnion of stratified lakes.

Henderson-Sellers (1976) reviewed five expressions for K_{zo} :

$$K_{zo} = \frac{1}{Pr} \; \frac{w_*^2}{\left| \frac{\partial U}{\partial z} \right|} \tag{34}$$

$$K_{zo} = \frac{1}{Pr} \, k \; w_* \, (z_s - z) \tag{35}$$

$$K_{zo} = c w_* \tag{36}$$

$$K_{zo} = \frac{1}{Pr} \, k^2 \, (z_s - z)^2 \left| \frac{\partial U}{\partial z} \right| \tag{37}$$

$$K_{zo} = \frac{1}{Pr} \, k^2 \, \frac{\left| \frac{\partial U}{\partial z} \right|^3}{\left| \frac{\partial^2 U}{\partial z^2} \right|^2} \tag{38}$$

where

Pr = Prandtl number = 1 for water, dimensionless

w_* = shear velocity, m/sec

$\dfrac{\partial U}{\partial z}$ = vertical velocity gradient, (m/sec)/m

k = von Karman's constant (~0.4)

z_s = elevation of water surface, m

z = elevation, m

c = empirical coefficient, m

and recommended Equation 34. The major difficulty with Equations 34,
37, and 38 is that they require a priori knowledge of the current struc-
ture. Although it is possible to assume a simple characteristic veloc-
ity profile such as parabolic or exponential under isothermal, steady-
state conditions, stratification significantly modifies these profiles.
In addition, the impact on the current profile of the time-varying
inflow density currents, withdrawal zones, wind vectors, and complicated
reservoir geometry is totally unknown. The practicality of formulations
for K_{zo} which require the velocity gradient is therefore questionable.
Physically, Equation 35 is questionable, since K_{zo} increases with
depth, which is contrary to field observations. Equation 36 is
desirable since the K_{zo} increases with wind shear velocity in water
but undesirable since K_{zo} is constant with depth and c is not
dimensionless.

The form of the Richardson number (Ri) in Equation 33 can be taken
as

$$Ri = \frac{\dfrac{-g}{\rho}\left(\dfrac{\partial \rho}{\partial z}\right)}{\left(\dfrac{\partial U}{\partial z}\right)^2} \tag{39}$$

or

$$Ri = \frac{\dfrac{-g}{\rho}\left(\dfrac{\partial \rho}{\partial z}\right)}{\dfrac{w_*^2}{(z_s - z)^2}} \tag{40}$$

89

where

g = acceleration due to gravity, m/sec^2

$\frac{\partial \rho}{\partial z}$ = local density gradient

As with the formulations for K_{zo}, Equation 40 is preferable over Equation 39 since the velocity gradient is not known.

Substitution of Equation 36 and 40 into Equation 33 yields

$$K_z = \frac{cw_*}{\left\{ 1 + a \left[\frac{- \frac{g}{\rho} \left(\frac{\partial \rho}{\partial z} \right)}{\frac{w_*^2}{(z_s - z)^2}} \right] \right\}^b} \tag{41}$$

If a lake does not stratify (i.e., Ri = 0), Equation 41 reduces to

$$K_z = cw_* \tag{42}$$

and if a lake stratifies such that Ri >> 1, Equation 41 reduces to

$$K_z = \frac{c_* w_* \left[\frac{w_*^2}{(z_s - z)^2} \right]^b}{\left[- \frac{g}{\rho} \left(\frac{\partial \rho}{\partial z} \right) \right]^b} \tag{43}$$

where $c_* = c/a^b$, in meters.

Ozmidov (1965) took a different approach to formulating an eddy diffusion coefficient. He assumed that mixing was done at the smaller length scales and that a local steady state existed such that the rate of turbulent energy input at larger length scales is in balance with

rate of dissipation at smaller scales. Ozmidov (1965) used an equation similar to Equation 43 with $b = 1$

$$K_z = \frac{c_1 \bar{\epsilon}}{N^2} \tag{44}$$

where

K_z = global vertical diffusion coefficient, m^2/sec

c_1 = dimensionless calibration coefficient

$\bar{\epsilon}$ = dissipation rate of TKE, m^2/sec^3

$N^2 = \frac{g}{\rho} \frac{\partial \rho}{\partial z}$ = buoyancy frequency, sec^{-2}

If all of the TKE is derived from the wind, the local dissipation per unit volume is proportional to the TKE input per unit surface area (i.e., $\propto w_*^3$) (see Equations 53 and 54) divided by the water column depth z . That is,

$$\bar{\epsilon} \propto \frac{w_*^3}{z} \tag{45}$$

and Equation 45 is similar to the numerator of Equation 43 if $b = 1$.

Other formulations for eddy diffusion coefficients have been proposed, but they are all variations of the above relationships and therefore will not be discussed.

4.3.3 Assumptions and Limitations

The major assumption of eddy diffusion models is that the effects of all mixing processes can be combined into a single diffusion coefficient K_z , which is coupled to the mean concentration gradient $\partial C/\partial z$ (see Section 2.4.4). If the concentration gradient becomes small or goes to zero (i.e., as in the epilimnion), the diffusion coefficient must be made infinitely large to compensate for the decrease in gradient

91

and still result in a finite value of the flux, $K_z \partial C/\partial z$. The method, therefore, breaks down when vertical transport is under way. According to Tennekes and Lumley (1972), the concept makes sense only for flows with a single characteristic scale. Since mixing in reservoirs is characterized by many scales of motion, the validity of the concept is questionable. Since turbulence may be decoupled from the mean gradient, the concept is physically meaningless (Zeman 1981).

From a practical viewpoint, the one major limitation of the various empirical formulations for the K_z is lack of knowledge concerning the internal current structure (i.e., $\partial U/\partial z$) in reservoirs. Since the one-dimensional models under consideration in this study do not and are not capable of simulating the internal current structure of reservoirs (i.e., that is not their purpose), formulations for K_z that include $\partial U/\partial z$ are not practically viable alternatives.

4.4 Mixed-Layer Models

4.4.1 Background

In reservoirs, mixing is primarily caused by turbulence (Sections 2.4.4 and 3.2.3). Since turbulence is highly dissipative, it requires a constant source of energy to be maintained. In addition, energy is also expended when mixing occurs (Section 2.3). It is therefore logical that a turbulent kinetic energy (TKE) budget be used to analyze mixing. TKE budgets have been used by atmospheric scientists to study entrainment at the inversion base (e.g., Tennekes 1973; Stull 1976a,b; Zeman and Tennekes 1977; Deardorff 1979; Mahrt 1979), by oceanographers to investigate entrainment into the upper mixed layer (e.g., Kraus and Turner 1967; Turner and Kraus 1967; Pollard, Rhines, and Thompson 1973; Niiler 1975; Niiler and Kraus 1977; Garnich and Kitaigorodskii 1977, 1978), and by physical limnologists to study entrainment in lakes and reservoirs (e.g., Stefan and Ford 1975a,b; Hurley-Octavio, Jirka, and Harleman 1977; Imberger et al. 1978; Bloss and Harleman 1980; Ford and Stefan 1980b; Imberger and Patterson 1981). Atmospheric scientists generally perform the energy budget at the density interface, while

oceanographers and engineers generally employ a vertically integrated energy budget. These models are therefore sometimes referred to as integral energy models or mixed-layer models. According to Tennekes and Driedonks (1980), there are no substantial differences in these two approaches. The differences deal primarily with notation.

Mixed-layer models have their origin with the laboratory experiments of Rouse and Dodu (1955). They studied mixing across a density interface by generating turbulence in the upper layer of a two-layered density-stratified fluid using an oscillating grid (Figure 45). The turbulence formed a well-mixed layer, bounded by a sharp interface which moved away from the stirrer as fluid was entrained from the underlying quiescent layer into the upper well-mixed layer. Since then, other experiments employing oscillating grids (e.g., Cromwell 1960; Bouvard and Dumas 1967; Turner 1968; Brush 1970; Wolanski 1972; Crapper 1973; Crapper and Linden 1974; Linden 1973, 1975; Thompson and Turner 1975; Wolanski and Brush 1975; Hopfinger and Toly 1976), moving screens at the water surface (e.g., Kato and Phillips 1969; Kantha, Phillips, and Azad 1977), wind (e.g., Wu 1973), and oppositely directed jets (e.g., Moore and Long 1971), have indicated:

a. The turbulence produces and maintains a well-mixed layer.

b. The turbulence sharpens the interface.

c. The turbulence causes mixing across the interface.

d. The entrainment velocity or advancement speed of the interface is a function of the Richardson number.

e. Mixing takes place largely through a process which looks like the intermittent breaking of steep-faced internal waves which tend to thicken the interface, followed by the sweeping away of this fluid by the stirring in the layers, which sharpens the interface again.

f. The turbulence reflects the characteristics of the generation mechanism (e.g., grid), and therefore the scale of the generated turbulence is smaller than the mixed-layer depth.

g. The TKE generated by stirring mechanisms decays with distance from the mechanism.

The results from these experiments are summarized in Turner (1973); Sherman, Imberger, and Corcos (1978); and Pederson (1980).
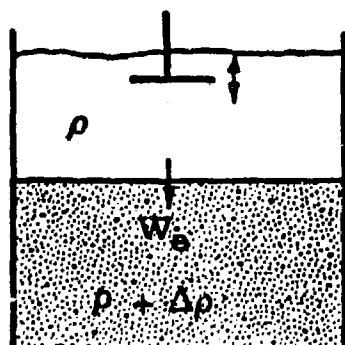
Figure 45. Schematic
of an oscillating grid
laboratory experiment

4.4.2 Description

Results from the experiments described in Section 4.4.1 and others
are used to parameterize and solve the TKE equation, which is the basis
of mixed-layer models. The TKE equation is derived by scalar multipli-
cation of the momentum equations with the turbulent velocity field and
assuming: (a) the Boussinesq approximation; (b) the main flow is
horizontal and in the direction of U ; and (c) the turbulence is homo-
geneous in the horizontal plane (see, e.g., Van Mieghem 1973, Ford 1976,
and Phillips 1977):

$$\frac{\partial}{\partial t} \overline{q^2} + \frac{\partial}{\partial z} \overline{(u(\frac{p'}{\rho_o} + q^2))} = \overline{-u_x u_z} \frac{\partial \overline{U}_x}{\partial z} - \frac{g}{\rho_o} \overline{u_z \rho'} - \epsilon \qquad (46)$$

$$\quad (1) \qquad\qquad (2) \qquad\qquad\quad (3) \qquad\quad (4) \qquad\quad (5)$$

where

$$\overline{q^2} = \overline{(u_x^2 + u_y^2 + u_z^2)}/2 = \text{TKE per unit mass}$$

u_x, u_y, u_x = turbulent fluctuations of the horizontal (x, y) and
vertical (z) velocity components, m/sec

94

p' = turbulent fluctuations of pressure, Pa

ρ' = turbulent fluctuations of density, kg/m^2

ρ_o = mean density, kg/m^2

ε = rate of dissipation of TKE, m^2/sec^3

$\bar{U}_x$ = mean horizontal velocity, m/sec

t = time, sec

z = vertical coordinate, m

In Equation 46, term (1) represents the temporal change in TKE; term (2) represents the redistribution in space of the TKE by turbulence; term (3) represents the rate of transfer of TKE from the mean flow by the Reynolds stresses; term (4) represents the gain or loss of TKE due to the release or increase of potential energy of the mean density (temperature) field; and term (5) represents the rate of dissipation of TKE.

In its present form, Equation 46 cannot be solved directly for any parameter of practical interest. The equation must therefore be parameterized in terms of variables of interest and practical significance. Following the parameterization scheme of Tennekes and Driedonks (1980), Equation 46 becomes

$$c_t \frac{\sigma w_e^2}{h} - c_f \frac{\sigma^3}{h} = -gw_e \frac{\Delta\rho}{\rho} - c_d \frac{\sigma^3}{h} \tag{47}$$

where

c_t, c_f, c_d = constants determined from experimental data

σ = velocity scale, m/sec

h = depth of mixed layer, m

$w_e = \frac{dh}{dt}$ = entrainment velocity, m/sec

Early mixed-layer models (i.e., Kraus and Turner 1967; Stefan and Ford 1975a,b; Hurley-Octavio, Jirka, and Harleman 1977; Imberger et al. 1978) assumed the temporal and shear terms (terms (1) and (3) in Equation 46) were zero and that the local dissipation equaled local

production such that Equation 47 reduced to:

$$\frac{w_e}{w_*} \propto \frac{\rho w_*^2}{g \Delta \rho h} = Ri^{-1} \tag{48}$$

when σ was assumed to scale with w_*. This dependence of the entrainment speed on the inverse of the Richardson number was found in many of the laboratory experiments previously discussed in this section. Models based on Equation 48 did an excellent job of simulating mixed-layer dynamics during periods of strong stratification but overpredicted mixed-layer depth during periods of weak stratification (Bloss and Harleman 1980).

Bloss and Harleman (1980) corrected this deficiency by using the parameterization of Zilitinkevich (1975) for the transient term (term (1) in Equation 46). Assuming shear was still small and using the constant from Zeman and Tennekes (1977), Bloss and Harleman (1980) expressed Equation 47 as a function of Richardson number,

$$f(Ri) = 0.057 \ Ri \left[\frac{29.46 - \sqrt{Ri}}{14.20 + Ri} \right] \tag{49}$$

where $Ri = \dfrac{g \ \Delta \rho \ h}{\rho w_*^2}$.

This function (Figure 46) is actually an efficiency factor for the conversion of TKE into potential energy. This modification significantly improved model predictions during periods of weak stratification.

Another deficiency of mixed-layer models was noted by Imberger and Patterson (1981). They observed that mixed-layer models always cause the metalimnetic gradient to sharpen, while field observations indicated times when the gradient was more diffuse. This prompted Imberger and Patterson to include shear (term (3) in Equation 46) in their

96
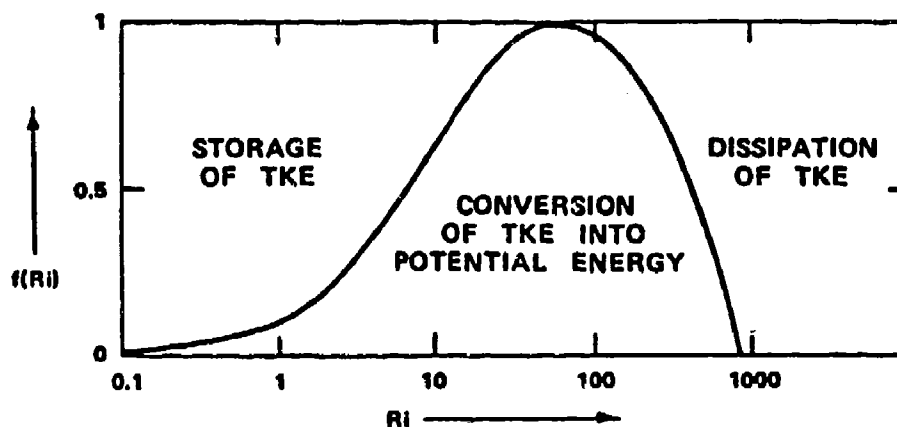
Figure 46. Efficiency factor for mixing
(after Bloss and Harleman 1980)

formulation. This improvement requires computing the slope of
thermocline under wind forcing.

4.4.3 Assumptions and Limitations

TKE or mixed-layer models assume that a well-mixed layer overlies
a region of density gradient. The depth of the upper mixed layer is
determined by the TKE input at the air/water interface and the retarding
buoyancy force of the underlying, density-stratified layer. The models
predict averaged parameters for the mixed layer but do not consider the
dynamics of the underlying density-stratified layer. Its major limita-
tion is, therefore, that it does not simulate the lower density-
stratified layer.

4.5 Summary

The review of diffusion and TKE models indicates that both
approaches have significant advantages and limitations. More important,
however, is the fact that the two approaches model different physical
mixing processes (i.e., diffusion and entrainment) and, since both of
these processes are important reservoir mixing processes, both should be
included in the recommended algorithm.

97

SECTION 5. ALGORITHM DEVELOPMENT

5.1 Introduction

The second objective of this study was to develop a mathematical algorithm that realistically represents all major mixing processes occurring in CE reservoirs. Since this algorithm is intended to be used in a generalized one-dimensional water quality model (e.g., CE-QUAL-R1 (Environmental Laboratory 1982)) to predict changes in reservoir water quality resulting from changes in hydrometeorological conditions and project operation, several requirements had to be considered during algorithm development.

First, the algorithm had to be generalized with respect to CE reservoirs. Sizes of CE reservoirs range over four orders of magnitude (Ford 1978). Some reservoirs are small and round (e.g., Eau Galle Lake, Wisconsin, and C. J. Brown Lake, Ohio) while others are large and dendritic in shape with many islands (e.g., DeGray Lake, Arkansas). Elevations and proximity to major cities (i.e., a source of meteorological data) also vary. Since there is no typical CE reservoir or location, the algorithm must therefore not be constrained by extensive morphometric and hydrometeorological data requirements. In addition, it is highly unlikely that similar mixing processes dominate in all reservoirs.

Second, the algorithm is to be used in a one-dimensional water quality model (CE-QUAL-R1). The one-dimensional assumption (Section 4.2) not only limits model applicability to certain types of lakes and problems but also limits the types of formulations that can be used. For example, one-dimensional models do not generally compute the internal current structure. Water quality is defined to include the kinds and amounts of dissolved and suspended matter in water, the physical-chemical characteristics of the water, and the ecological relations with and among aquatic organisms; therefore, the algorithm must be capable of accurately describing the vertical transport of all water quality parameters and yet not be sensitive to concentration gradients.

98

Historically, temperature predictions have been relatively insensitive to diffusion formulations when compared with other water quality parameters because temperatures are physically constrained between $0°$ and $35°$ C by heat transfer at the air/water interface, and gradients are usually no more than a few degrees Celsius per metre. In contrast, the magnitudes and gradients of other water quality parameters may vary over several orders of magnitude and may not be as physically constrained to a specific range. Model simulations of these parameters can therefore be sensitive to changes in diffusion coefficients (Thornton et al. 1979).

Third, the algorithm must be able to predict changes in the mixing regime resulting from changes in hydrometeorological conditions and project operation. As previously stated (Section 3.2), mixing in reservoirs results from hydrometeorological forcing. Superimposed on the seasonal variation in hydrometeorological forcing are short-term fluctuations. The mixing regime responds to both of these forcing scales. Different mixing regimes result depending on the timing of the forcing mechanism and the formation of stratification. A change in project operation also results in a change in the mixing regime. For example, increasing the pool level may change the mixing regime from an advective-dominated to a buoyancy-dominated regime. Lowering the outlet depth from the surface to the bottom increases hypolimnetic mixing. The algorithm must be able to simulate these changes in mixing regime, without coefficient changes, in order to be used for evaluation of management alternatives.

5.2 Evaluation Procedures

Two approaches were used in this study to evaluate alternative mixing algorithms:

a. Investigation of physical basis.

b. Applications to different reservoirs.

Although our knowledge of reservoir mixing is more qualitative than quantitative, the potential sources of TKE for mixing and the basic

functional relationships are well known (Section 3.2). Based on the review of reservoir mixing processes in Section 3.2, the important sources of TKE were identified to be the wind, inflows, and outflows (including location) and solar and atmospheric heating and cooling (i.e., convective mixing). It is also shown that mixing increases non-linearly with increases in wind speed and inflow rate. Improvements to existing formulations and/or alternative formulations were therefore first evaluated on how realistically they approximated the physical phenomena to be modeled. For example, several of the formulations for eddy diffusion coefficients (i.e., Equation 32) were discarded since they did not accurately portray mixing processes and/or did not support field observations (Section 4.3.2).

After the proposed improvements or alternative formulations were determined to be physically viable, they were evaluated by applications to a number of different reservoirs and hydrometeorological conditions. When comparing model simulations with field data, it is important to consider the previous discussion on data interpretation (Section 2.2.5), especially the uncertainty associated with field measurements. For example, in Figure 47 there is up to a $3°$ C difference in metalimnetic temperature during a 3-day period. Since this was a period of calm weather and low, steady inflows and outflows, there is little reason to expect seiching and internal waves that could cause larger temperature deviations in the metalimnion. The difference in temperatures is probably representative of field measurement errors and should be considered when comparing field data with model predictions.

Based on the review of the influence of mixing on reservoir water quality (Section 3.3), it was determined that the mixing algorithm should be able to accurately predict the onset of stratification, mixed-layer depth dynamics, metalimnetic gradient, variable mixing in the hypolimnion, fall overturn, inverse stratification during winter months, and effects of project operation to adequately address reservoir water quality problems.

An accurate representation of the onset of stratification includes not only the timing but also the depth and gradient. As explained in

100
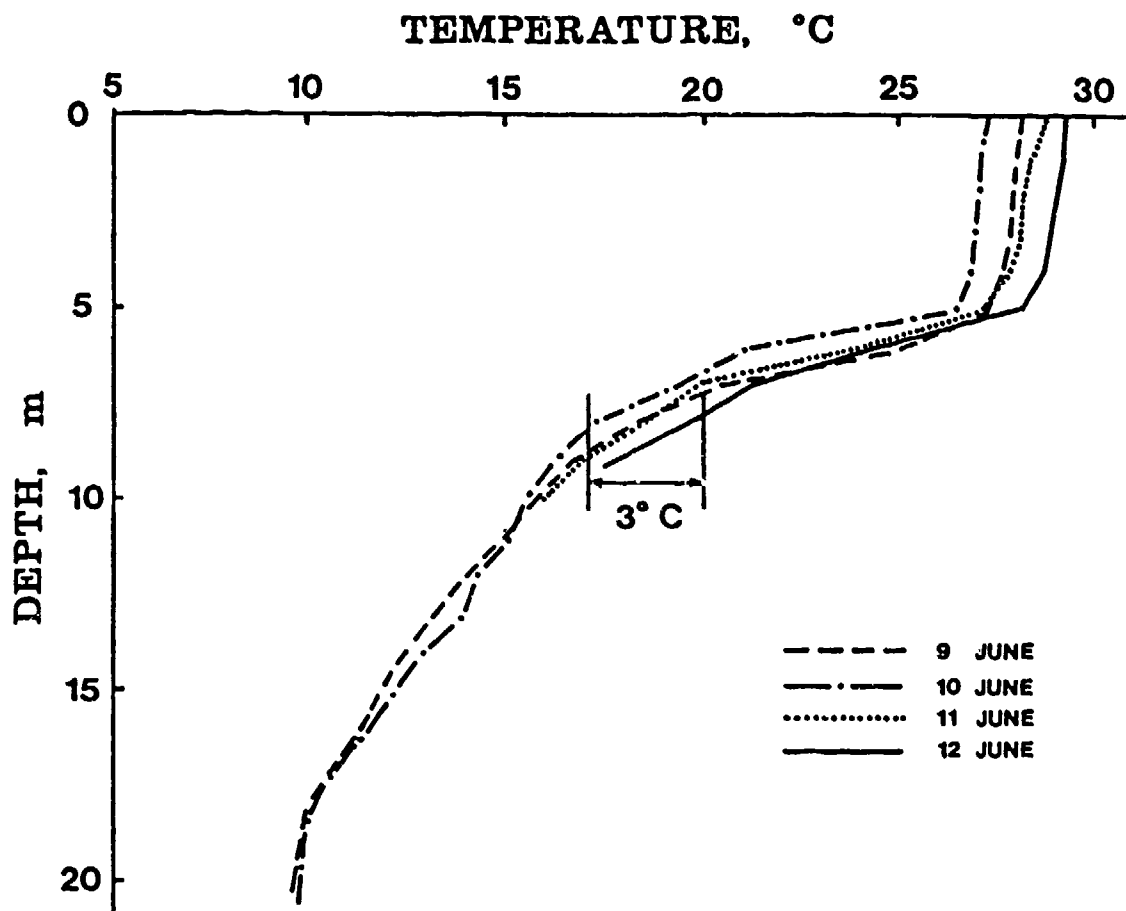
Figure 47. Daily variation in temperature profiles,
DeGray Lake, Arkansas

Section 2.2 and shown in Figure 48, reservoir stratification starts at
the bottom of a lake and moves upward, not from the water surface down-
ward as some older diffusion models predict. In many shallow
reservoirs, it is possible for stratification to form and break up sev-
eral times prior to the permanent summer stratification forming.

Daily variations in mixed-layer depths result from synoptic varia-
tions in hydrometeorological forcing as well as diel variations (Sec-
tion 2.2.3). Since the one-dimensional assumption limits the
computational time interval to 1 day (Section 4.2), it is not possible
to simulate diel variation in mixed-layer dynamics. Daily variations in
mixed-layer depths and temperatures resulting from synoptic variations
in hydrometeorological forcing are, however, significant. As indicated
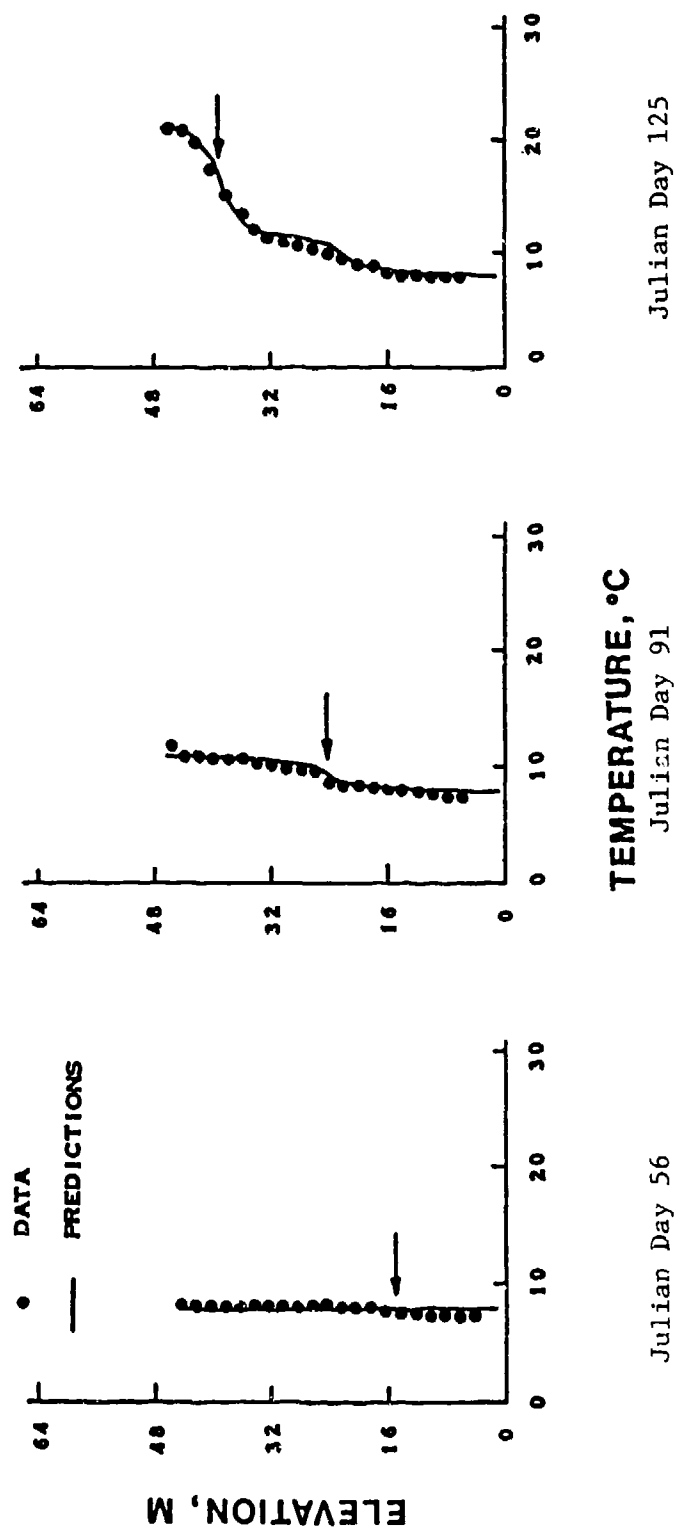
Figure 48. Simulation of the onset of stratification in Lake Greeson, Arkansas

in Section 2.2.5, it is sometimes difficult to separate diel variations from synoptic variations because most temperature data are collected at midday, not in the early morning hours.

Since density gradients inhibit mixing in the metalimnion, the dynamics of the metalimnion are sometimes ignored. An accurate representation of the metalimnetic gradient requires first an accurate portrayal of the onset of the stratification and, second, the inclusion of mixing from synoptic hydrometeorological forcing. It is important to simulate the sharpening of the metalimnetic gradient due to entrainment (Figure 49) as well as the weakening of the gradient due to advection and shear (Figure 50).

Variable mixing in the hypolimnion is dependent on hydrometeorological forcing and project operation. Although little is known about hypolimnetic mixing, it is known that mixing levels increase with hydrometeorological forcing and use of bottom gates. Because hypolimnetic temperatures can remain relatively constant, it is difficult to determine the significance of hypolimnetic mixing using only temperature data.

With fall overturn, complete vertical mixing returns to the lake. Consideration must be given to both the water temperature (i.e., heat transfer, Section 3.2.1) and the magnitude of entrainment (Figure 51). Accurate simulation of this process may require the inclusion of penetrative convection (Section 2.4.6). Because of the triangular longitudinal profile of most reservoirs (Figure 52), fall overturn appears to start at the upstream end of the reservoir and move downstream toward the dam.

Many CE reservoirs are located in cold climates and experience ice and snow covers that isolate the lakes from exchanges across the air/ water interface. The lakes then become inversely stratified, and mixing is dominated by inflow and outflow processes. The actual formation of complete ice cover may take as little time as a few hours during a cold, calm night in small reservoirs, to several weeks in large reservoirs. Some reservoirs may never experience complete ice cover. To accurately simulate mixing during the period of ice formation, a measure of the
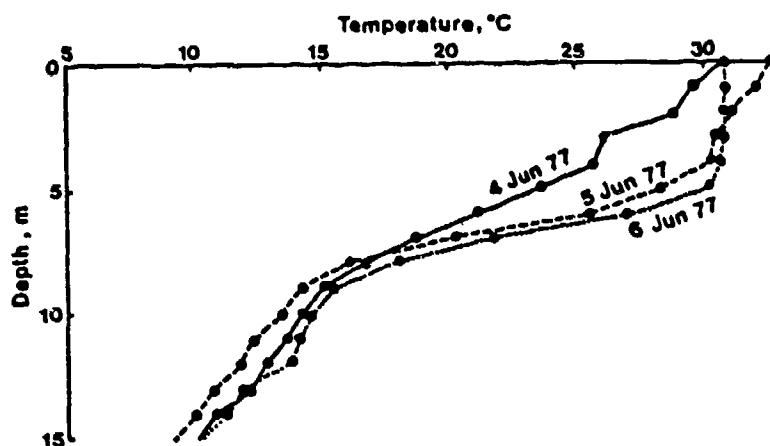
Figure 49. Sharpening of the metalimnetic
gradient due to entrainment, DeGray Lake,
Arkansas
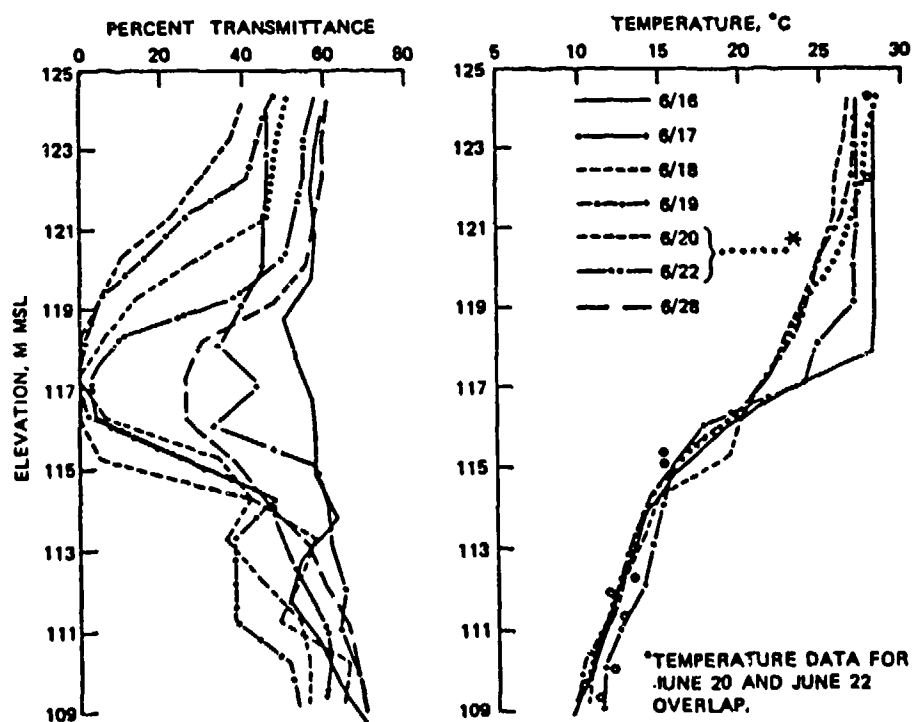
STATION 12, JUNE 1977

Figure 50. Weakening or diffusion of the metalimnetic
gradient due to shear (inflow), DeGray Lake, Arkansas
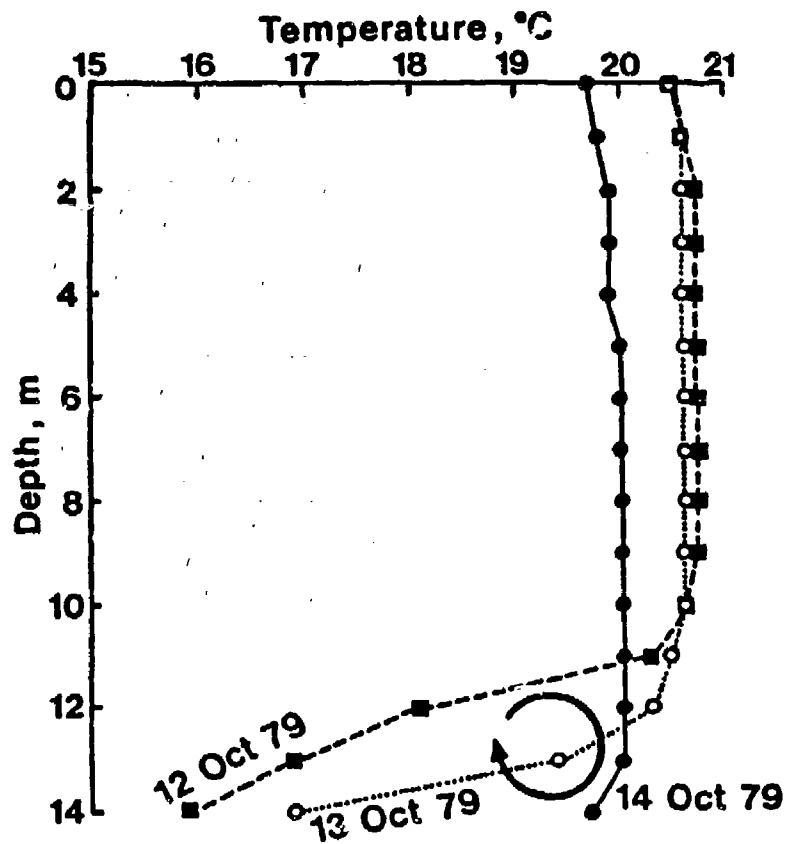
Figure 51. Fall overturn in DeGray Lake, Arkansas
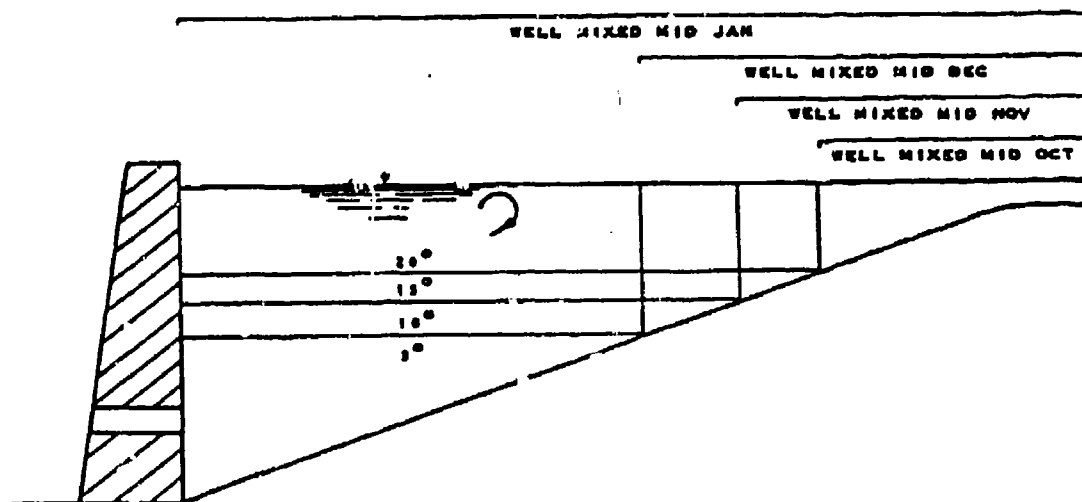
Figure 52. Triangular shape of a reservoir

size of ice-free water is required, necessitating the use of partial
area ice cover algorithm (Schultz International, Ltd. 1984).

As previously described (Section 3.2.6), project operation can
alter the mixing regime in a reservoir. In addition to considering the
nonlinear effects of localized TKE input and its interactions with den-
sity stratification, an accurate representation of the mixing regime
must consider other algorithms that compute effects of project operation
such as selective withdrawal zones.

5.3 Historical Development

5.3.1 WQRRS

Initial work on the mixing algorithm began with the 1974 version of
the Water Quality for River-Reservoir Systems model (WQRRS) (Hydrologic
Engineering Center 1974.) WQRRS was the basis from which CE-QUAL-R1
evolved (Environmental Laboratory 1982). WQRRS used the eddy diffusion
coefficient formulation shown in Figure 53. Eddy diffusion coefficients
were constant and equal in both the epilimnion and hypolimnion. Meta-
limnetic coefficients were decreased based on the density gradient and a
calibration coefficient, A3. The metalimnion was distinguished form the
epilimnion and hypolimnion using a user-specified stability criterion,
GSWH. The major limitations of this formulation were the assump-
tions of equal, constant eddy diffusion coefficients in the epilimnion

WIND MIXING / DIFFUSION
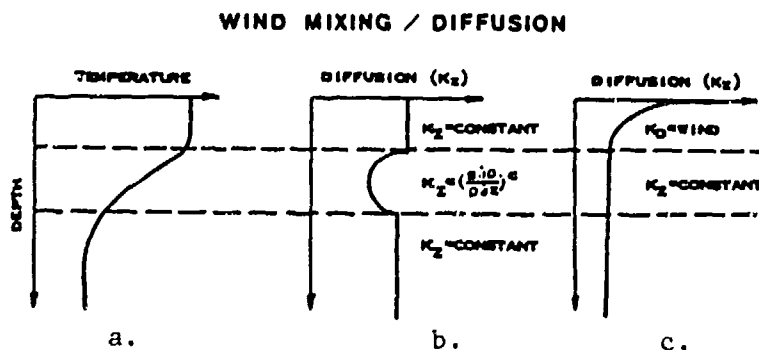
Figure 53. WQRRS diffusion coefficient
formulations

and hypolimnion and no consideration of the wind as a mixing mechanism (Figure 53b).

WQRRS did contain an alternative formulation that considered the wind (Figure 53c), but in this formulation the dependence on the wind speed was linear and therefore not physically correct. This formulation also did not consider the reduced mixing in the metalimnion resulting from density gradients. As discussed in Section 4.3.2, the need for reduced mixing in the metalimnion is critical, and models that do not reduce metalimnetic eddy diffusion coefficients with increasing density gradients characteristically predict a metalimnetic gradient that is too weak even if the simulations are started with a measured temperature profile after stratification forms (e.g., Figure 54).
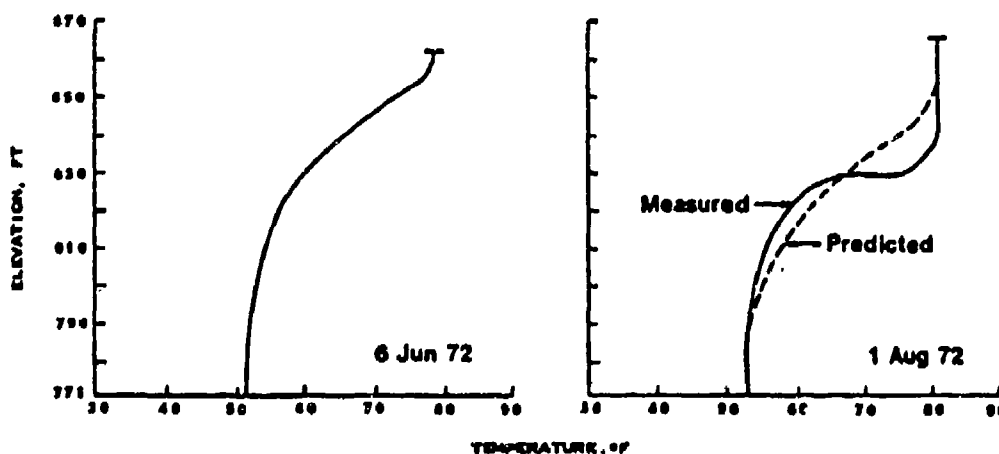
Figure 54. Diffused metalimnetic gradient resulting from using a constant diffusion coefficient

Both of these formulations received numerous applications and, for the most part, did an adequate job of representing the thermal regime in reservoirs. In many simulations (e.g., Figure 55), hypolimnetic temperatures were too low in the spring and too high in late summer, indicating insufficient mixing during spring turnover and too much hypolimnetic mixing during the summer stratified period.

In order to eliminate these deficiencies and improve model simulations, the formulation in WQRRS was modified to include the effects of
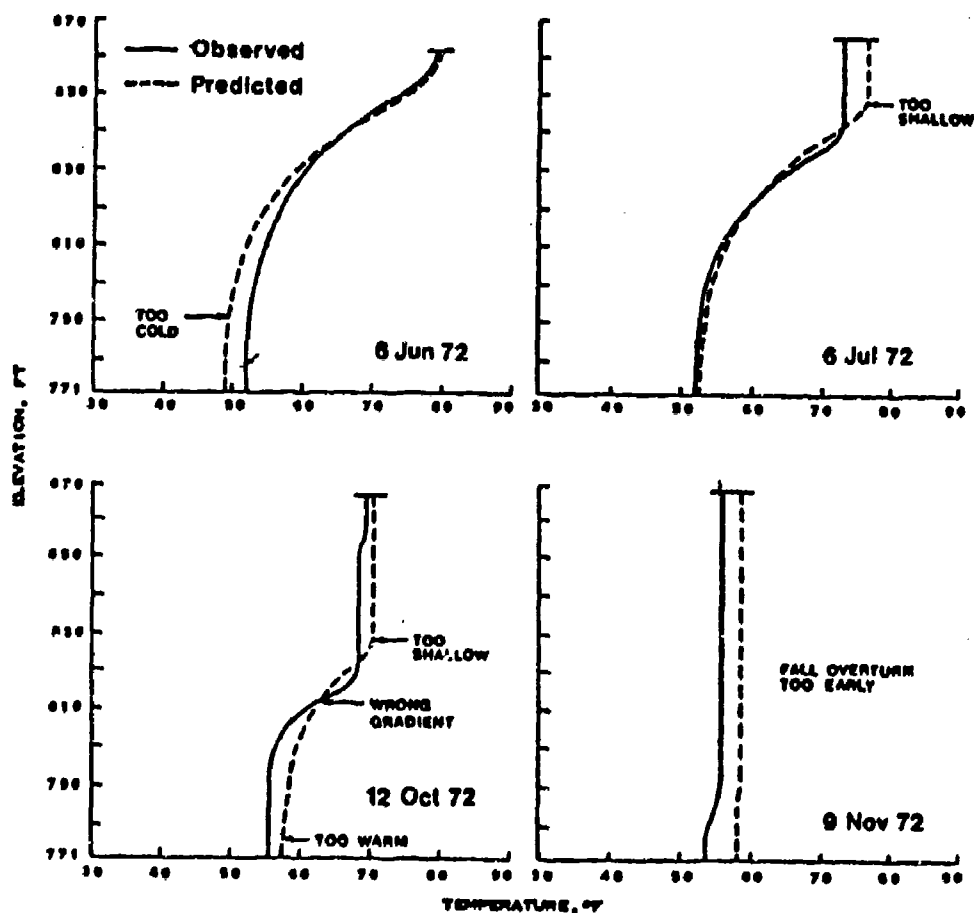
Figure 55. General characteristics of predictions
using WQRRS, Stockton Lake, Missouri (to convert
feet to metres, multiply by 0.3048; to convert
degrees Fahrenheit to degrees Celsius, use the
following formula: C = (5/9)(F - 32))

the wind and to separate mixing in the epilimnion from mixing in the

hypolimnion (Figure 56). The formulation retained the stability

criteria and metalimnetic formulation from WQRRS. The hypolimnetic

mixing coefficient was a separate user-specified diffusion coefficient

that was considered constant throughout the simulation period; the epi-

limnetic mixing coefficient was dependent on the wind shear stress

(i.e., wind speed squared) and either decreased linearly with depth to

the hypolimnetic diffusion coefficient value (Figure 56a) or was con-

stant with depth (Figure 56b). Simulations of a number of different

reservoirs indicated the linear decreasing formulation was preferable.
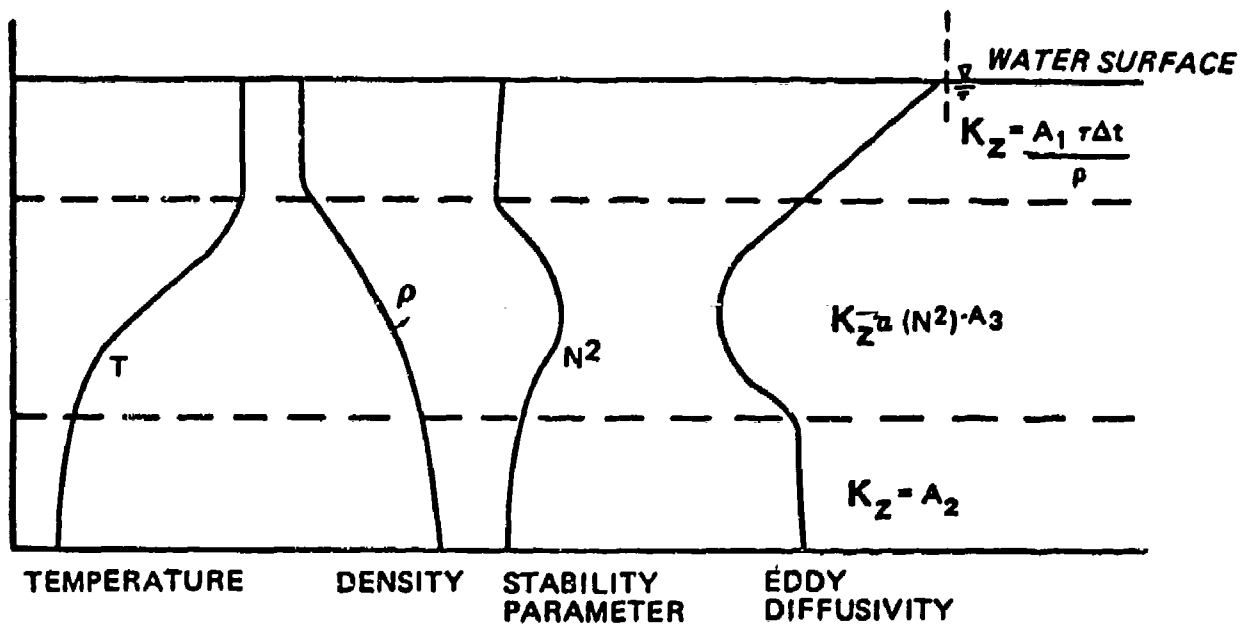
a. Linear with depth
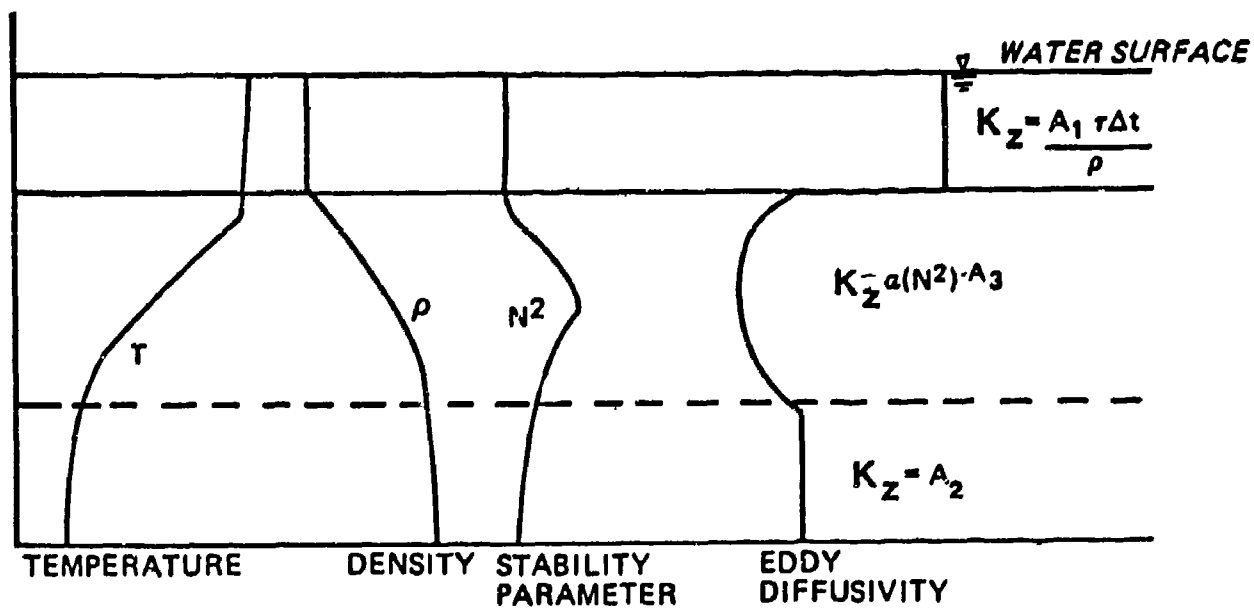
b. Constant with depth

Figure 56. Modified WQRRS diffusion coefficient formulation

As with WQRRS, the stability criterion GSWH was used to define the density-dependent metalimnion.

This eddy diffusion coefficient formulation considered similar physical processes to those in the Richardson number formulations discussed in Section 4.3.2 but had more coefficients to calibrate to match field data. Stafford (1978) showed that although he could match the temperature structures of Lakes Greeson, Arkansas, and Sardis, Mississippi, for any single year, it was not possible to match temperature structures for 5 consecutive years using the same calibration coefficients. Selected calibration profiles from Lake Greeson (from 1972) are compared with verification simulations from 1974 in Figure 57. It is readily apparent from Figure 57 that the formulation was either not correctly calibrated or not capable of simulating different hydrometeorological conditions without recalibration. Simulations using other Richardson number-based formulations produced similar results, indicating that a Richardson number-type formulation for the diffusion coefficients, alone, was not adequate to accurately simulate changes in a lake's thermal structure resulting from hydrometeorological conditions.

5.3.2 Variable Layer Formulation

One of the problems associated with the 1974 Lake Greeson predictions (Figure 57) was excessive metalimnetic mixing. This mixing resulted, in part, from the vertical advective term (term (2)) in Equation 29 for two reasons. First, reduction of the mixing coefficients to produce molecular diffusion in this region did not improve model predictions. Second, the outlet was located in the metalimnion at the same elevation where excessive mixing was observed.

To reduce this numerical mixing, the variable layer concept or Lagrangian approach of Imberger et al. (1978) was incorporated into the model. With this approach there is no vertical advection term and the layers are allowed to expand or contract with layer inflows and outflows. A simple example illustrating the differences between the fixed layer model and variable layer model is shown in Figure 58. With the fixed layer model, the net result of the mass inflow to the top layer and withdrawal from the bottom layer is an increase in bottom layer

110
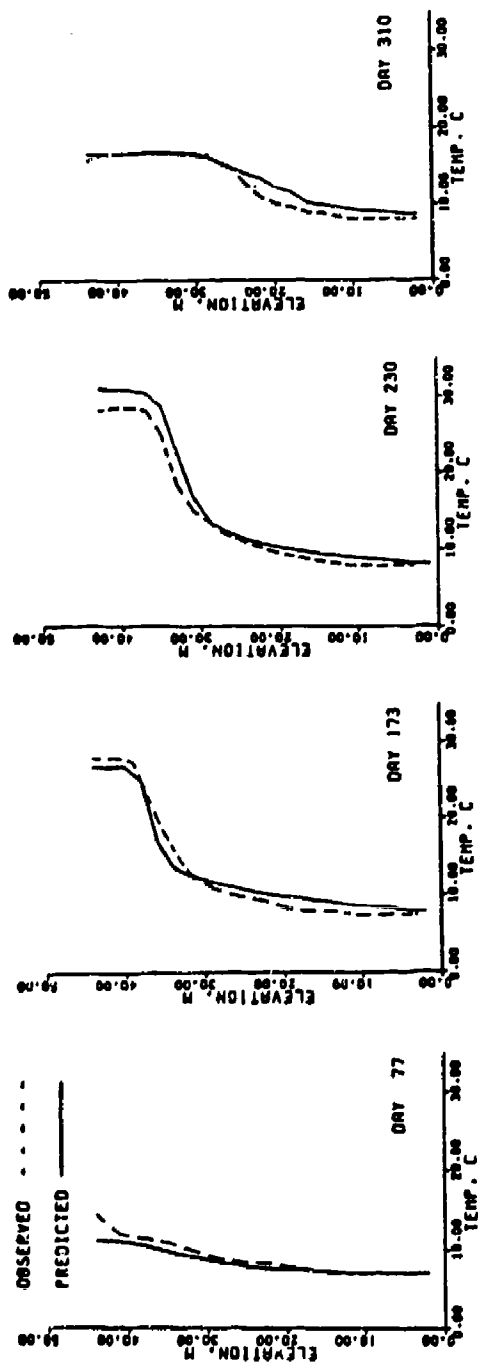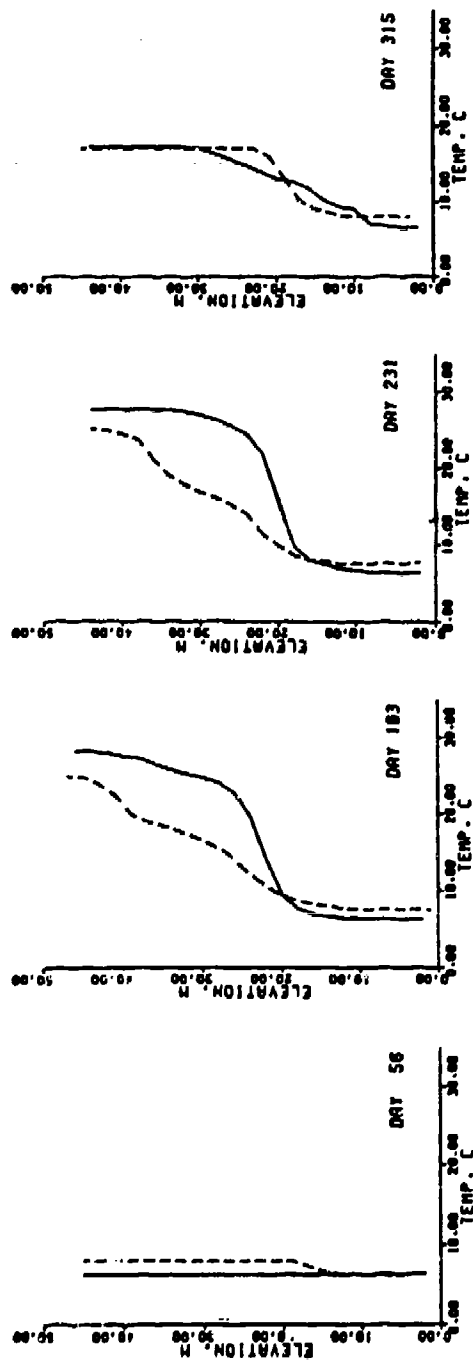
Figure 57. Calibration and verification simulations from Lake Greeson, Arkansas (after Stafford 1978)

111
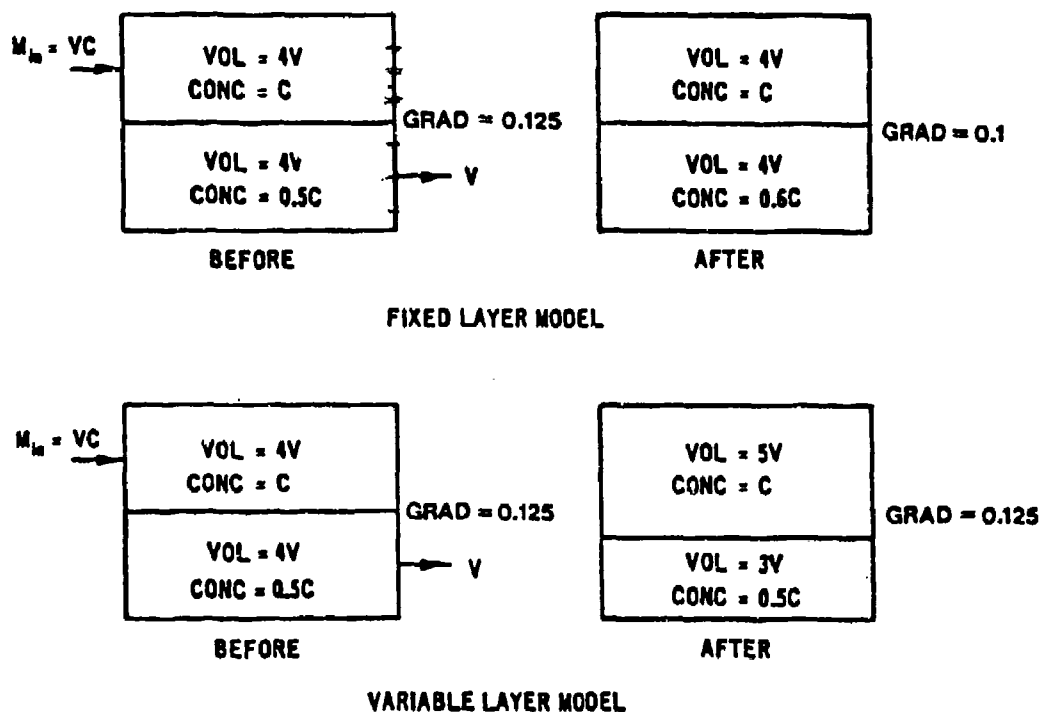
Figure 58. Schematic comparing fixed and variable
layer formulations

concentration (0.5C to 0.6C) and decrease in the vertical concentration
gradient between the two layers. The volumes or sizes of the two layers
remain constant. In contrast, with the variable layer model, the top
layer increases in size and the bottom layer decreases in size while the
layer concentrations and the gradient remain unchanged.

A comparison of model predictions using the variable and fixed
layer formulations is shown in Figure 59. As expected, there was less
metalimnetic mixing with the variable layer formulation.

5.3.3 Mixed-Layer Dynamics

In addition to problems associated with simulating consecutive
years on Lake Greeson, the modified WQRRS formulation also did not accu-
rately portray the onset of stratification and mixed-layer dynamics.
Since Ford (1976) showed that a simple TKE formulation (Section 4.4) was
able to accurately reproduce the onset of stratification and mixed-layer
dynamics in small natural lakes and Hurley-Octavio, Jirka, and Harleman
(1977) and Imberger et al. (1978) were able to simulate the thermal

112
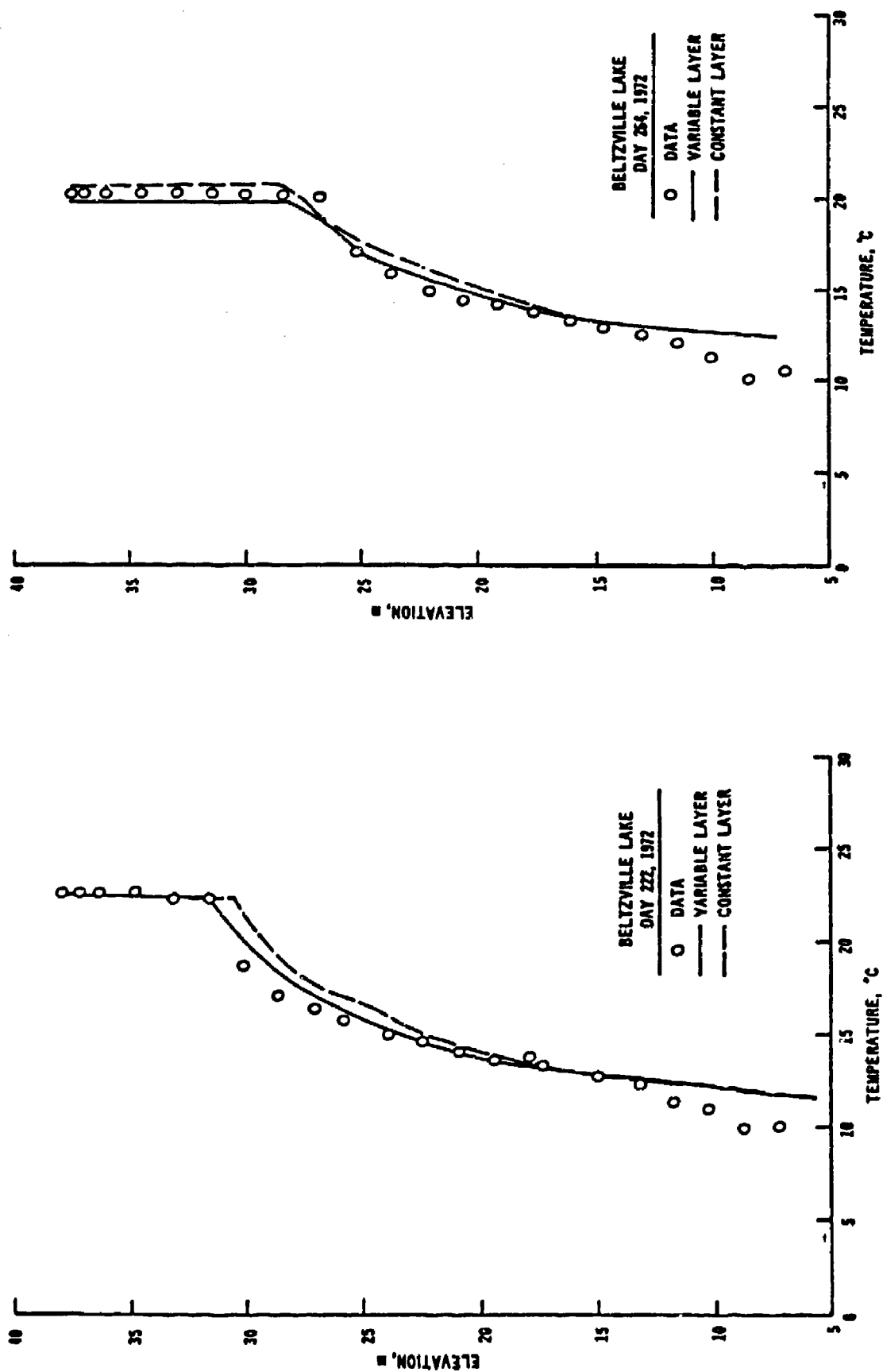
Figure 59. Comparison of thermal predictions using fixed and variable layer formulations

structure of larger reservoirs using similar formulations, a TKE
formulation or mixed-layer formulation was incorporated into the mixing
algorithm.

Initially, the mixed layer formulation followed the approach of
Ford (1976) and Hurley-Octavio, Jirka, and Harleman (1977) and did not
consider dissipation of TKE with depth. Although the simulations of the
onset of stratification improved (Ford et al. 1981), there was too much
entrainment during periods of weak stratification (i.e., the predicted
mixed-layer depths were too deep) (Figure 60). Imberger et al. (1978)
avoided this problem by dissipating the TKE with depth using a cubic
function. There was, however, no physical basis for the function. Not-
ing the same problem with the Hurley-Octavio model, Bloss and Harleman
(1980) developed an efficiency function for entrainment based on the
Richardson number (Section 4.4). This function significantly improved
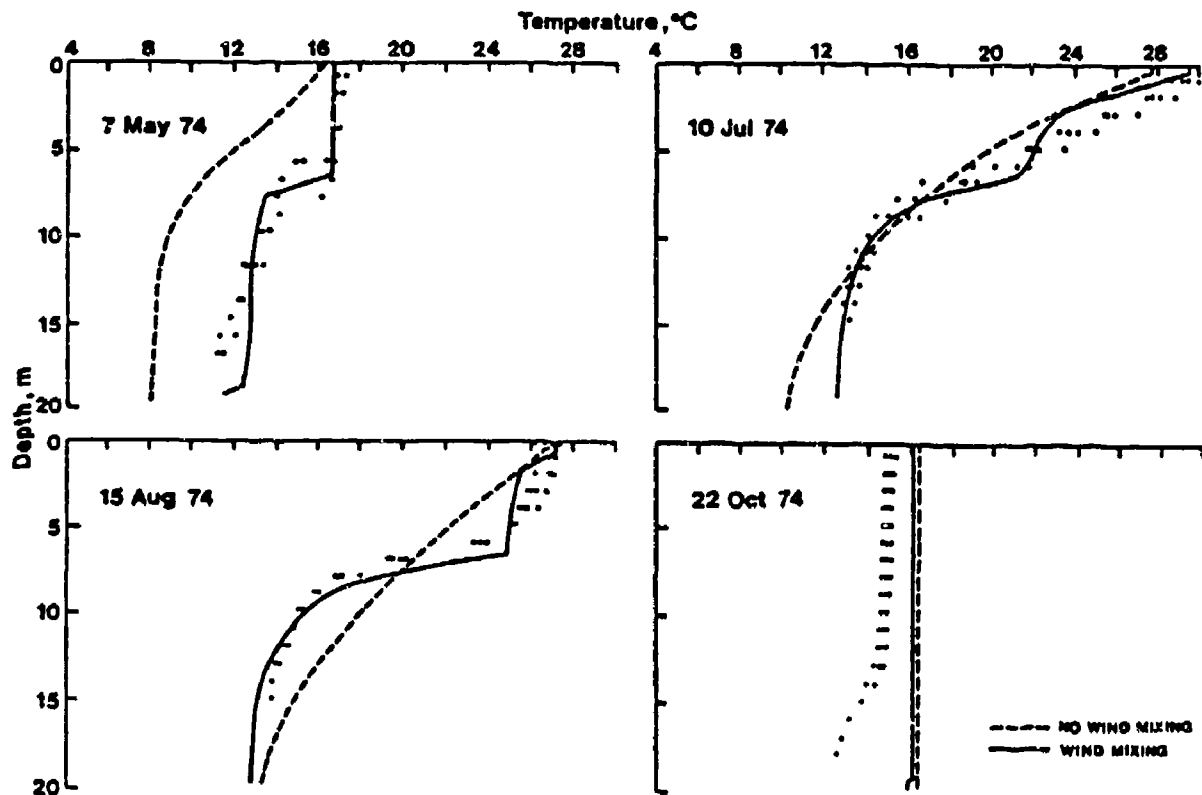
Figure 60. Comparison of simulation results from a diffusion and
TKE model, Lake Anna, Virginia (after Hurley-Octavio, Jirka, and
Harleman 1977)

114

model simulations (Figure 61). Johnson and Ford (1981) were able to
simulate 6 years of data at DeGray Lake, Arkansas, and 5 years at Lake
Greeson, Arkansas (including the years Stafford (1978) had problems
with). Figures 62 and 63 compare Stafford's results using a diffusion
model with Johnson and Ford's results using the TKE formulation in a
diffusion model.

In the 1975 simulations (Figure 62), the onset of stratification
(Julian Day (JD) 91), mixed-layer depths, metalimnetic gradients, and
hypolimnetic temperatures (JD 167, 251, and 321) were all more accu-
rately simulated with the mixed-layer formulation. The 1973 simulations
(Figure 63) were also significantly better with respect to these param-
eters. As shown in Figure 64, the mixed-layer depth or TKE formulation
was able to accurately predict differences in metalimnetic gradients
resulting from hydrometeorological forcing. As previously indicated
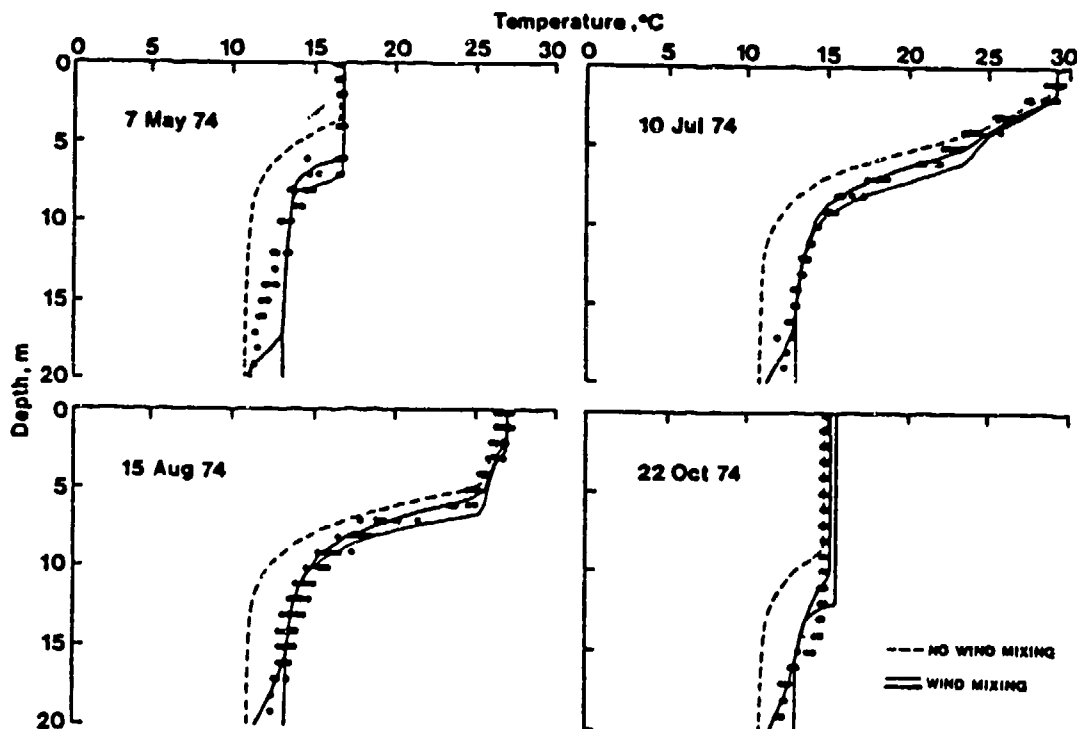
Figure 61. Comparison of simulation results with and without
dissipation function, Lake Anna, Virginia (after Bloss and
Harlemann 1980)
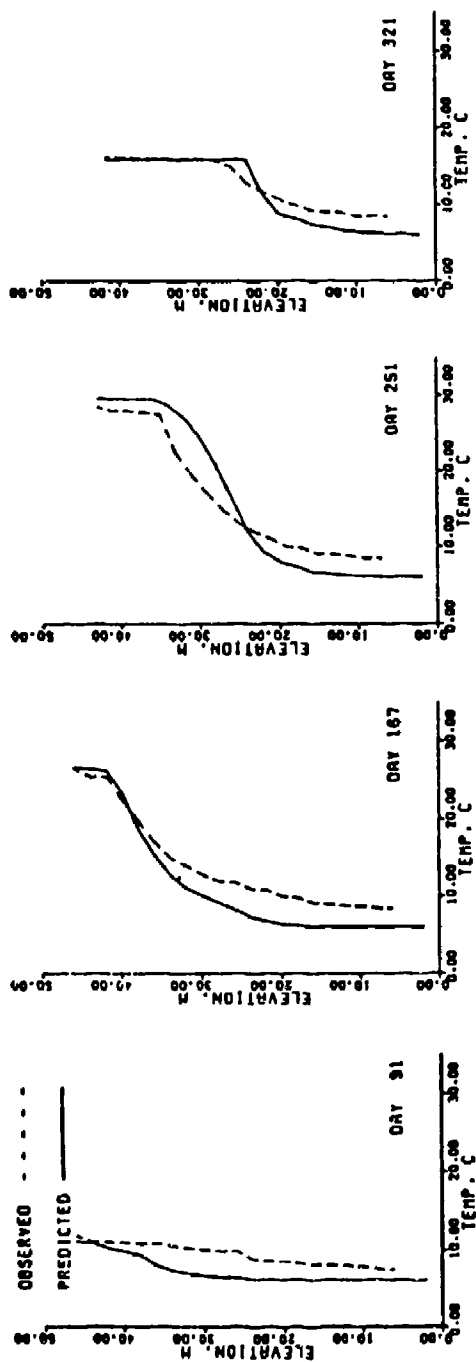
a. Diffusion model only
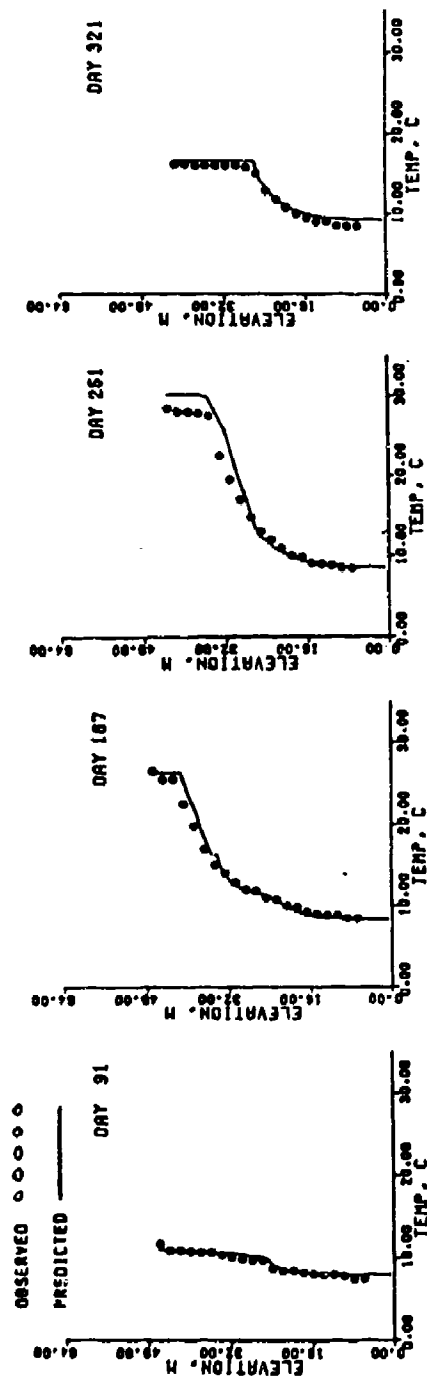
b. TKE formulation included

Figure 62. Comparison of diffusion and TKE model results, Lake Greeson, Arkansas, 1975

116
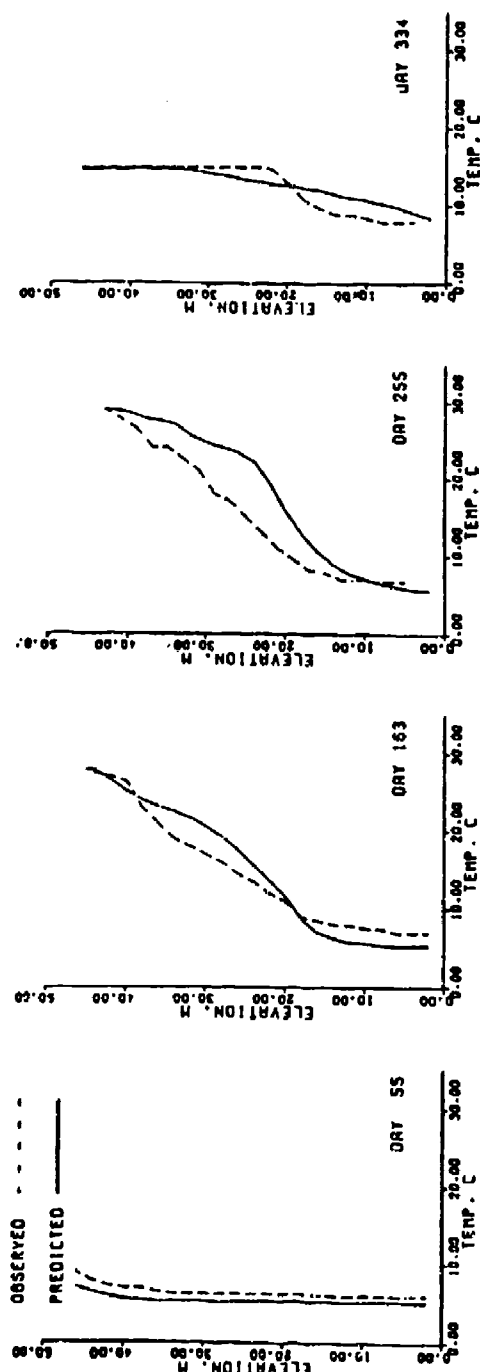
a. Diffusion model only
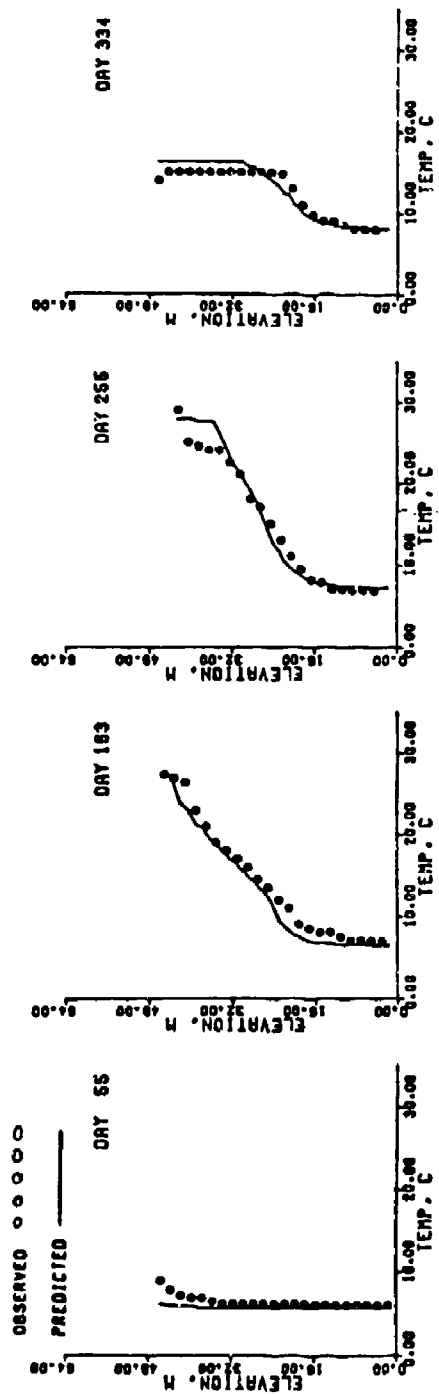
b. TKE formulation included

Figure 63. Comparison of diffusion and TKE model results, Lake Greeson, Arkansas, 1973

117
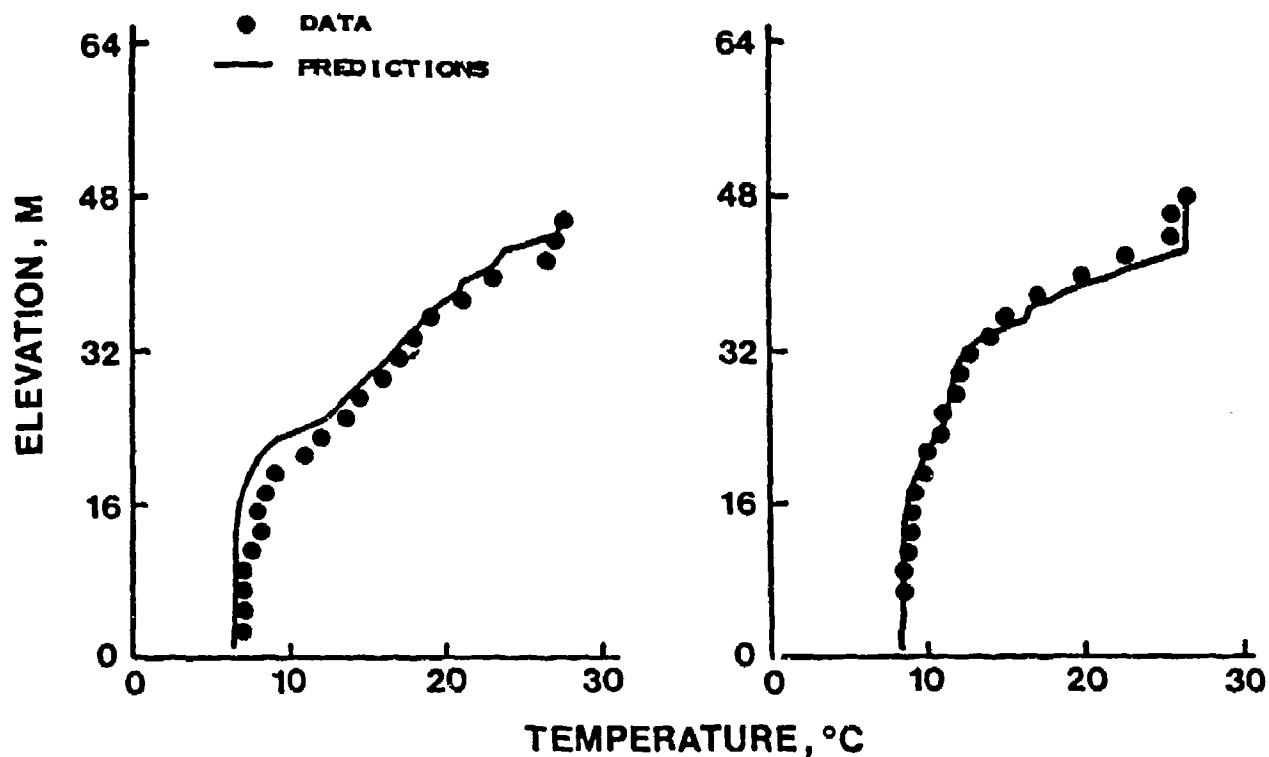
Figure 64.   Simulation of metalimnetic gradient, Lake Greeson, Arkansas

(Section 5.3.1), pure diffusion models based on Richardson number for-
mulations were not able to reproduce these differences.

5.3.4   Diffusion Coefficient Formulation

The incorporation of the variable layer concept and mixed-layer
dynamics into the model reduced numerical dispersion (Section 5.3.2),
improved mixed-layer depth predictions (Section 5.3.3), and identified
the need to modify the diffusion coefficient formulacion. Model simu-
lations using the modified formulation indicated that mixing from
inflows and outflows was not being adequately considered and that the
hypolimnetic mixing coefficient should be variable and dependent on the
wind speed.

Analysis of storm event data from DeGray Lake, Arkansas, clearly
showed that mixing from inflows diffuses or weakens the metalimnetic
temperature gradient (Figure 50). In the fixed layer formulation,
mixing from inflows and outflows was introduced through the numerical
dispersion introduced from the vertical advection. Elimination of this

dispersion with the incorporation of the variable layer concept also eliminated much of the mixing associated with inflows and outflows in the model. Since Ozmidov (1965) related the eddy diffusion coefficient to the dissipation rate of TKE (Equation 44), mixing from inflows and outflows was incorporated into the eddy diffusion coefficient by computing the TKE input associated with advection in a horizontal layer i :

$$TKE_a = \frac{1}{2} \rho_w Q_i U_i^2 \qquad (50)$$

where

Q_i = flow rate in layer i, m^3/sec

U_i = flow velocity in layer i, m/sec

Equation 44 was used to incorporate variable mixing into the hypolimnion of a lake. Since wind-generated TKE can indirectly enter the metalimnion and hypolimnion via seiche motion and breaking of internal waves, the wind-generated TKE was assumed to be dissipated throughout the entire reservoir.

These formulations were incorporated in CE-QUAL-R1 and used by Johnson and Ford (1983) to simulate the thermal structures of Lakes DeGray and Greeson.

5.4 Recommended Algorithm

Based on an investigation of the physical basis for a number of algorithms and applications to reservoirs representing different regions of the country, different hydrometeorological conditions, and different operating conditions, it is recommended that the generalized, one-dimensional model capable of simulating changes in the mixing regime include:

<u>a</u>. Variable layer formulation.

119

<u>b</u>. Mixed-layer dynamics using the efficiency function of Bloss and Harleman (1980) and considering penetrative convection.

<u>c</u>. Variable diffusion coefficient that depends on wind, inflows, outflows, and density differences.

5.4.1 Variable Layer Formulation

A Lagrangian or variable layer formulation is recommended to reduce numerical diffusion and to allow calibration of the mixing resulting from inflows and outflows. Although the details and advantages of the variable formulation using power functions for the area $A(z)$

$$A(z) = a_1 \, Z \, \exp \, (a_2) \tag{51}$$

and the volume $V(z)$

$$V(z) = \frac{a_1}{a_2 + 1} \, Z \, \exp \, (a_2 + 1) \tag{52}$$

are fully described in the CE-QUAL-R1 User's Manual (Environmental Laboratory 1982), experience has shown that these simple power functions do not always provide a sufficiently accurate representation of reservoir geometry for water quality simulations. It is therefore recommended that a polynomial function or a lookup table of actual areas and volumes be used in future versions of CE-QUAL-R1.

5.4.2 Mixed-Layer Dynamics

A mixed layer of TKE formulation is recommended to accurately simulate the onset of stratification and mixed-layer dynamics. This type of formulation ensures that stratification starts at the bottom of the lake and moves up, and that the dynamics of hydrometeorological forcing determine the shape of the metalimnetic temperature gradient. An accurate representation of mixed-layer dynamics during periods of cooling requires consideration of penetrative convection.

<u>Wind.</u> The TKE available for possible entrainment from the wind shear can be estimated by

$$TKE_w = \int_{A_s} c_t \, w_* \, \tau_s \, \Delta t \, dA \qquad (53)$$

where

TKE_w = wind shear turbulent kinetic energy, $(kg-m^2)/sec^2$

A_s = water surface area, m^2

c_t = empirical coefficient

w_* = shear velocity of water, m/sec

τ_s = shear stress at the air/water interface, $kg/(m-sec^2)$

Δt = time step, sec

The shear velocity w_* is defined by

$$w_I = \sqrt{\frac{\tau_s}{\rho_w}} \qquad (54)$$

in which ρ_w = water density, kg/m^3.

The shear stress at the air/water interface is given by:

$$\tau_s = \rho_a \, C_d W^2 \qquad (55)$$

where

ρ_a = air density ($1.177 \ kg/m^3$)

C_d = dimensionless drag coefficient

W = wind speed, m/sec

The drag coefficient is taken from Safaie (1978):

$$C_d = 0.00052 \, W^{0.44} \qquad (56)$$

In many lakes, the wind stress does not act on the entire surface area because of sheltering effects from the surrounding terrain. The TKE_w (Equation 53) is therefore modified by a site-dependent sheltering

coefficient that is the ratio of the water surface area exposed to the wind to the total water surface area. The coefficient has a maximum value of 1 when sheltering is insignificant. It may also be necessary in some regions to modify Equation 56 for the drag coefficient to consider nonneutral atmospheric conditions.

Penetrative convection. TKE produced by convection currents during periods of cooling is assumed to be proportional to the net heat flux H_n, when H_n is negative. The energy available for entrainment from overturn convection can be estimated by:

$$TKE_c = -c_c \, H_n \, A_s \, h \, g \, \alpha \, \Delta t / c_p \tag{57}$$

where

TKE_c = turbulent kinetic energy, $(kg\text{-}m^2)/sec^2$

c_c = empirical calibration coefficient

H_n = net heat flux across the air/water interface, W/m^2

h = depth of mixed layer, m

g = acceleration due to gravity, m/sec^2

α = coefficient of thermal expansion for water, per °C

c_p = specific heat of water, $J/(kg\text{-}°C)$

In Equation 57, TKE_c equals 0 when H_n is positive. The total TKE available for entrainment is:

$$TKE = TKE_w + TKE_c \tag{58}$$

Mixing efficiencies. Because mixing processes are dissipative and not efficient and because different processes dominate at different times, Equation 58 must be modified. Based on parameterization of the TKE balance at a density interface, Bloss and Harleman (1980) determined a Richardson number function $f(R_i)$ to modify the TKE:

$$f(R_i) = 0.057 \, R_i \, \frac{29.46 - \sqrt{R_i}}{14.20 + R_i} \tag{59}$$

122

where

R_i = Richardson number = $hg\Delta\rho/\rho_w w_*^2$

$\Delta\rho$ = density difference across the interface

The total TKE available for entrainment is

$$TKE = TKE * F(R_i) \qquad (60)$$

Entrainment. Prior to calculating entrainment, a temporary temperature (density) structure is computed for the computation interval. This structure considers internal absorption of solar radiation, net heat transfer at the air/water interface, inflows, and outflows. It does not consider mixing between layers.

The work W_L required to entrain or lift the mass $\Delta\rho\Delta V$ from its position immediately below the mixed layer to the center of mass of the mixed layer is

$$W_L = \Delta\rho \; \Delta V \; g \; (h - h_g) \qquad (61)$$

where

W_L = entrainment work, $(kg\text{-}m^2)/sec^2$

$\Delta\rho$ = density difference between the mixed layer and underlying layer, kg/m^3

ΔV = incremental volume to be entrained, m^3

g = acceleration due to gravity, m/sec^2

h_g = depth of the center of mass of the mixed layer, m

The depth of the mixed layer is calculated after comparing Equations 60 and 61. If the TKE is larger than W_L, entrainment occurs and h increases. Entrainment continues until TKE is no longer larger than W_L.

As indicated in Section 4.4.2, this type of formulation always sharpens the metalimnetic gradient. Diffusion or weakening of the gradient is discussed in the next section.

123

5.4.3 Diffusion Coefficient Formulation

Following the work of Ozmidov (1965), the recommended form of the diffusion coefficient for stratified conditions is

$$K_z = c_1 \frac{\bar{\epsilon}}{N^2} \qquad (62)$$

where

K_z = global vertical diffusion coefficient, m^2/sec

c_1 = dimensionless calibration coefficient

$\bar{\epsilon}$ = local dissipation rate of TKE, m^2/sec^3

$N^2 = \frac{g}{\rho} \frac{\partial \rho}{\partial z}$ = buoyancy frequency, sec^{-2}

This equation assumes a local steady state or equilibrium such that the rate of input of TKE at larger scales is in balance with the rate of dissipation at smaller scales. Equation 62 has been theoretically justified by Weinstock (1978), who assumed mixing was done in the inertial subrange. These assumptions are acceptable since turbulence is highly dissipative. Values for c_1 vary from 0.8 (Weinstock 1978) to 0.25 (Linden 1979, McEwan 1980, Oakey 1982). Equation 62 states that mixing or the diffusion coefficient increases with increasing energy input and decreases with increasing density gradient.

The computation of the local dissipation rate needs to consider the TKE inputs from the wind, inflows, and outflows separately, since the inputs from the inflows and outflows are not spread uniformly over the entire lake as the wind is but are restricted to the zone of inflow or outflow (Imberger and Patterson 1981). This finding was also verified in simulations of DeGray Lake.

The total TKE input rate from the wind is given by Equation 53. The rate of energy dissipation for wind per unit mass is

$$\bar{\epsilon}_w \ \alpha \ \frac{\rho_w \ w_*^3 \ A_s}{\rho_w \ V} \ \alpha \ \frac{w_*^3}{D_m} \tag{63}$$

where

V = volume, m^3

D_m = mean depth, m

This relationship is similar to the rate of dissipation in an unstratified uniform stress layer where shear-generated turbulence cascades to dissipation scales (e.g., Turner 1973). This is

$$\epsilon = \overline{u_x \ u_z} \ \frac{\partial U}{\partial z} \ \approx \ \frac{w_*^3}{kz} \tag{64}$$

where

$\overline{u_x \ u_z}$ = Reynolds stress, m^2/sec^2

$\frac{\partial U}{\partial z}$ = velocity gradient, (m/sec)/m

k = von Karman's constant (~0.4)

This relationship has been found to be valid in the surface layer of a reservoir (Dillon et al. 1981) and in the mixed layer off the Nova Scotia continental shelf (Oakey and Elliott 1980, 1982).

The TKE input from the inflow and outflow is given by Equation 50. The dissipation rate is therefore

$$\bar{\epsilon}_a = \frac{TKE_a}{\rho_w \ V_i} = \frac{1}{2} \left(\frac{Q_i \ U_i^2}{V_i} \right) \tag{65}$$

where V_i = volume of layer i, m^3.

With the substitution of Equations 63 and 65 into Equation 62, the diffusion coefficient becomes

125

$$K_z = \frac{c_w \bar{\epsilon}_w + c_a \bar{\epsilon}_a}{N^2} \qquad (66)$$

where

c_w = calibration coefficient for wind mixing, dimensionless

c_a = calibration coefficient for advective mixing, dimensionless

There are two problems with Equation 66. First, the diffusion coefficient becomes infinitely large when the density gradient (i.e., N^2) goes to zero (i.e., a well-mixed condition). Second, the diffusion coefficient is dependent on the density gradient to the -1 power, but field data indicate this power varies between -1/2 and -2 (Section 4.3.2). These deficiencies were corrected by defining the dimensionless stability factor

$$S_f = \frac{H}{\Delta\rho} \frac{\partial\rho}{\partial z} \qquad (67)$$

where

H = depth of lake, m

$\Delta\rho$ = density differential between bottom and surface waters, kg/m^3

For well-mixed conditions, $S_f = 1$. Incorporation of S_f into Equation 66 requires the addition of a time constant to keep Equation 66 dimensionally correct. This time constant was assumed to be the computation interval. The formulation for the diffusion coefficient is therefore

$$K_z = \frac{\left(c_w \bar{\epsilon}_w + c_a \bar{\epsilon}_a\right) \Delta t^2}{(S_f)^n} \qquad (68)$$

where n = calibration coefficient.

126

This formulation for the diffusion coefficient has several desirable features:

    a. Mixing increases with energy input.

    b. Mixing resulting from the wind and flow can be calibrated separately.

    c. The formulation is density dependent.

    d. The density dependency can be varied.

5.5 Applications and Verification

During the period 1976 to 1983, the recommended algorithm and its predecessors were used to simulate the thermal structures of over 15 reservoirs and lakes and numerous proposed reservoirs (i.e., over 40 data sets). A partial listing is given in Table 3. The reservoirs and lakes are from seven states and one province in Canada and represent all types of hydrometeorological conditions. The lakes vary in size from F. E. Walter Reservoir, Pennsylvania, which has a volume of $2.47 \times 10^6 \ m^3$ and mean annual hydraulic residence time of 1.7 days (Ford, Thornton, and Norton 1983), to Williston Reservoir which has a volume of $5.7 \times 10^{10} \ m^3$ and a mean annual hydraulic residence time of several years (Schultz International, Ltd. 1984).

The applications clearly illustrate that the recommended one-dimensional algorithm is:

    a. Sufficiently general to simulate the thermal structures of all types and sizes of CE reservoirs.

    b. Capable of simulating differences in a lake's thermal structure resulting from hydrometeorological conditions.

    c. Capable of simulating differences in a lake's thermal structure resulting from changes in operation (i.e., different withdrawal depth, different rule curve).

    d. Capable of simulating the thermal structure of a proposed reservoir after being calibrated on a morphometrically similar, existing reservoir.

To illustrate the last point, the model was calibrated on 1979 data from DeGray Lake using bottom withdrawal and then applied to Lakes Greeson, Ouachita, Hamilton, and Catherine. These four lakes are located within

Table 3

Summary of Model Applications

Reservoir	Simulation Year(s)	Purpose
Beltzville Lake, Pennsylvania	1972	Verification of 1981 F. E. Walter calibration
	1981	Verification of 1981 F. E. Walter calibration
Lake Catherine, Arkansas	1982	Verification using 1979 DeGray calibration
Lake Calhoun, Minnesota	1974	Calibration
	1975	Verification
C. J. Brown Reservoir, Ohio	1974	Simulation of filling
	1975	Calibration
Lake Coralville, Iowa	1966-67	Calibration
	1969	Calibration
DeGray Lake, Arkansas	1974-78	Verification, surface withdrawal
	1979	Calibration, bottom withdrawal
	1980	Verification, bottom withdrawal
	1982	Verification, bottom withdrawal
F. E. Walter Reservoir, Pennsylvania	1977	Verification of 1981 on shallow pool, 16.8 m deep
	1979	Verification of 1981 on shallow pool, 16.8 m deep
	1981	Calibration on high pool, 44.8 m deep
Lake Greeson, Arkansas	1972-76	Verification of 1979 DeGray calibration
	1982	Verification of 1979 DeGray calibration
Lake Hamilton, Arkansas	1982	Verification of 1979 DeGray calibration

(Continued)

128

Table 3 (Concluded)

Reservoir	Simulation Year(s)	Purpose
McCarrons Lake, Minnesota	1974	Verification of 1974 Calhoun calibration
	1975	Verification of 1974 Calhoun calibration
Lake Ouachita, Arkansas	1982	Verification of 1979 DeGray calibration
Sardis Lake, Mississippi	1966	Verification of 1968 calibration
	1967	Verification of 1968 calibration
	1968	Calibration
	1969	Verification of 1968 calibration
	1970	Verification of 1968 calibration
Lake Shelbyville, Illinois	1973	Calibration
	1975	Verification of 1973-77 calibration
	1977	Calibration
Williston Lake, British Columbia	1976-77	Verification of 1981-82 calibration
	1981-82	Calibration

50 km of DeGray Lake in southwestern Arkansas. Their major morphometric characteristics are compared in Table 4. Johnson and Ford (1983) discuss the applications to several years of data for Lake Greeson while FTN (1983) presents the results for Lakes Ouachita, Hamilton, and Catherine.

Table 4

Comparison of Major Morphometric Characteristics

Characteristic	Lake DeGray	Lake Greeson	Lake Ouachita	Lake Hamilton	Lake Catherine
Total drainage area, km^2	1,173	614	2,700	3,779	4,011
Normal pool elevation, m NGVD	124.5	167.0	176.3	122.0	93.0
Volume, 10^6 m^3	791	345	2,653	233.7	43.5
Surface area, km^2	53.4	29.1	162.3	29.1	7.9
Maximum depth, m	57	51	45.7	29.7	18.3
Mean depth, m	14.8	11.8	16.3	8.0	5.5
Hydraulic residence time, days (years)	504 (1.38)	369 (1.01)	680 (1.86)	55 (0.15)	8.2 (0.02)

131

SECTION 6. SUMMARY AND CONCLUSIONS

6.1 Literature Review Findings

The review of reservoir mixing processes indicated the observed thermal structure in a reservoir results from the cumulative effects of a number of complex, nonlinear, interdependent mixing processes. Although the sources of TKE for mixing are limited to solar and atmospheric heating, wind, inflows, and outflows (including outlet location), quantitative knowledge of specific mixing mechanisms such as wind mixing, penetrative convection, turbulent diffusion, and Kelvin-Helmholtz instabilities is limited. The TKE budgets for the entire lake do, however, clearly identify the physical causes of observed motion and thermal stratification. They also indicate which source of energy is controlling mixing at a particular time. It is common for wind to dominate at one time and inflows to dominate at another time.

The review of the influence of mixing on reservoir water quality indicated that mixing significantly impacts and sometimes controls the observed water quality by controlling horizontal and vertical constituent distributions and thereby influencing the physical, chemical, and biological regimes. The review also indicated that in order for a one-dimensional model to accurately simulate the effects of project operation on reservoir water quality, the mixing algorithm should be capable of accurately simulating the:

a. Onset of stratification.

b. Daily variations in mixed-layer depths and dynamics of short-term mixing events.

c. Metalimnetic gradient.

d. Variable mixing in the hypolimnion.

e. Fall overturn.

f. Inverse stratification during winter months.

g. Effects of project operation.

The review of one-dimensional predictive techniques indicated that the recommended mixing algorithm should include formulations for both diffusion and mixed-layer dynamics (i.e., TKE models). Inclusion of only one type of formulation severely limits the applicability of the model for CE reservoirs.

6.2 Recommended Algorithm

Since the recommended mixing algorithm is intended to be used in a generalized one-dimensional water quality model (CE-QUAL-R1) to predict changes in reservoir water quality resulting from changes in hydrometeorological conditions and project operation, several requirements were considered during algorithm development:

a. The algorithm had to be generalized with respect to CE reservoirs and therefore not be constrained by extensive morphometric and hydrometeorological data requirements nor limited in the mixing processes considered.

b. The algorithm is to be used in a one-dimensional water quality model that does not compute the internal current structure.

c. The algorithm must include all major mixing processes in order to predict changes in the mixing regime resulting from changes in hydrometeorological conditions and project operation.

Based on the review of reservoir mixing processes, an investigation of the physical basis for a number of algorithms, and applications to reservoirs representing different regions of the country, different hydrometeorological conditions, and different operating conditions, the recommended one-dimensional algorithm includes:

a. Variable layer formulation (Section 5.4.1) to reduce numerical dispersion and to allow direct calibration of mixing resulting from inflows and outflows.

b. Mixed-layer dynamics using the TKE available for possible entrainment from wind shear (Equation 53), TKE produced by convective currents during periods of cooling (Equation 57), and the efficiency function of Bloss and Harleman (1980) (Equation 59).

133

<u>c</u>. Variable diffusion coefficient that depends on the energy
   inputs from the wind, inflows, and outflows and on the density
   gradient (Equation 68).

The recommended algorithm was used to simulate the thermal struc-
tures of over 15 reservoirs and lakes of varying geographical location,
size, hydrometeorological regime, and operation configurations.

REFERENCES

Abbott, M. R., et al. 1984. "Mixing and Dynamics of the Deep Chlorophyll Maximum in Lake Tahoe," Limnology and Oceanography, Vol 29, pp 862-878.

Akiyama, J., and Stefan, H. G. 1981. "Theory of Plunging Flow into a Reservoir," St. Anthony Falls Hydraulic Laboratory Internal Memorandum I-97, Minneapolis, Minn.

Armstrong, F. A., and LaFond, E. C. 1966. "Chemical Nutrient Concentrations and Their Relationship to Internal Waves and Turbidity off Southern California," Limnology and Oceanography, Vol 11, pp 538-547.

Bengtsson, L. 1978. "Wind Induced Circulation in Lakes," Nordic Hydrology, Vol 9, pp 75-94.

Birge, E. A. 1910. "An Unregarded Factor in Lake Temperatures," Transactions of the Wisconsin Academy of Science and Arts Letters, No. 16, pp 989-1005.

Blanton, J. O. 1973. "Vertical Entrainment into the Epilimnion of Stratified Lakes," Limnology and Oceanography, Vol 18, No. 5, pp 697-704.

Bloss, S., and Harleman, D. R. F. 1980. "Effects of Wind Induced Mixing on the Seasonal Thermocline in Lakes and Reservoirs," Second International Symposium on Stratified Flow, Vol I, T. Carstens and T. McClimans eds., Trondheim, Norway, Tapir.

Bohan, J. P., and Grace, J. L. 1973. "Selective Withdrawal from Man-Made Lakes," Technical Report H-73-4, US Army Engineer Waterways Experiment Station, Vicksburg, Miss.

Bolz, R., and Tuve, G., eds. 1976. CRC Handbook of Tables for Applied Engineering Science, 2d ed., CRC Press, Cleveland, Ohio.

Bouvard, M., and Dumas, H. 1967. "Application de la Methode du fil Chaud a la Mesure de la Turbulence dans L'eau," Houille Blanche, Vol 22, pp 257-278, 723-733.

Boyce, F. M. 1974. "Some Aspects of Great Lakes Physics of Importance to Biological and Chemical Processes," Journal of the Fisheries Research Board of Canada, Vol 31, No. 5, pp 689-730.

Brush, L. M., Jr. 1970. "Artificial Mixing of a Stratified Fluid Formed by Salt and Heat in a Laboratory Reservoir," New Jersey Water Research Institute.

Coulter, G. W. 1968. "Hydrological Processes and Primary Production in Lake Tangayika," Proceedings of the 11th Conference on Great Lakes Research, International Association for Great Lakes Research, pp 609-626.

Crapper, P. F. 1973. "An Experimental Study of Mixing Across Density Interfaces," Ph. D. Thesis, University of Cambridge.

Crapper, P. F., and Linden, P. F. 1974. "The Structure of Turbulent Density Interfaces," Journal of Fluid Mechanics, Vol 65, pp 45-63.

Cromwell, T. 1960. "Pycnoclines Created by Mixing in an Aquarium Tank," Journal of Marine Research, Vol 18, pp 73-82.

Csanady, G. T. 1975. "Hydrodynamics of Large Lakes," Annual Review of Fluid Mechanics, Vol 7, pp 357-386.

Davis, J. E., Holland, J. P., and Wilhelms, S. C. 1985. "SELECT: A Numerical One-Dimensional Model of Selective Withdrawal," Instruction Report in preparation, US Army Engineer Waterways Experiment Station, Vicksburg, Miss.

Davison, W., Woof, C., and Rigg, E. 1982. "The Dynamics of Iron and Manganese in a Seasonally Anoxic Lake; Direct Measurement of Fluxes Using Sediment Traps," Limnology and Oceanography, Vol 27, pp 987-1003.

Deardorff, J. W. 1970. Convective Velocity and Temperature Scales for the Unstable Planetary Boundary Layer and for Raleigh Convection," Journal of Atmospheric Science, Vol 27, pp 1121-1213.

_____. 1979. "Prediction of Convective Mixed-Layer Entrainment for Realistic Capping Inversion Structure," Journal of Atmospheric Science, Vol 36, pp 424-436.

Denman, K. L. 1976. "Covariability of Chlorophyll and Temperature in the Sea," Deep-Sea Research, Vol 23, pp 539-550.

_____. 1977. "Short Term Variability in Vertical Chlorophyll Structure," Limnology and Oceanography, Vol 22, No. 3, pp 434-441.

Denman, K. L., and Gargett, A. E. 1983. Time and Space Scales of Vertical Mixing and Advection of Phytoplankton in the Upper Ocean," Limnology and Oceanography, Vol 28, pp 801-815.

Denman, K. L., and Platt, T. 1975. "Coherences in the Horizontal Distributions of Phytoplankton and Temperature in the Upper Ocean," Memoires Societe Royale des Sciences de Liege, Vol 6, No. 7, pp 19-30.

Denton, R. A. 1978. "Entrainment by Penetrative Convection at Low Peclet Number," Ph. D. Thesis, University of Canterbury, Christchurch, New Zealand.

De Pinto, J. V., Young, T. C., and Martin, S. C. 1982. "Aquatic Sediments," Journal of the Water Pollution Control Federation, Vol 54, pp 855-862.

Dillon, T. M., et al. 1981. "Near-Surface Turbulence Measurements in a Lake," Nature, Vol 290, pp 390-392.

Dortch, M. S. 1981. "Investigation of Release Temperatures for Kinzua Dam, Allegheny River, Pennsylvania," Technical Report HL-81-9, US Army Engineer Waterways Experiment Station, Vicksburg, Miss.

Dunst, R. C. 1974. "In-Lake Nutrient Retention During Artificial Circulation and Bottom Water Discharge," presentation at American Society of Limnologists and Oceanographers meeting, Seattle, Wash.

Edinger, J. E., Brady, D. K., and Geyer, J. C. 1974. Heat Exchange and Transport in the Environment," Cooling Water Discharge Project (RP-49), EPRI Report No. 14, Electric Power Research Institute, Palo Alto, Calif.

Environmental Laboratory. 1982. "CE-QUAL-R1: A Numerical One-Dimensional Model of Reservoir Water Quality; User's Manual," Instruction Report E-82-1, US Army Engineer Waterways Experiment Station, Vicksburg, Miss.

Farmer, D. M., and Carmack, E. 1982. "Wind-Mixing and Restratification in a Lake near the Temperature of Maximum Density," Journal of Physical Oceanography, Vol 11, pp 1516-1533.

Fasham, M. J. R., and Pugh, P. R. 1976. "Observations on the Horizontal Coherences of Chlorophyll a and Temperature," Deep-Sea Research, Vol 23, pp 527-538.

Fee, E. J. 1976. "The Vertical and Seasonal Distribution of Chlorophyll in Lakes of the Experimental Lakes Area, Northwestern Ontario: Implications for Primary Production Estimates," Limnology and Oceanography, Vol 21, No. 6, pp 767-783.

Fischer, H. B., et al. 1979. Mixing in Inland and Coastal Waters, Academic Press, New York.

Fogg, G. E. 1975. Algal Cultures and Phytoplankton Ecology, The University of Wisconsin Press, Madison, Wis.

Ford, D. E. 1976. "Water Temperature Dynamics of Dimictic Lakes: Analysis and Predictions Using Integral Energy Concepts," Ph. D. Thesis, University of Minnesota, Minneapolis.

_____. 1978. "Temperature and Dissolved Oxygen Data Interpretation," Proceedings of a Seminar on Water Quality Data Interpretation, US Army Corps of Engineers Committee on Water Quality.

Ford, D. E., and Johnson, M. C. 1983. "An Assessment of Reservoir Density Currents and Inflow Processes," Technical Report E-83-7, US Army Engineer Waterways Experiment Station, Vicksburg, Miss.

Ford, D. E., Johnson, M. C., and Monismith, S. G. 1980. "Density Inflows to DeGray Lake, Arkansas," Second International Symposium on Stratified Flow, Vol II, T. Carstens and T. McClimans, eds., Trondheim, Norway, Tapir.

Ford, D. E., and Stefan, H. G. 1980a. "Stratification Variability in Three Morphometrically Different Lakes Under Identical Meteorological Forcing," Water Resources Bulletin, Vol 16, No. 2, pp 243-247.

_____. 1980b. "Thermal Predictions Using Integral Energy Model," Journal of the Hydraulics Division, Proceedings of the American Society of Civil Engineers, Vol 106, No. HY1, pp 39-55.

Ford, D. E., and Thornton, K. W. 1979. "Time and Length Scales for the One-Dimensional Assumption and Its Relation to Ecological Models," Water Resources Research, Vol 15, No. 1, pp 113-120.

Ford, D. E., Thornton, K. W., and Norton, J. L. 1983. "Thermal Analysis of the Proposed Francis E. Walter Reservoir Modification: Guidance on Selective Withdrawal," prepared by Ford, Thornton, Norton and Associates for US Army Engineer District, Philadelphia, Philadelphia Pa.

Ford, D. E., et al. 1981. "A Water Quality Management Model for Reservoirs," Proceedings of the Symposium on Surface Water Impoundments, H. G. Stefan, ed., American Society of Civil Engineers, New York, Vol 1, pp 624-633.

Frink, C. R. 1969. "Chemical and Mineralogical Characteristics of Eutrophic Lake Sediments," Soil Science Society of America Proceedings, Vol 33, pp 369-372.

FTN. 1983. "Arkansas Lakes Interim Study: Thermal Modeling of Lakes Ouachita, Hamilton, and Catherine," prepared by Ford, Thornton, Norton and Associates for Ouachita Baptist University, Arkadelphia, Ark., under contract to US Army Engineer District, Vicksburg, Vicksburg, Miss.

Garnich, N. G., and Kitaigorodskii, S. A. 1977. "On the Rate of Deepening of the Oceanic Mixed Layer," Isv. Akad. Nauk USSR, Atmos. and Ocean. Phys., Vol 13, pp 1287-1296.

_____. 1978. "On the Theory of the Deepening of the Upper Quasi-Homogeneous Ocean Layer Owing to the Processes of Purely Wind-Induced Mixing," Isv. Akad. Nauk USSR, Atmos. and Ocean. Phys., Vol 14, pp 748-755.

Garrett, C., and Munk, W. 1979. "Internal Waves in the Ocean," Annual Review of Fluid Mechanics, Vol 11, pp 339-370.

Gregg, M. C., and Briscoe, M. G. 1979. "Internal Waves, Finestructure, Microstructure and Mixing in the Ocean," Review of Geophysics and Space Physics, Vol 17(T), pp 1524-1548.

Hannan, H. H., and Cole, T. M. 1984. "Dissolved Oxygen Dynamics In (On-Stream) Reservoirs," Perspectives in Reservoir Limnology in preparation, K. W. Thornton, ed., John Wiley and Sons, New York.

Harleman, D. R. F. 1982. "Hydrothermal Analysis of Lakes and Reservoirs," Journal of the Hydraulics Division, Proceedings of the American Society of Civil Engineers, Vol 108, No. HY3, pp 302-325.

Harris, G. P. 1980. "Temporal and Spatial Scales in Phytoplankton Ecology; Mechanisms, Methods, Models, and Management," Canadian Journal of Fish and Aquatic Science, Vol 37, pp 877-900.

Haugen, K. A., ed. 1973. Workshop in Micrometeorology, American Meteorology Society, Boston, Mass.

Henderson-Sellers, B. 1976. "Role of Eddy Diffusivity in Thermocline Formation," Journal of the Environmental Engineering Division, Proceedings of the American Society of Civil Engineers, Vol 102, No. EE3, pp 517-531.

Hirshburg, R. I., Goodling, J. S., and Maples, G. 1976. "The Effects of Diurnal Mixing on Thermal Stratification of State Impoundments," Water Resources Bulletin, Vol 12, No. 6, pp 1151-1159.

Hopfinger, E. J., and Toly, J. A. 1976. "Spatially Decaying Turbulence and Its Relation to Mixing Across Density Interfaces," Journal of Fluid Mechanics, Vol 78, pp 155-177.

Huber, W. C., and Harleman, D. R. F. 1968. "Laboratory and Analytical Studies of the Thermal Stratification of Reservoirs," Technical Report No. 112, Ralph M. Parsons Laboratory, Massachusetts Institute of Technology, Cambridge, Mass.

Hurley-Octavio, K. A., Jirka, G. H., and Harleman, D. R. F. 1977. "Vertical Heat Transport Mechanisms in Lakes and Reservoirs," Technical Report No. 227, Ralph M. Parsons Laboratory, Massachusetts Institute of Technology, Cambridge, Mass.

Hutchinson, G. E. 1941. "Limnological Studies in Connecticut; IV. The Mechanism of Intermediary Metabolism in Stratified Lakes," Ecological Monographs, Vol 11, pp 21-69.

_____. 1957. A Treatise on Limnology, John Wiley and Sons, New York.

Hydrologic Engineering Center. 1974. "Water Quality for River-Reservoir Systems; User's Manual (Draft)," US Army Engineer Hydrologic Engineering Center, Davis, Calif.

Imberger, J. 1980. "Selective Withdrawal: A Review," Second International Symposium on Stratified Flow, Vol I, T. Carstens and T. McClimans, eds., Trondheim, Norway, Tapir.

Imberger, J., and Hamblin, P. F. 1982. "Dynamics of Lakes, Reservoirs, and Cooling Ponds," Annual Review of Fluid Mechanics, Vol 14, pp 153-187.

Imberger, J., and Patterson, J. C. 1981. "A Dynamic Reservoir Simulation Model-DYRESM; 5. Transport Models for Inland and Coastal Waters," H. B. Fischer, ed., Academic Press, New York.

Imberger, J., et al. 1978. "Dynamics of a Reservoir of Medium Size," Journal of the Hydraulics Division, Proceedings of the America Society of Civil Engineers, Vol 104, No. HY5, pp 725-743.

Imboden, D. M., and Emerson, S. 1978. "Natural Radon and Phosphorus as Limnologic Tracers: Horizontal and Vertical Eddy Diffusion in Greifensee," Limnology and Oceanography, Vol 23, No. 1, pp 77-90.

Imboden, D. M., et al. 1977. "Lake Tahoe Geochemical Study; 1. Lake Chemistry and Tritium Mixing Study," Limnology and Oceanography, Vol 22, No. 6, pp 1039-1051.

Jassby, A., and Powell, T. 1975. Vertical Patterns of Eddy Diffusion During Stratification in Castle Lake, California," Limnology and Oceanography, Vol 20, No. 4, pp 530-542.

Jirka, G. H., and Harleman, D. R. F. 1979. "Cooling Impoundments: Classification and Analyses," Journal of the Energy Division, Proceedings of the American Society of Civil Engineers, Vol 105, No. EY20, pp 291-309.

Jirka, G. H., and Watanabe, M. 1980. "Thermal Structure of Cooling Ponds. Journal of the Hydraulics Division, Proceedings of the American Society of Civil Engineers, Vol 106, No. HY5, pp 701-715.

Johnson, L. S., and Ford, D. E. 1981. "Verification of a One-Dimensional Reservoir Thermal Model," presented at 1981 American Society of Civil Engineers Convention and Exposition, St. Louis, Mo.

_____. 1983. "Thermal Modeling of DeGray Lake," Symposium on DeGray Lake, J. Nix and R. H. Kennedy, eds., Technical Report in preparation, US Army Engineer Waterways Experiment Station, Vicksburg, Miss.

Kaeff, J., and Knoechel, R. 1978. "Phytoplankton and Their Dynamics in Oligotrophic and Eutrophic Lakes," Annual Review of Ecological Systems, Vol 9, pp 475-495.

Kantha, L. H., Phillips, O. M., and Azad, R. S. 1977. "On Turbulent Entrainment at a Density Interface," Journal of Fluid Mechanics, Vol 79, pp 753-768.

Kato, H., and Phillips, O. M. 1969. "On the Penetration of a Turbulent Layer into a Stratified Fluid," Journal of Fluid Mechanics, Vol 37, pp 643-655.

Kennedy, R. H., Gunkel, R. C., and Carlile, J. M. 1983. "Riverine Influence on the Water Quality Characteristics of West Point Lake," Technical Report in preparation, US Army Engineer Waterways Experiment Station, Vicksburg, Miss.

Kimmel, B. L., Lind, O. T., and Paulson, L. J. 1984. "Reservoir Primary Production," Perspectives in Reservoir Limnology in preparation, K. W. Thornton, ed., John Wiley and Sons, New York.

Knapp, R. T. 1942. "Density Currents: Their Mixing Characteristics and Their Effect on the Turbulence Structure of the Associated Flow," Proceedings of the Second Hydraulic Conference, University of Iowa, Iowa City, pp 289-306.

Koberg, G. E. 1962. "Methods to Compute Long Wave Radiation from the Atmosphere and Reflected Solar Radiation from a Water Surface," Geological Survey Professional Paper, US Geological Survey, Washington, DC.

Kraus, E. B. 1977. Modeling and Prediction of the Upper Layers of the Ocean, Pergamon, Oxford.

Kraus, E. B., and Turner, J. S. 1967. "A One-Dimensional Model of the Seasonal Thermocline; Part 2: The General Theory and Its Consequences," Tellus, Vol 19, pp 98-106.

Kullenburg, G., Murthy, C. R., and Westerberg, H. 1973. "An Experimental Study of Diffusion Characteristics in the Thermocline and Hypolimnion Regions of Lake Ontario," Proceedings of the Sixteenth Conference on Great Lakes Research.

LaFond, E. C. 1962. "Internal Waves: Part 1," The Sea, Vol 1, M. N. Hill, ed., Wiley Interscience, New York, pp 731-751.

Langmuir, I. 1938. "Surface Motion of Water Induced by Wind," Science, Vol 87, pp 119-123.

Larson, D. W. 1979. "Turbidity-Induced Meromixis in an Oregon Reservoir: Hypothesis," Water Resources Research, Vol 15, No. 6, pp 1560-1566.

Leibovich, S. 1983. "The Form and Dynamics of Langmuir Circulations," Annual Review of Fluid Mechanics, Vol 15, pp 391-427.

Lerman, A. 1971. "Time to Chemical Steady-States in Lakes and Oceans," Advances in Chemistry Series, Vol 106.

Linden, P. F. 1973. "The Interaction of a Vortex Ring with a Sharp Density Interface: A Model for Turbulent Entrainment," Journal of Fluid Mechanics, Vol 75, No. 2, pp 305-320.

_____. 1975. "The Deepening of a Mixed Layer in a Stratified Fluid," Journal of Fluid Mechanics, Vol 71, pp 385-405.

_____. 1979. "Mixing in Stratified Fluids," Geophysical and Astrophysical Fluid Dynamics, Vol 13, pp 3-23.

Lund, J. W. G. 1950. Studies on Asterionella formosa Hass; Vol II: Nutrient Depletion and the Spring Maximum," Journal of Ecology, Vol 38, pp 1-35.

_____. 1954. "The Seasonal Cycle of the Plankton Diatom, Melosira italica (Ehr.) Kuitz., Subsp. Subarctica O. Mull.," Journal of Ecology, Vol 42, pp 151-179.

Lund, J. W. G., Mackereth, F. J. H., and Mortimer, C. H. 1963. Changes in Depth and Time of Certain Chemical and Physical Conditions and of the Standing Crop of Asterionella formosa Hass. in the North Basin of Windermere in 1947," Phil. Trans. Roy. Soc., Vol B246, pp 255-290.

Mahrt, L. 1979. "Penetrative Convection at the Top of a Growing Boundary Layer," Quarterly Journal of the Royal Meteorological Society, Vol 105, pp 469-485.

McEwan, A. D. 1980. "Mass and Momentum Diffusion in Internal Breaking Events," Second International Symposium on Stratified Flow, Vol I, T. Carstens and T. McClimans, eds., Trondheim, Norway, Tapir.

Mellor, G. L., and Yamada, T. 1974. "A Hierarchy of Turbulence Closure Models for Planetary Boundary Layers," _Journal of Atmospheric Science_, Vol 31, pp 1791-1806.

Monismith, S. G. 1983. "Dynamic Response of Stratified Reservoirs to Surface Shear Stress," Ph. D. Thesis, University of California, Berkeley, Calif.

Moore, M. J., and Long, R. R. 1971. "An Experimental Investigation of Turbulent Stratified Shearing Flow," _Journal of Fluid Mechanics_, Vol 49, pp 635-656.

Mortimer, C. H. 1974. "Lake Hydrodynamics," _International Association of Applied Limnology Mitteilungen_, Vol 20, pp 124-197.

Munk, W., and Anderson, E. R. 1948. "Notes on a Theory of the Thermocline," _Journal of Marine Research_, Vol 7, pp 276-295.

Neal, V. T., Neshyba, S. J., and Denner, W. T. 1971. "Temperature Microstructure in Crater Lake, Oregon," _Limnology and Oceanography_, Vol 16, pp 695-700.

Niiler, P. P. 1975. "Deepening of the Wind-Mixed Layer," _Journal of Marine Research_, Vol 33, pp 405-422.

Niiler, P. P., and Kraus, E. B. 1977. "One Dimensional Models of the Upper Ocean," _Modeling and Prediction of the Upper Layer of the Ocean_, E. B. Kraus, ed., Pergamon Press, Oxford, England.

Nix, J. 1981. "Contribution of Hypolimnetic Water on Metalimnetic Dissolved Oxygen Minima in a Reservoir," _Water Resources Research_, Vol 17, pp 329-332.

_____. 1984. "Transport of Iron and Manganese in a Deep Storage Reservoir," _Symposium on DeGray Lake_, J. Nix and R. H. Kennedy, eds., Technical Report in preparation, US Army Engineer Waterways Experiment Station, Vicksburg, Miss.

Norton, W. R., Roesner, L. A., and Orlob, G. T. 1968. "Mathematical Models for Prediction of Thermal Energy Changes in Impoundments," EPA Water Pollution Control Research Series, US Environmental Protection Agency.

Oakey, N. S. 1982. "Determination of the Rate of Dissipation of Turbulent Energy from Simultaneous Temperature and Velocity Shear Microstructure Measurements," _Journal of Physical Oceanography_, Vol 12, pp 256-271.

Oakey, N. S., and Elliott, J. A. 1980. "Dissipation in the Mixed Layer near Emerald Basin," _Marine Turbulence_, J. C. Nihoul, ed., pp 123-133.

_____. 1982. "Dissipation Within the Surface Mixed Layer," _Journal of Physical Oceanography_, Vol 12, pp 171-185.

Ottesen Hansen, N-E. 1978. "Mixing Processes in Lakes," _Nordic Hydrology_, Vol 9, pp 57-74.

Ozmidov, R. V. 1965. "On the Turbulent Exchange in a Stably Stratified Ocean," *Atmospheric and Oceanic Physics Series,* Vol 1, pp 853-860.

Pedersen, F. B. 1980. "A Monograph of Turbulent Entrainment and Friction in Two-Layer Stratified Flow," Series Paper No. 25, Institute of Hydrodynamics and Hydraulic Engineering, Technical University of Denmark.

Phillips, O. M. 1977. *The Dynamics of the Upper Ocean,* Cambridge University Press, London and New York.

Pita, F. W., and Hyne, N. J. 1974. "The Depositional Environment of Zinc, Lead, and Cadmium in Reservoir Sediments, *Water Research,* Vol 9, pp 701-706.

Pharo, C. H., and Carmack, E. C. 1979. "Sedimentation Processes in a Short Residence-Time Intermontane Lake Kamloops, B. C.," *Sedimentology,* Vol 24, pp 523-542.

Platt, T. 1972. "Local Phytoplankton Abundance and Turbulence," *Deep-Sea Research,* Vol 19, pp 183-187.

Platt, T., and Denman, K. L. 1975a. "Spectral Analysis in Ecology," *American Review of Ecology and Systematics,* Vol 6, pp 189-210.

_____. 1975b. "A General Equation for the Mesoscale Distribution of Phytoplankton in the Sea," *Memoires Societe Royale des Sciences de Liege,* Vol 6, No. 7, pp 31-42.

Pollard, R. T. 1977. "Observations and Theories of Langmuir Circulations and Their Role in Near Surface Mixing," *A Voyage to Discovery,* Martin Angel, ed., Supplement to Deep-Sea Research, Pergamon Press, Oxford, England, pp 235-251.

Pollard, R. T., Rhines, P. B., and Thompson, R. O. R. Y. 1973. "The Deepening of the Wind-Mixed Layer," *Geophysical Fluid Dynamics,* Vol 3, pp 381-404.

Powell, T. M., et al. 1975. "Spatial Scales of Current Speed and Phytoplankton Biomass Fluctuations in Lake Tahoe," *Science,* Vol 189, pp 1088-1090.

Quay, P. D., et al. 1980. "Vertical Diffusion Rates Determined by Tritium Tracer Experiments in the Thermocline and Hypolimnion of Two Lakes," *Limnology and Oceanography,* Vol 25, No. 2, pp 201-218.

Rao, D. V. S. 1977. "Effect of Physical Processes on the Production of Organic Matter in the Sea," *Symposium on Modeling of Transport Mechanisms in Oceans and Lakes,* Manuscript Report Series, Vol 43, pp 161-169, Marine Sciences Directorate, Department of Fisheries and the Environment, Ottawa.

Reid, J. L. 1956. "Observations of Internal Tides in October 1950," *Transactions of the American Geophysical Union,* Vol 37, pp 278-286.

Reynolds, C. S., and Rogers, D. A. 1976. "Seasonal Variations in the Vertical Distribution and Buoyancy of *Microcystis aeruginosa* Kuitz. Emend. Elenkin in Rostherne Mere, England," Hydrobiologia, Vol 48, No. 1, pp 17-23.

Roberts, P. J. W. 1981. "Jet Entrainment in Pumped Storage Reservoirs," Technical Report E-81-3, US Army Engineer Waterways Experiment Station, Vicksburg, Miss.

Roberts, P. J. W., and Dortch, M. S. 1985. "Entrainment Descriptions for Mathematical Modeling of Pumped-Storage Inflows in Reservoirs," Technical Report E-85-12, US Army Engineer Waterways Experiment Station, Vicksburg, Miss.

Rouse, H., and Dodu, J. 1955. "Turbulent Diffusion Across a Density Discontinuity," La Houille Blanche, Vol 10, pp 530-532.

Ruttner, F. 1963. Fundamentals of Limnology, University of Toronto Press.

Safaie, B. 1978. "Mixing of Horizontal Buoyant Surface Jet Over Sloping Bottom," Report HEL-27-4, Hydraulic Engineering Laboratory, University of California, Berkeley, Calif.

Schultz International, Ltd. 1984. "Development of a Reservoir Water Quality Model for Reservoirs in British Columbia," Technical Report prepared for British Columbia Hydro Power Authority, Vancouver, B. C.

Sharpley, A. N., and Segers, J. K. 1979. "Phosphorus Inputs into a Stream Draining an Agricultural Watershed; Vol II: Amounts Contributed and Relative Significance of Runoff Types," Water, Air, and Soil Pollution, Vol 11, pp 417-428.

Sherman, F. S., Imberger, J., and Corcos, G. M. 1978. "Turbulence and Mixing in Stably Stratified Waters," Annual Review of Fluid Mechanics, Vol 10, pp 267-288.

Simpson, J. H., and Woods, J. D. 1970. "Temperature Microstructure in a Fresh Water Thermocline," Nature, Vol 226, pp 832-834.

Smith, F. B. 1975. "Turbulence in the Atmosphere Boundary Layer," Scientific Programs of Oxford, Vol 62, pp 127-151.

Smith, I. R. 1979. "Hydraulic Conditions in Isothermal Lakes," Freshwater Biology, Vol 9, pp 119-145.

Stafford, J. P., III. 1978. "Thermal Analysis of Lake Greeson, Arkansas and Sardis Lake, Mississippi," M.S. Thesis, Mississippi State University, Starkville, Miss.

Stauffer, R. E., and Lee, G. F. 1974. "The Role of Thermocline Migration in Regulating Algal Blooms," Modeling the Eutrophication Process, E. J. Middlebrooks, D. H. Falkenborg, and T. E. Maloney, eds., Ann Arbor Science Publishers, Inc., Ann Arbor, Mich., pp 73-82.

Stefan, H., and Ford, D. E. 1975a. "Mixed Layer Depth and Temperature Dynamics in Temperate Lakes," <u>Verh. Internat. Verin. Limnol.,</u> Vol 19, pp 149-157.

_____. 1975b. "Temperature Dynamics in Dimictic Lakes," <u>Journal of the Hydraulics Division, Proceedings of the American Society of Civil Engineers,</u> Vol 101, No. HY1, pp 97-114.

Steward, R. W. 1959. "The Natural Occurrence of Turbulence," <u>Journal of Geophysical Research,</u> Vol 64, No. 12, pp 2112-2115.

Stull, R. B. 1976a. "The Energetics of Entrainment Across a Density Interface," <u>Journal of Atmospheric Science,</u> Vol 33, pp 1260-1267.

_____. 1976b. "Mixed-Layer Depth Model Based on Turbulent Energetics," <u>Journal of Atmospheric Science,</u> Vol 33, pp 1268-1278.

Sundaram, T. R. 1973. "A Theoretical Model for the Seasonal Thermocline Cycle of Deep Temperate Lakes," <u>Proceedings of the Sixteenth Conference on Great Lakes Research,</u> pp 1009-1025.

Sundaram, T. R., and Rehm, R. G. 1971. "Formation and Maintenance of Thermoclines in Temperate Lakes," <u>American Institute of Aeronautics and Astronautics Journal,</u> Vol 9, No. 7, pp 1322-1329.

_____. 1973. "The Seasonal Thermal Structure of Deep Temperate Lakes," <u>Tellus,</u> Vol 25, No. 2, pp 157-167.

Tennekes, H. 1973. "A Model for the Dynamics of the Inversion Above a Convection Boundary Layer," <u>Journal of Atmospheric Science,</u> Vol 30, pp 558-567.

Tennekes, H., and Driedonks, A. G. M. 1980. "Basic Entrainment Equations for the Atmospheric Boundary Layer," <u>Second International Symposium on Stratified Flow,</u> Vol I, T. Carstens and T. McClimans, eds., Trondheim, Norway, Tapir.

Tennekes, H., and Lumley, J. L. 1972. <u>A First Course in Turbulence,</u> The MIT Press, Cambridge, Mass.

Tennessee Valley Authority. 1972. "Heat and Mass Transfer Between a Water Surface and the Atmosphere," Water Resources Research Laboratory Report 14, Norris, Tenn.

Thompson, S. M., and Turner, J. S. 1975. "Mixing Across an Interface Due to Turbulence Generated by an Oscillating Grid," <u>Journal of Fluid Mechanics,</u> Vol 67, No. 2, pp 349-368.

Thornton, K. W., Nix, J. F., and Bragg, J. D. 1980. "Coliforms and Water Quality: Use of Data in Project Design and Operation," <u>Water Resources Bulletin,</u> Vol 16, pp 86-92.

Thornton, K. W., et al. 1979. "Improving Ecological Simulation Through Sensitivity Analysis," <u>Simulation,</u> Vol 32, No. 5, pp 155-166.

Turner, J. S. 1968. "The Influence of Molecular Diffusivity on Turbulent Entrainment Across a Density Interface," <u>Journal of Fluid Mechanics,</u> Vol 33, pp 639-656.

Turner, J. S. 1973. Buoyancy Effects in Fluids, Cambridge University Press, London and New York.

Turner, J. S., and Kraus, E. B. 1967. "A One-Dimensional Model of the Seasonal Thermocline; Part 1: A Laboratory Experiment and Its Interpretation," Tellus, Vol 19, pp 88-97.

US Army Engineer District, Baltimore. 1974. Thermal Simulation of Lakes, User's Manual," Program Numbers 722-F5-E1010 and 722-F5-E1011, Baltimore, Md.

Van Mieghem, J. 1973. Atmospheric Energenics, Clarendom Press, Oxford, England.

Walters, R. A., Carey, G. F., and Winter, D. F. 1978. "Temperature Computation for Temperate Lakes," Applied Mathematical Modeling, Vol 2, No. 3, pp 41-48.

Ward, P. R. B. 1977. "Diffusion in Lake Hypolimnia," Proceedings of the Congress of the International Association of Hydraulic Research, 17th Baden-Baden, Vol 2, pp 103-110.

Weinstock, J. 1978. "Vertical Diffusion in a Stably Stratified Fluid," Journal of Atmospheric Science, Vol 35, pp 1022-1027.

Welander, P. 1968. "Theoretical Forms for the Vertical Exchange Coefficients in a Stratified Fluid with Application to Lakes and Seas," Acta. R. Soc. Sci. Litt., Gothoburgensis, Geophysics, Vol 1, pp 1-16.

Wetzel, R. G. 1983. Limnology, 2d ed., Saunders College Publishing, Philadelphia, Pa.

Whitney, L. V. 1938. "Microstratification of Inland Lakes," Transactions of the Wisconsin Academy of Science and Arts Letters, Vol 31, pp 155-173.

Williams, D. T., et al. 1981. "Determination of Light Extinction Coefficients in Lakes and Reservoirs," Proceedings of the Symposium Surface Water Impoundments, H. G. Stefan, ed., American Society of Civil Engineers, New York, Vol 2, pp 1329-1335.

Wolanski, E. J. 1972. "Turbulent Entrainment Across Stable Density-Stratified Liquids and Suspensions," Ph. D. Thesis, The Johns Hopkins University, Baltimore, Md.

Wolanski, E. J., and Brush, L. M. 1975. "Turbulent Entrainment Across Stable Density Step Structures," Tellus, Vol 27, No. 3, pp 259-262.

Wu, J. 1973. "Wind Induced Entrainment Across a Stable Density Interface," Journal of Fluid Mechanics, Vol 61, pp 275-287.

_____. 1980. Wind Stress Coefficients over Sea Surface near Neutral Conditions - A Revisit," Journal of Physical Oceanography, Vol 10, pp 727-740.

Zeman, O. 1981. "Progress in the Modeling of Planetary Boundary Layers," Annual Review of Fluid Mechanics, Vol 13, pp 253-272.

Zeman, O., and Tennekes, H. 1977. "Parameterization of the Turbulent Energy Budget at the Top of the Daytime Atmospheric Boundary Layer," Journal of Atmospheric Science, Vol 34, pp 111-123.

Zilitinkevich, S. S. 1975. "Comments on 'A Model for the Dynamics of the Inversion Above a Convective Boundary Layer,'" Journal of Atmospheric Science, Vol 32, pp 991-992.

APPENDIX A: STRATIFICATION COMPUTATIONS

A.1 Introduction

Most lakes and reservoirs stratify, albeit weakly and intermittently, at one time or another. The major factors that limit stratification are the lake depth, flowthrough rate, and the wind. These factors have been used by several investigators to develop criteria for stratification potential (i.e., the likelihood that a particular body of water will stratify). In general, lakes with depths greater than 10 m and mean annual residence times greater than 20 days stratify. These numbers differ slightly from Harleman (1982), who states that lakes with depths greater than 5 m stratify except if the residence time is less than 36 days. In addition to these general rules, several computations can be made to evaluate the stratification potential of a reservoir. Note, however, that these calculations are merely indicators and, as shown in the examples, all methods do not always yield the same conclusion.

A.2 Densimetric Froude Number

A.2.1 Description

Norton, Roesner, and Orlob (1968) proposed a more scientifically based stratification criterion in the form of the densimetric Froude number

$$F_d = \sqrt{\frac{1}{ge}} \frac{L\tilde{Q}}{D_m V} \tag{A1}$$

where

F_d = densimetric Froude number, dimensionless
g = acceleration of gravity, m/sec^2
e = dimensionless density gradient, 10^{-6}/m
L = reservoir length, m

A1

$\bar{Q}$ = average reservoir discharge, m^3/sec

D_m = reservoir mean depth, m

V = reservoir volume, m^3

An $F_d \gg 1/\pi$ indicates a well-mixed system; $F_d \ll 1/\pi$ indicates a strongly stratified system; while $F_d \sim 1/\pi$ indicates a weakly or intermittently stratified system.

This criterion compares the destratifying force of the flowthrough with the stratifying potential of the assumed density gradient. It can be simplified and rewritten in terms of the residence time t_r (t_r = volume/flow rate)

$$F_d = \frac{319}{t_r} \frac{L}{D_m} \qquad (A2)$$

For the critical F_d of $1/\pi$ and a residence time of 20 days, $L/D_m = 1,724$ or the bottom slope is on the order of 5.8×10^{-4}. Since this slope is characteristic of many CE reservoirs, the critical residence time of 20 days is consistent with the Norton, Roesner, and Orlob (1968) criterion.

A.2.2 Examples

DeGray Lake is a CE impoundment located on the Caddo River in south-central Arkansas. It has the following characteristics:

$$L = 32,000 \text{ m}$$

$$D_m = 14.8 \text{ m}$$

$$V = 7.91 \times 10^8 \text{ m}^3$$

$$\bar{Q} = 18.2 \text{ m}^3/sec$$

The densimetric Froude number is, therefore,

$$F_d = \sqrt{\frac{1}{g}} \frac{L\bar{Q}}{D_m V} = \sqrt{\frac{1}{(9.8)(10^{-6})} \frac{(32,000)(18.2)}{(14.8)(7.91 \times 10^8)}} = 0.02$$

A2

Since $F_d = 0.02 \ll 1/\pi$, DeGray Lake should be a strongly stratified system, which it is (see Figure 6). Its maximum depth of 57 m and mean annual residence time of 1.38 years also confirm this conclusion.

F. E. Walter Reservoir is a small CE project located on the Lehigh River in the Pocono Mountains of northeastern Pennsylvania. It has the following characteristics:

$$L = 2,700 \text{ m}$$

$$D_m = 6.8 \text{ m}$$

$$V = 2.47 \times 10^6 \text{ m}^3$$

$$\bar{Q} = 17.6 \text{ m}^3/\text{sec}$$

The densimetric Froude number is, therefore,

$$F_d = \sqrt{\frac{1}{ge} \frac{L\bar{Q}}{D_m V}} = \sqrt{\frac{1}{(9.8)(10^{-6})} \frac{(2,700)\ (17.6)}{(6.8)(2.47 \times 10^6)}} = 0.9$$

indicating a weakly or intermittently stratified system. In contrast, its maximum depth of 16.8 m would indicate a stratified system and its mean annual residence time of 1.7 days would indicate a well-mixed system. Since F. E. Walter Reservoir intermittently stratifies, the densimetric Froude number computation gives the proper result while the conflicting maximum depth and residence time criteria compensate one another.

A.3 Wind Mixing Depth

A.3.1 Description

The depth of the lake is important when evaluating stratification potential since the effects of wind mixing and the penetration of solar radiation are depth limited. If solar radiation does not penetrate to the bottom of the lake, wind mixing is required to prevent stratification

from forming. Since the average Secchi disc depth of CE reservoirs is 1.1 m (Thornton, Nix, and Bragg 1980), wind mixing is required in most CE reservoirs to mix the heat to depths greater than 2.2 m. The importance of wind mixing can be evaluated using the length or depth scale (Sundaram 1973):

$$D_t = \frac{w_*^3}{\beta \alpha g \dfrac{H_n}{\rho_w c_p}} \tag{A3}$$

where

w_* = shear velocity of wind in water, m/sec

β = empirical coefficient, dimensionless

α = volumetric coefficient of thermal expansion, $1.8 \times 10^{-4}/°C$

H_n = net surface heat flux, W/m^2

ρ_w = density of water, kg/m^3

c_p = specific heat of water, 4,186 J/(kg-°C)

The value for empirical coefficient β can be taken as 0.4 (i.e., von Karman's constant) although Sundaram (Mortimer 1974) recommends 0.2 to 0.4. The surface heat flux can be estimated from

$$H_n = K(T_e - T_s) \tag{A4}$$

where

K = heat exchange coefficient, $W/(m^2 - °C)$

T_e = equilibrium temperature, °C

T_s = surface temperature, °C

Procedures for computing K and T_e can be found in Edinger, Brady, and Geyer (1974).

The physical significance of D_t is that it is a measure of the depth the wind can distribute a given surface heat input. Lakes with depths greater than D_t and not dominated by advection (flowthrough) will probably stratify.

A4

A.3.2 Examples

Since the wind mixing depth scale (Equation A3) is dependent only on meteorological conditions, computations will be made for southern Minnesota (Minneapolis) and central Louisiana (Monroe) to illustrate geographic variations in D_t . Equation A3 reduces to

$$D_t = \frac{5.9 \times 10^9 \, w_*^3}{H_n} \qquad (A5)$$

with substitution for the various coefficients and constants. Assuming a drag coefficient C_d of 1.3×10^{-3} (see Equations 54 and 55), the shear velocity w_* can be obtained directly from the wind speed W using

$$w_* = 1.27 \times 10^{-3} \, W \qquad (A6)$$

where W = wind speed, m/sec.

The surface heat is obtained from Equation A4 using Figure A1 to obtain K and approximating T_e by

$$T_e = T_d + \frac{H_s}{K} \qquad (A7)$$

where

T_d = dew point temperature, °C

H_s = gross rate of solar radiation, W/m^2

Computation of D_t therefore requires values for the wind speed, dew point temperature, water surface temperature, and solar radiation for the period of interest. Assuming the period of interest for Minnesota was May through September and for Louisiana was April through November, the following meteorological parameters were obtained from historical records and used as input.
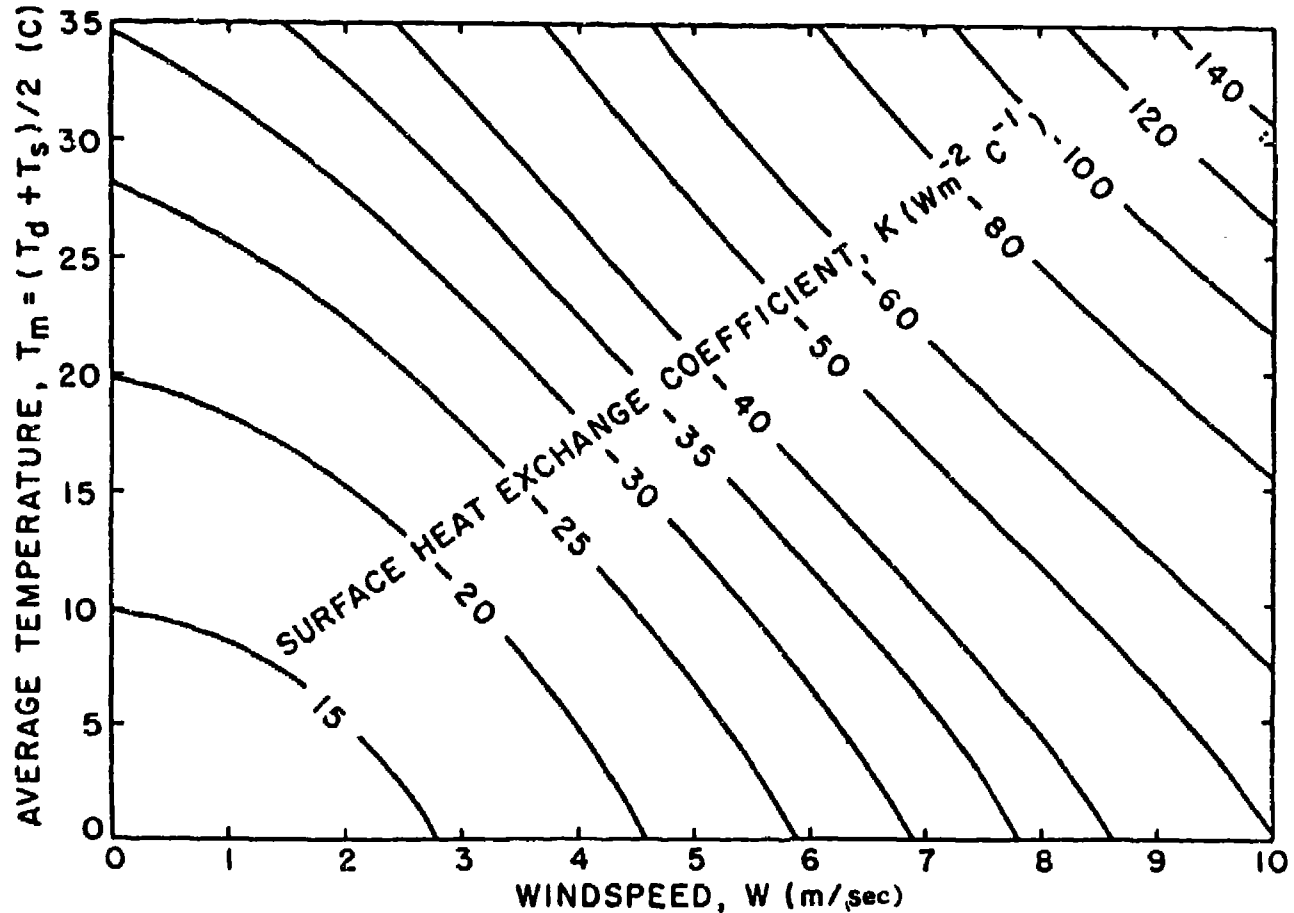
Figure A1. Design curve for surface heat exchange coefficient K
(after Edinger, Brady, and Geyer 1974)

	Minnesota	Louisiana
Wind speed, m/sec	4.3	2.6
Dew point temperature, °C	11.3	16.7
Solar radiation, W/m^2	230	223
Water surface temperature, °C	15.2	23.0

The computed quantities are:

		Minnesota	Louisiana
K	from Figure A1	29	29
T_e	from Equation A7	19.2	24.8
H_n	from Equation A4	117	49.8
w_*	from Equation A6	0.0055	0.0033
D_t	from Equation A5	8.4	4.3

Since these D_t values are less than the general rule of 10 m, they indicate the importance of other mixing processes in determining the stratification potential.

A.4 Pond Number

A.4.1 Description

For reregulation pools or multiple reservoirs in series, a more sophisticated stratification criterion has been proposed by Jirka and Harleman (1979) and Jirka and Watanabe (1980). Although this criterion was originally developed for cooling ponds, it can be used on any system characterized by large unsteady inflows of different density (temperature) water. Jirka and Harleman (1979) proposed the Pond number, Po, which is defined by:

$$ Po = \left[\frac{f_i}{4} \frac{Q^2}{\alpha \Delta T g D_m^3 B_c^2} D_v^3 \frac{L}{D_m} \right]^{1/4} \tag{A8} $$

where

f_i = interfacial friction coefficient (~0.01), dimensionless

α = coefficient of thermal expansion, per °C

ΔT = temperature differential between inflow water and ambient reservoir water, °C

D_v = dilution ratio for entrance mixing (~1.0), dimensionless

The Pond number includes four separate factors:

a. The parameter $f_i/4$ describes the magnitude of the internal turbulent shear.

b. The densimetric Froude number $Q^2 (\alpha \Delta T g D_m^3 B_c^2)^{-1}$ compares the destabilizing kinetic energy of inflow with the stabilizing buoyant energy.

c. The factor D_v^3 considers the destabilizing entrance mixing.

d. The parameter L/D_m is an aspect ratio comparing length to depth dimensions.

The larger the values of Po , the weaker the stratification. If
Po < 0.3 , the pool is well stratified. If 0.3 ≤ Po ≤ 1.0 , the pool
is weakly stratified with a vertical temperature difference of ΔT_v =
$0.45 T_o$ (1-Po) , where T_o = epilimnetic temperature, °C. If Po > 1.0 ,
the pool is vertically well mixed.

A.4.2 Examples

Lakes Catherine and Hamilton are two small hydropower projects
located downstream of Lake Ouachita, a large CE reservoir, on the
Ouachita River in south-central Arkansas. All of these projects have
bottom releases and are operated in series such that the cold,
hypolimnetic releases from Lake Ouachita pass through Lake Hamilton as
an underflow and then through Lake Catherine as an underflow. The Pond
number criterion is used to evaluate the stratification potential of
Lakes Catherine and Hamilton because there is a large unnatural tempera-
ture difference between the inflowing release waters from the upstream
reservoir and natural reservoir surface temperatures.

In this example, the following coefficients were used

$$f_1 = 0.01$$

$$\alpha = 1.8 \times 10^{-4}/°C$$

$$g = 9.8 \text{ m/sec}^2$$

$$D_v = 1.0$$

reducing Equation A8 to

$$Po = 1.09 \left[\frac{Q^2}{\Delta T D_m^3 B^2} \frac{L}{D_m} \right]^{1/4} \tag{A9}$$

The lakes have the following morphometric characteristics:

Characteristic, m	Catherine	Hamilton
D_m	5.5	8.0
B	400	970
L	19,500	29,900

A8

and mean monthly values were used for the flows Q and the temperature differentials. The temperature differentials were obtained from sine curves fitted to field measurements (see Figure A2). The following values were used

	Catherine	Hamilton
May – Q, m^3/sec	42.5	42.0
ΔT, °C	9.0	9.8
July – Q, m^3/sec	28.3	25.0
ΔT, °C	10.5	10.3
October – Q, m^3/sec	34.0	27.0
ΔT, °C	2.3	2.5

which, when substituted into Equation A9, resulted in the following Pond numbers:

	Catherine	Hamilton
May	0.44	0.21
July	0.34	0.19
October	0.55	0.25

These results indicate Lake Hamilton should be well stratified since Po < 0.3 and Lake Catherine should be weakly stratified since $0.3 \le Po \le 1.0$. Field measurements verify these results with midsummer temperatures in Lake Hamilton varying from 14° C in the hypolimnion to 30° C in the epilimnion and in Lake Catherine varying from 18° C in the hypolimnion to 28° C in the epilimnion. In Lake Catherine, the vertical temperature differential can be estimated from

$$\Delta T = 0.45 T_o \ (1 - Po)$$

If Po = 0.34 and T_o = 28° C, then ΔT = 8.3° C, which is similar to the measured 10° C.

A9
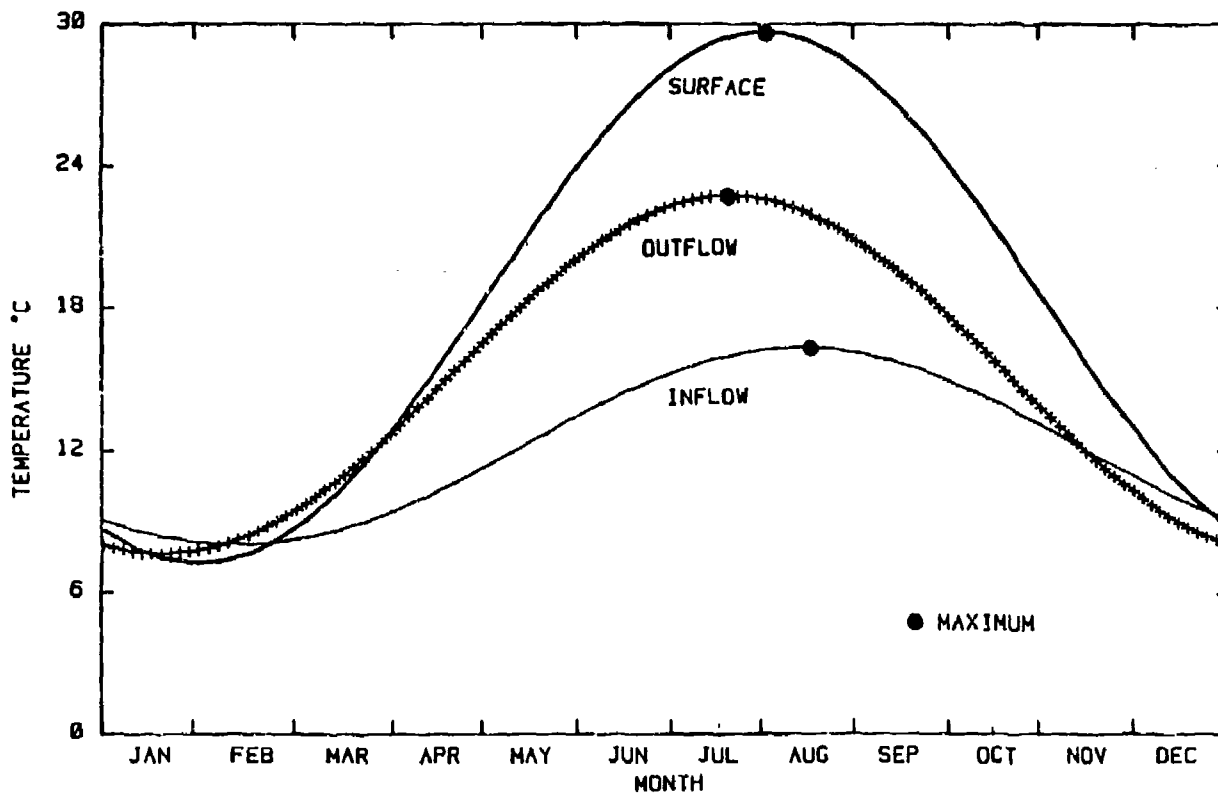
Figure A2. Sine curves fit to surface, outflow, and inflow
temperatures for Lake Hamilton

A.5 Summary

The methods presented to evaluate the stratification potential of a
reservoir range from a general rule to simple computations. Used inde-
pendently, these methods can provide an indication of the stratification
potential. However, because of the many factors involved in the
development and maintenance of stratification, the use of more than one
of the methods is suggested to provide a broader basis for the
evaluation of the stratification potential of a given reservoir (see
Section A.2.2).

NOTATION

A_j	Cross-sectional area of inflow, m^2
A_s	Water surface area, m^2
$A(z)$	Horizontal area of reservoir at elevation z, m^2
a	Dimensionless coefficient
B_c	Width of zone of conveyance, m
$B(z)$	Reservoir width at elevation z, m
C	Concentration, g/m^3
C_d	Drag coefficient, dimensionless
c	Empirical coefficient or proportionality constant, m
c_1	Dimensionless calibration coefficient
c_a	Calibration coefficient for advective mixing
c_c	Empirical calibration coefficient
c_p	Heat capacity of water, $J/(kg-°C)$
c_t, c_f, c_d	Constants determined from experimental data
c_w	Calibration coefficient for wind mixing
c_*	c/a^b, m
D	Water depth, m
D_1	Thickness of top layer, m
D_m	Reservoir mean depth, m
D_t	Wind mixing depth scale, m
D_v	Dilution ratio for entrance mixing (~1.0), dimensionless
$\dfrac{dz}{dx}$	Slope of water surface, m/m
e	Dimensionless density gradient = $10^{-6}/m$
F_d	Densimetric Froude number, dimensionless
f	Coriolis parameter ($f = 2_\omega \sin ∅$)
f_i	Interfacial friction coefficient (~0.01), dimensionless
GSWH	WQRRS stability criterion
g	Acceleration due to gravity, m/sec^2
H	Thickness, depth, or height, m
H_n	Net heat flux across the air/water interface, W/m^2
H_s	Surface heat flux, W/m^2

H_w Wave height, m

H_z Heat flux at elevation z, W/m^2

h   Depth (thickness) of upper turbulent layer or mixed layer, m

h_g Depth of center of mass of the mixed layer, m

h_p Hydraulic plunge depth, m

K   Heat exchange coefficient, $W/(m^2-°C)$

KE   Kinetic energy, J

K_d Dispersion coefficient, m^2/sec

K_m Molecular diffusivity or diffusion coefficient, m^2/sec

K_t Turbulent diffusion coefficient, m^2/sec

K_z Global vertical diffusion coefficient, m^2/sec

K_{zo} Eddy diffusion coefficient at neutral stability, m^2/sec

k   von Karman's constant (~0.4)

L   Length scale or reservoir length, m

M   Mass, kg

m   Total mass of the reservoir, kg

N^2 $\frac{g}{\rho}\frac{\partial \rho}{\partial z}$ = buoyancy frequency, sec^{-2}

n   Coefficient, dimensionless

Po   Pond number, dimensionless

Pr   Prandtl number = 1 for water, dimensionless

PE   Potential energy, J

p'   Turbulent fluctuations of pressure, Pa

$\bar{Q}$ Average reservoir discharge, m^3/sec

Q_i Flow rate in layer i, m^3/sec

Q_j Inflow rate, m^3/sec

Q_v Vertical flow rate, m^3/sec

q^2 TKE per unit mass = $(u_x^2 + u_y^2 + u_z^2)/2$

q_d Flux due to dispersion, $kg/(m^2-sec)$

q_m Flux due to molecular diffusion, $kg/(m^2-sec)$

q_t Flux due to turbulent diffusion, kg/m^2-sec

Ri   Richardson number, dimensionless

RPE   Relative potential energy, J

r	Radius of an inertial circle, m
S	Water surface slope, m/m
S_f	Stability factor, dimensionless
S_i	Interface slope, m/m
T	Water temperature, °C
TKE_a	Turbulent kinetic energy from advection, $(kg\text{-}m^2)/sec^2$
TKE_c	Turbulent kinetic energy from convection, $(kg\text{-}m^2)/sec^2$
TKE_w	Wind shear turbulent kinetic energy, $(kg\text{-}m^2)/sec^2$
T_d	Dew point temperature, °C
T_e	Equilibrium temperature, °C
T_j	Inflow temperature, °C
T_s	Surface temperature, °C
t	Time, sec
t_r	Hydraulic residence time, sec
t_s	Seiche period, sec
U	Velocity in direction of flow, m/sec
$\bar{U}$	Mean horizontal component, m/sec
U_i	Flow velocity in layer i, m/sec
U_j	Inflow velocity, m/sec
U_x, U_y, U_z	Instantaneous velocity components, m/sec
$\bar{U}_x$, $\bar{U}_y$, $\bar{U}_z$	Mean velocity components, m/sec
$u_j(z)$	Inflow velocity distribution, m/sec
$u_o(z)$	Outflow velocity distribution, m/sec
u_s	Surface drift velocity, m/sec
$\overline{u'w'}$	Reynolds stress, m^2/sec^2
u_x, u_y, u_z	Turbulent fluctuations of the horizontal (x,y) and vertical (z) velocity components, m/sec
$\overline{u_x u_z}$	Reynolds stress, m^2/sec^2
u^2	$\overline{u_x^2 + u_y^2 + u_z^2}$
V	Volume, m^3
V_i	Volume of layer i, m^3
W	Wind speed, m/sec

W_e	Wedderburn number
W_L	Entrainment work, $(kg\text{-}m^2)/sec^2$
w_e	$\dfrac{dh}{dt}$ = entrainment velocity, m/sec
w_*	Shear or friction velocity, m/sec
Z_j	Difference in depth between center of mass of inflow and center of mass of inflow placement, m
Z_m	Maximum elevation or depth, m
z	Vertical coordinate, m
z_s	Elevation of water surface, m
$< >$	Ensemble mean (i.e., mean over many trials)
$<u^2>^{1/2}$	Root mean square velocity, m/sec
α	Coefficient of thermal expansion of water, per °C
β	Coefficient, dimensionless
ΔD	Setup of water surface, m
ΔT	Temperature differential between inflow water and ambient reservoir water, °C
ΔV	Incremental volume to be entrained, m^3
Δt	Time step, sec
$\Delta \rho$	Density difference, kg/m^3
$\Delta \rho_j$	Density difference between inflow and reservoir surface waters, kg/m^3
$\bar{\varepsilon}$	Rate of dissipation of TKE, m^2/sec^3
ε	Local dissipation rate of TKE, m^2/sec^3
λ	Wavelength, m
ρ	Density, kg/m^3
ρ'	Turbulent fluctuations of density, kg/m^2
ρ_a	Density of air, 1.177 kg/m^3
ρ_j	Inflow density, kg/m^3
ρ_m	Maximum water density, kg/m^3
ρ_o	Mean density, kg/m^3
ρ_w	Water density, kg/m^3
$\rho(z,t)$	Reservoir density at elevation z and time t, kg/m^3
σ	Velocity scale, m/sec

τ	Shear stress, $kg/(m\text{-}sec^2)$
τ_s	Shear stress at air/water interface, $kg/(m\text{-}sec^2)$
$\emptyset$	Latitude
$\dfrac{\partial C}{\partial x}$	Concentration gradient, $mg/\ell/m$
$\dfrac{\partial U}{\partial z}$	Velocity gradient, $(m/sec)/m$
$\dfrac{\partial \rho}{\partial z}$	Local density gradient
ω	Angular velocity of the earth's rotation, 7.29×10^{-5} rad/sec